Projekt

# Junge (känozoische) tektonische Entwicklung der Kristallingebiete in Sachsen

## Anlage 1

***Recent tectonics in the Eger rift (Saxony and NW Czech Republic): Insights from geomorphic indices (L. Andreani, K. Stanek, R. Gloaguen)***

***Inhaltsverzeichnis***

# Recent tectonics in the Eger rift (Saxony and NW Czech Republic): Insights from geomorphic indices

L. ANDREANI [a,1,2], K. STANEK[1] AND R. GLOAGUEN[1,2]

[(1)] *Institute of Geology, TU Bergakademie Freiberg, B. von-Cotta-Str. 2, 09599, Freiberg, Germany.*

[(2)] *Remote Sensing Group, Helmholtz Institute Freiberg for Resource Technology, Halsbrueckerstr. 34, 09599, Freiberg, Germany.*

## Abstract

We analyse in this report the response of landscapes to recent tectonic events along the Eger rift. The Eger rift is located in the northern part of the Bohemian Massif. The main rifting event began at the end of the Eocene and lasted until the early Miocene. The post-rift evolution of the Eger Graben is associated to a NW- to NNW-trending compression which mainly resulted in the uplift of the Erzgebirge mountains. We analysed both topographic surfaces and drainage networks by using topographic profiles and geomorphic indices. Our results show that in spite of low deformation rates the areas located around the Bohemian Massif are suitable for a morphotectonic analysis. The topography of Saxony and NW Czech Republic appears to be geomorphically young. Topographic profiles and geomorphic maps show that large portions of the landscape consist in relatively well preserved surfaces which may represent relicts of the Paleogene "etchplain". These surfaces are associated to well defined relict base-levels in river profiles. Geomorphic indices also suggest a close relationship between main structures and landscapes. The Eger rift basins are well defined in our geomorphic maps. The Erzgebirge block is mainly tilted along the Krušné Hory fault. Our results show that it is divided in three main compartments (Eibenstock, Marienberg and Mittelsachsen) by NW-trending lineaments (Mariánské-Lázně, Gera-Jáchymov, Flöha, Elbe lineaments). Alongstrike changes in incisions suggest that the uplift was initiated along the western compartment and then propagated toward the east. Others areas consist mainly in tilted panels and plateaus with different elevations. The most recent event observed in river profiles is mainly associated to a 100 to 150m base-level drop along the Elbe valley. This event can be correlated with the Pleistocene Elbe terrace sequence.

[a]Corresponding author e-mail: andreani.louis@gmail.com

# CONTENTS



# LIST OF FIGURES

## 1. Introduction

The Eger Graben is the easternmost part of the European Cenozoic Rift System (ECRIS) which transects all Variscan Massifs in the foreland of the Alps (e.g., Dèzes et al., 2004; Ziegler & Dèzes, 2007). The Eger Graben is a subject of intense research and controversy regarding the causes and mechanisms of extension as well as post-rift deformation (e.g., Rajchl et al., 2009; Cajz & Valečka, 2010). The onset of extension in the Eger graben is associated with the latest Eocene main volcanic pulse in NW Bohemian Massif (e.g., Cajz et al., 1999; Ulrych et al., 1999). Magnetostratigraphic and palaeobotanical data suggest that the syn-rift deposition in Eger rift basins ended during early Miocene (Teodoridis & Kvaček, 2006). The post-rift evolution of the Eger Graben is commonly associated to a NW- to NNW-trending compression (Müller et al., 1997; Jarosinski, 2006) which mainly resulted in the uplift and erosion of its northwestern rim (Erzgebirge mountains) during the Plio-Quaternary (Ziegler & Dèzes, 2007).

Present-day tectonic rates are low in Central Europe (< 2 mm/yr, Grenerczy et al., 2005). However, earthquake swarms (e.g. Fischer & Horálek, 2005; Babuška et al., 2007), $CO_2$-emanation (Bräuer et al., 2003; Weinlich et al., 2003) and geological studies (e.g. Peterek et al., 2011) provide evidences for active magmatism and ongoing tectonic activity along NW part of the Bohemian Massif. From a geomorphic point of view the Plio-Quaternary uplift of the Bohemian Massif resulted in the increase of incision rates for main rivers and thus in the entrenchment of the drainage network. Available data about terraces indicate for example 180 m of incision since the late Pliocene (3.5 Ma) for the Eger river and 160 m of incision during the last 1.9 Ma for the Vltava river (Westaway, 2002; Tyráček et al., 2004).

We propose here to analyze the landscapes of the Eger rift and surrounding regions and their response to tectonics by using a set of geomorphic indices. Landscapes affected by recent or active tectonics result from a competition between vertical uplift and erosional processes (e.g., Snyder et al., 2000; Burbank & Anderson, 2001). In tectonically active areas, erosion processes are enhanced as drainage networks respond to base-level changes (e.g., Mather, 2000; Mather et al., 2000). Geomorphic indices are commonly used to detect landscapes responses to recent deformation processes (e.g., Keller & Pinter, 1996; Burbank & Anderson, 2001, and references therein). In addition geomorphic indices can be obtained easily. During the last years the Remote Sensing Group in TU Bergakademie Freiberg focused on the development of new remote sensing tools in order to extract geomorphic indices and quantify regional deformation. The main contribution of our group is the development of TecDEM, a MATLAB-based software able to extract from digital elevation models and analyze the most commonly used geomorphic indices (Shahzad & Gloaguen, 2011a,b).

We analyse in this report both topographic surfaces and drainage networks. While surface analyses (e.g., hypsometry, incision and surface roughness) are commonly used to classify landscapes between different erosional (and thus evolutionary) stages (e.g., Strahler, 1952; Schumm, 1956; Ohmori, 1993; Grohmann, 2004; Grohmann et al., 2007; Pérez-Peña et al., 2009), river profile analyses proved to be useful in detecting active structures, delineating spatial patterns in rock uplift rates and, in some cases, estimating the amount of uplift or incision for different segments of a river (e.g., Hack, 1973; Wobus et al., 2006; Kirby & Whipple, 2012). A major concern in geomorphic studies is that in slowly deformed areas erosion processes may suppress the effects of active tectonics on present-day topography, thus questioning the suitability of geomorphic indices to characterize recent and active tectonics. For this reason only a few works were done in intra-plate settings or in areas with low deformation rates (e.g., Pedrera et al.,

2009; Font et al., 2010). However, our results show that the areas located around the Bohemian Massif are suitable for a morphotectonic analysis. Geomorphic indices suggest a tight relationship between main tectonic features and landscapes and provide new insights into the evolution of the northern Bohemian Massif.

## 2. Tectonic setting

The Bohemian Massif (Fig. 1) is located in Central Europe. It covers Czech Republic, eastern Germany, southern Poland and northern Austria. Its central part forms a rhombus shaped plateau limited by four major ranges: the Ore Mountains (Erzgebirge in german or Krušné Hory in czech) in the northwest, the Sudetes (which are themselves divided in several ranges such as the Jizera, Krkonoše and Hrubý Jeseník mountains) in the northeast, the Bohemian-Moravian Highlands in the southeast, and the Bohemian Forest in the southwest. The massif also encompasses a number of "mittelgebirges" and mainly consists of crystalline rocks deformed during the Variscan Orogeny.

The studied area is located along the Eger graben and corresponds to the easternmost part of the European Cenozoic Rift System (ECRIS) which transect all Variscan Massifs in the foreland of the Alps (Ziegler, 1992; Dèzes et al., 2004; Ziegler & Dèzes, 2007). The rifting started during the Eocene in the foreland of the Alps in response to collision-related intraplate stresses. During Oligocene and Neogene times the ECRIS evolved by passive rifting under changing stress fields, reflecting the increasing coupling of the Alpine Orogen with its foreland. The ECRIS is presently still active, as evidenced by its seismicity and geodetic data (Ziegler & Dèzes, 2007).

The main volcanic pulse occurred between the early Oligocene and early Miocene (Adamovic & Coubal, 1999; Ulrych et al., 1999) in the Eger volcano-tectonic zone, prior to a subsidence phase (Malkovský, 1987). Volcanic activity decreased during the middle Miocene (16 to 12 Ma) and intensified again during the late Miocene and Pliocene (11.4 to 3.95 Ma). It locally lasted until 0.11 Ma (Adamovic & Coubal, 1999; Ulrych et al., 1999). During the Burdigalian a N- to NW-trending drainage system developed in the Bohemian Massif area and up to 500 m of lacustrine and fluvial clastic deposits accumulated in the Eger depression during an extensional period (Malkovský, 1975, 1979). During the early Langhian (15 to 16 Ma) temporary marine incursions advanced northward along river valleys into the southern and eastern parts of the Bohemian Massif (Malkovský, 1979; Suk, 1984). The middle Miocene to present evolution of the Bohemian Massif is marked by a compressional reactivation of pre-existing fracture zones which produced a disruption of the initially flat landscape. This event resulted in the uplift of the marginal Thüringer Wald (Thuringian Forest), Böhmischer Wald (Bohemian Forest), Erzgebirge, Sudetic and Moravo–Silesian blocks. According to Suk (1984), uplifted remnants of early Langhian marine deposits are now found at 600 m above the present-day sea level in the southern parts of the Bohemian Massif.

The Plio-Quaternary uplift of the Bohemian Massif and surrounding areas is associated to a mainly NW- to NNW-trending compression (Müller et al., 1997; Jarosinski, 2006). Earthquake swarms (e.g. Fischer & Horálek, 2005; Babuška et al., 2007), $CO_2$-emanation (Bräuer et al., 2003) and geological studies (e.g. Peterek et al., 2011) provide evidences for active magmatism and ongoing tectonic activity along NW part of the Bohemian Massif. Leveling data indicate that the NW parts of the Bohemian Massif are being uplifted while the Cretaceous Basin located in the eastern part of the Bohemian Massif appears to gently subside (Frischbutter & Schwab, 1995). GPS data also indicate a differential horizontal motion

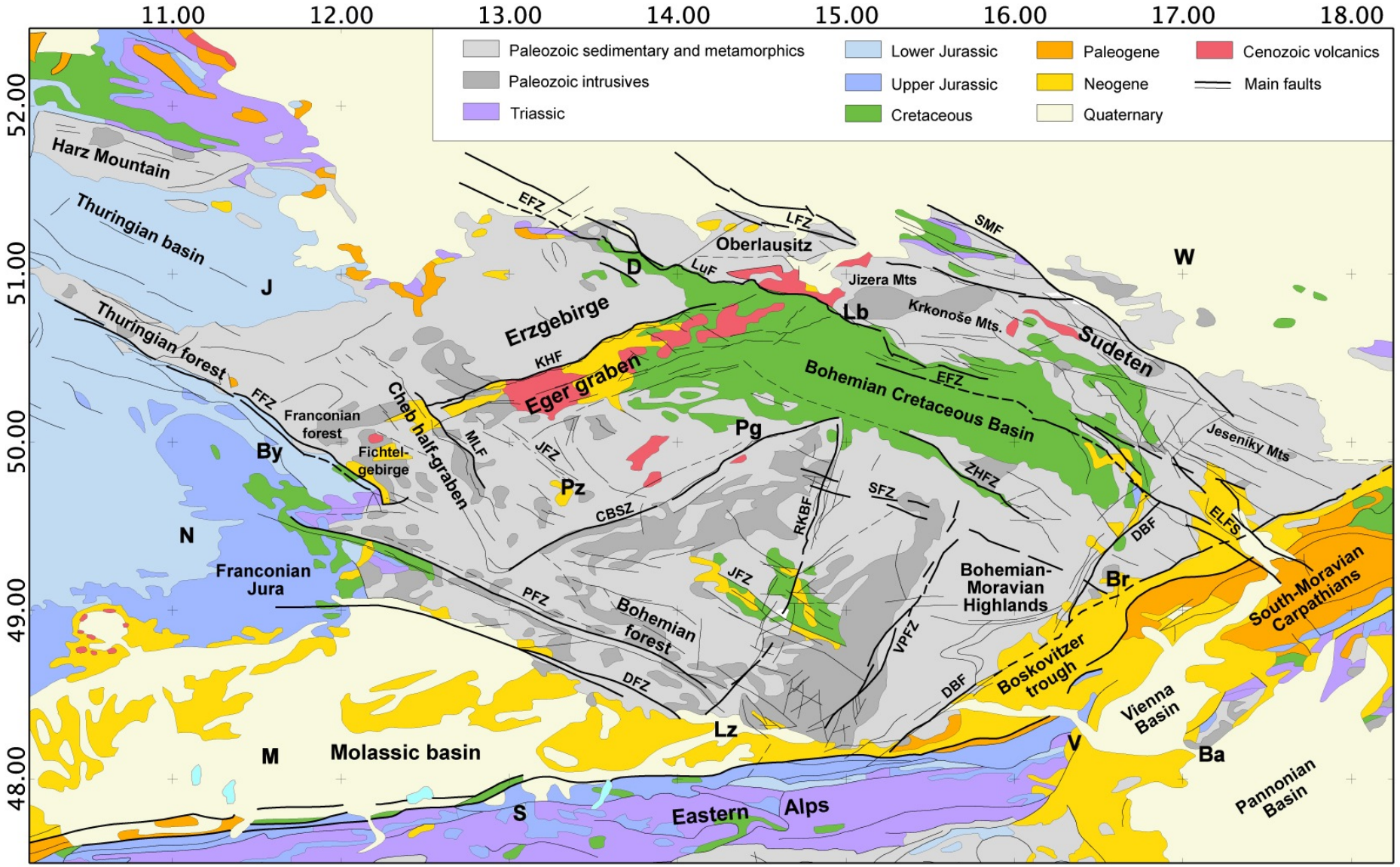


Fig. 1 – *Simplified geological map of the Bohemian Massif and surrounding areas (modified from Pawlewicz et al., 1997). Main structures: CBSZ - Central Bohemian Shear Zone, DBF - Diendorf-Boskovice fault, DFZ - Danube fault zone, EFZ - Elbe fault zone, ELFS - Elbe-Lužice fault system, FFZ - Franconian fault zone, JFZ - Jáchymov fault zone, KHF - Krušné hory fault, LFZ - Lauzitzer fault zone, LuF - Lusatian fault, MLF, Mariánské-Lázně fault, PFZ - Pfahl fault zone, RKBF - Rodl-Kaplice-Blanice fault system, SFZ - Sázava fault zone, SMF - Sudetic marginal fault, VPFZ - Vitis-Přibyslav fault zone, ZHFZ - Železné Hory fault zone. Bold letters indicate main cities: Ba - Bratislava, Br - Brno, By - Bayreuth, D - Dresden, J - Jena, Lb - Liberec, Lz - Linz, M - Munich, N - Nuremberg, Pg - Prag, Pz - Plzeň, S - Salzburg, V - Vienna, W - Wrocław.*

of a few mm/y between the Sudetic and Moravo-Silesian blocks (Schenk et al., 2000). From a geomorphic point of view the Plio-Quaternary uplift of the Bohemian Massif resulted in the increase of incision rates for main rivers and thus in the entrenchment of the drainage network. Available data about terraces indicate for example 180 m of incision since the late Pliocene (3.5 Ma) for the Eger river and 160 m of incision during the last 1.9 Ma for the Vltava river (Westaway, 2002; Tyráček et al., 2004).

## 3. Methods and tools

### *3.1. Surface analyses*

#### *3.1.1. Geomorphic indices*

Surface analyses of landforms are commonly used to differentiate between different erosional and thus evolutionary stages (e.g., Strahler, 1952; Ohmori, 1993) or in tectonic geomorphology (e.g., Pérez-Peña et al., 2009). Hypsometric integral (HI, Fig. 2) shows the distribution of landmass volume remaining beneath or above a basal reference plane (e.g., Strahler, 1952; Pike & Wilson, 1971; Schumm, 1956). Pike & Wilson (1971) show that the hypsometric integral can also be calculated using this simple formula:

$$HI = \frac{h_{mean} - h_{min}}{h_{max} - h_{min}} \tag{1}$$

with $h_{mean}$, $h_{min}$ and $h_{max}$ being the mean, minimum and maximum elevations of the analyzed area.

The surface roughness (SR, Fig. 2) is given by:

$$SR = \frac{TS}{FS} \tag{2}$$

with $TS$ and $FS$ being the areas of the analyzed topographic surface and the corresponding flat and horizontal surface (Grohmann, 2004; Grohmann et al., 2007). The ratio value is close to 1 for flat areas and increases rapidly as the real surface becomes irregular.

The topographic position index (TPI, Weiss, 2001; Jenness, 2006) compares the elevation of each cell in a digital elevation model to the mean elevation of a specified neighborhood around that cell. It is calculated using the following formula:

$$TPI = h - h_{mean} \tag{3}$$

with $h$ and $h_{mean}$ being the elevation of the cell and the mean elevation of neighboring cells. The TPI provides a simple method to classify landscapes between ridges (positive values) and valleys (negative values). TPI values near zero correspond either to flat areas (where the slope is near zero) or to areas with constant slope (where the slope of the point is significantly greater than zero). TPI values also reflect the degree of incision by the drainage network. For instance, gentle and rounded hills will show moderate TPI values while cliffs and canyons will display extreme values.

#### *3.1.2. Classification of landscapes according to their erosional stage*

Steady-state topography is marked by low-amplitude reliefs and surfaces related to a defined base-level. Topographic uplift or drop in sea level result in a change of this base-level and in the progressive erosion of the former steady-state topography through time. Hypsometric integral (HI) and surface roughness (SR) can be used to differentiate between erosional (and thus evolutionary) stages (Fig. 2). Landscapes

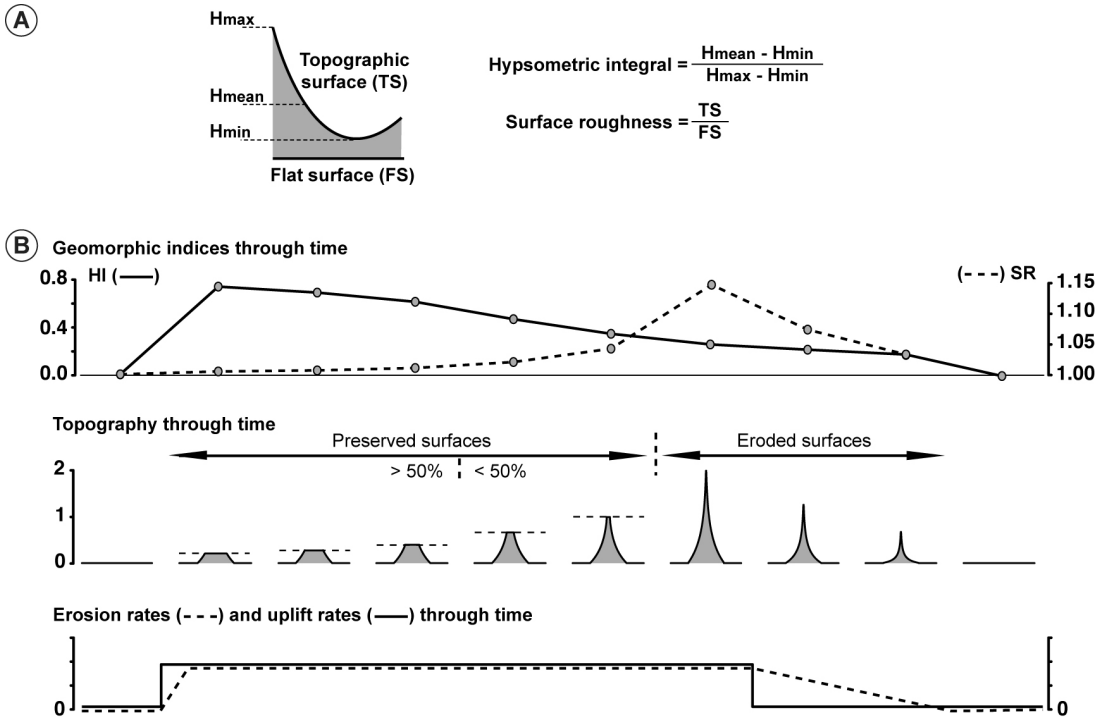


Fig. 2 – *Surface indices.* ***(A)*** *Calculation of the hypsometric integral (HI) and surface roughness (SR) indices within a moving window.* ***(B)*** *Evolution of hypsometric integral and surface roughness during the uplift and erosion of an initially flat surface. HI increases rapidly after the uplift started and then decreases as the uplifted surface is eroded. The peak of SR is associated to the latest stage of the uplift, when the paleo-surface is eroded.*

affected by recent base-level drop are characterized by high hypsometry and low surface roughness because recently uplifted surfaces are largely preserved and, in the case of tectonic activity, fault scarps are poorly eroded (e.g., Strahler, 1952; Delcaillau et al., 1998; Pérez-Peña et al., 2009; Cheng et al., 2012). In older landscapes these surfaces are almost completely eroded by the drainage network, resulting thus in the gradual increase of the surface roughness and decrease of hypsometric integral.

We propose a new index (referred hereafter as "Surface Index", SI) which combine the hypsometric integral, the surface roughness and the elevation. Our aim is to reveal on the same map peak values of hypsometry and surface roughness and to relate them to the intensity of the base-level change. Surface roughness values are strongly correlated to the differences in elevation and thus to the intensity of the initial base-level drop. It is not the case for hypsometric integral which mainly depends on the repartition of landmasses (i.e. two landscapes with the same shape but with different elevations will have the same hypsometric integral). In order to relate hypsometry to the elevations we converted both datasets to ratios and multiplied the hypsometry by the elevation. Then, we subtracted the ratios of the surface roughness from the resulting values according to the following formula:

$$SI = \left(\frac{HI - HI_{min}}{HI_{max} - HI_{min}}\right) \times \left(\frac{h - h_{min}}{h_{max} - h_{min}}\right) - \left(\frac{SR - SR_{min}}{SR_{max} - SR_{min}}\right) \quad (4)$$

$HI$, $h$ and $SR$ represent the values of hypsometry, elevation and surface roughness for the considered pixel while "$max$" and "$min$" represent the corresponding maximum and minimum values for the whole area. SI values around 0 correspond mainly to areas with low elevations or to flat areas characterized by low HI and SR values. Values between 0 and +1 correspond to preserved (i.e. poorly eroded) surfaces associated to a recent event (uplift or base-level drop). Increase of values is related to the increase in the elevation of these surfaces and thus to the intensity of the event. Negative values (between -1 and 0)

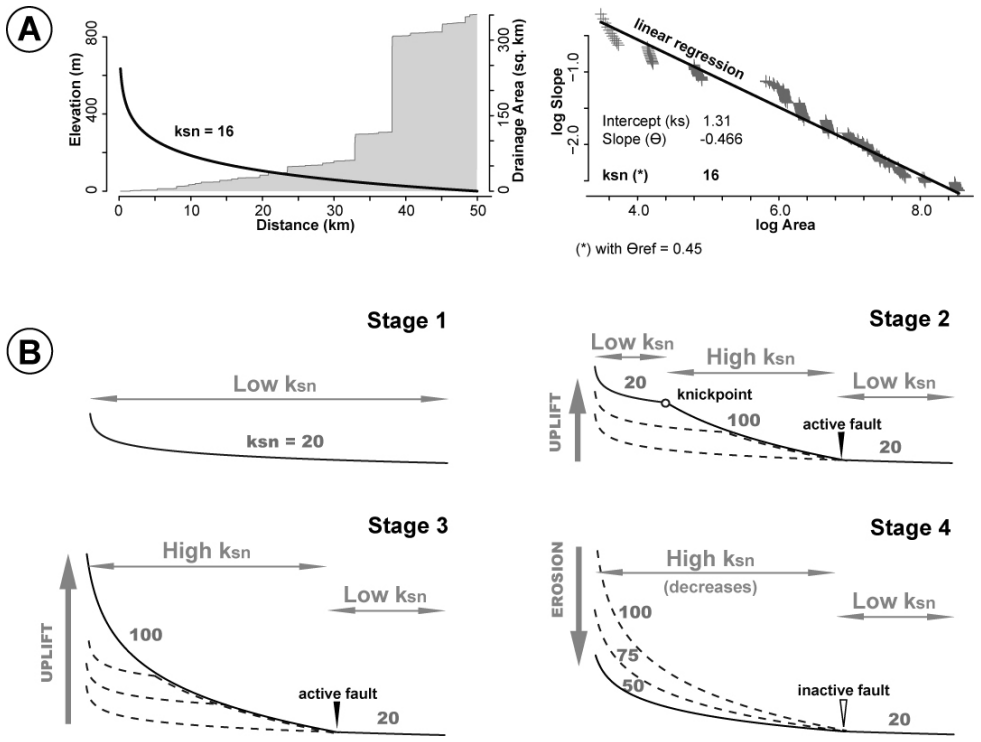


Fig. 3 – *River profile analysis.* ***(A)*** *Calculation of the normalized steepness index for a schematic river profile and corresponding drainage area. Slope of log(Slope) vs. log(Area) scaling is the concavity index $\theta$; y-intercept is the steepness index $k_s$. In this example the normalized steepness index $k_{sn}$is calculated using a reference concavity of 0,45.* ***(B)*** *Schematic river profiles corresponding to an initial steady-state (stage 1), recent uplift along a fault (stage 2, the profile displays a marked knickpoint and its uppermost segment is still preserved and shows low $k_{sn}$ values), continued uplift through time along the same fault (stage 3, the whole profile above the fault is equilibrated with respect to uplift and erosion rates and displays high $k_{sn}$ values) and end of the fault activity (stage 4, the river profile progressively evolves toward stage 1).*

---

are associated to eroded topography. They are related to the amount of incision by the drainage network and reflect both the age and the intensity of the base-level change. Values close to -1 indicate recent or high-amplitude events while negative values close to 0 reflect either low-amplitude events or older and strongly eroded topography.

### *3.2. Swath profiles*

Swath topographic profiles provide a useful way to characterize the topography of orogenic belts (e.g., Isacks, 1992; Masek et al., 1994; Duncan et al., 2003; Ponza et al., 2010). An elongated and rectangular patch of topography is extracted and the calculated topographic values (usually the maximum, minimum and mean elevations) are projected onto a vertical plane parallel to the long axis of the swath rectangle. The curve for maximum elevations provides informations on the initial topography while the curve for minimum elevations reflect the base-level of rivers. Swath profiles provide thus a quick estimate of the incision by the drainage network (the difference between the maximum and minimum elevations).

### *3.3. River networks and longitudinal profiles*

The study of the drainage networks and river longitudinal profiles is a suitable approach to explore neotectonics. As river networks are highly responsive and adapt quickly to the changes of surface slope, they may register tectonic activity better than hillslopes (e.g., Duvall et al., 2004; Pearce et al., 2004). Deviations from the typical concave-up shape of stream longitudinal profiles, such as knickpoints or convex segments, indicate a disequilibrium state resulting from tectonic, base-level or lithological perturbations

(e.g., Kirby & Whipple, 2001; Chen et al., 2003; Troiani & Della Seta, 2008; Pedrera et al., 2009; Font et al., 2010; Kirby & Whipple, 2012).

The normalized steepness index ($k_{sn}$, Fig. 3) is widely used to investigate tectonically induced perturbations in river longitudinal profiles as it shows a direct proportionality with uplift rates (e.g., Kirby & Whipple, 2001; Wobus et al., 2006; Whittaker et al., 2008; Kirby & Whipple, 2012). Assuming a known relationship between slope and catchment area, Hack (1957) suggested an expression for the equilibrium state channel gradient:

$$S = k_s \times A^{-\theta} \tag{5}$$

with

$$k_s = \left(\frac{U}{K}\right)^{\frac{1}{n}} \tag{6}$$

where S is the local channel slope, $\theta$ is the channel concavity, $k_s$ is the steepness index, A is the upstream drainage area, U is the rock uplift rate, and K is the dimensional coefficient of erosion. As suggested by Wobus et al. (2006), a normalized steepness index $k_{sn}$ is used, since $k_s$ and $\theta$ are strongly correlated. In a logarithmic plot of slope against catchment area, the segments of a river profile can be defined and regressed with a power-law function in order to obtain the values of $k_{sn}$ and $\theta$ (Fig. 3A; Kirby & Whipple, 2001; Wobus et al., 2006). According to the above equation the steepness index shows a direct proportionality with the rock uplift rate U and can be used as a relative uplift-rate value. Some streams show a single slope-area scaling for their entire length (e.g., stage 1 in Fig. 3B); in other cases, if a knickpoint is, for example, generated by an active fault (e.g., stages 2 and 3 in Fig. 3B), the upper part of the longitudinal profile will be characterized by one or two concave segments with changing values of $k_{sn}$ and $\theta$ (Wobus et al., 2006). Derived relative uplift-rate values can be plotted in maps for comparison with the specific geologic and tectonic settings.

The spatial distribution of stream height is also a useful proxy for investigating geologic or tectonic processes (e.g., Golts & Rosenthal, 1993; Grohmann et al., 2007, 2011). Drainage networks are commonly organized according to Strahler (1957) stream order. According to Golts & Rosenthal (1993) streams of similar orders are of similar geological age and are related to similar geological events. Hence the interpolation of isobase lines, which connect streams with a similar order, produce a surface resulting from the same erosional events. As suggested by Grohmann et al. (2007), isobase maps can be seen as a smoothed version of the original topographic surface, from which was removed the 'noise' of the 1st-order streams erosion. Sharp topographic changes affecting an isobase surface may indicate structures associated to tectonic movements or extreme lithological changes.

### *3.4. Extraction and analysis of geomorphic indices*

Extraction and analysis of geomorphic indices were made using TecDEM, a MATLAB-based software allowing the extraction of river networks, drainage basins and geomorphologic parameters from digital elevation models (Shahzad & Gloaguen, 2011a,b). We used 90m resolution SRTM data from CIAT (Jarvis et al., 2008) for regional scale analyses. We also used 30m resolution ASTER GDEM data (product of METI and NASA) and 20m resolution DGM data (provided by the Sächsisches Landesamt für Umwelt, Landwirtschaft und Geologie) for more local analyses. The drainage network was extracted from DEM

data by calculating flow directions at all points using the D8 algorithm (Fairfield & Leymarie, 1991; Jones, 2002). Stream longitudinal profiles were identified and selected based upon least cost path analyses, which compute paths of least down slope resistance (i.e. the downstream flow path) and Strahler orders. This method is highly efficient, but accuracy is limited by the resolution and quality of the DEM. As the extracted streams contain some error, smoothening algorithms are applied, depending upon the number of nodes. Associated drainage basins were extracted using a second grid corresponding to the contributing area for each pixel. Isobase maps were computed by interpolating the elevation of streams corresponding to Strahler order 2 and 3. Morphometric maps for topographic position index, hypsometric integral and surface roughness were calculated using a moving window. Issues related to the minimal size of the moving window are well documented (e.g., Ascione et al., 2008; Guzzetti & Reichenbach, 1994). The moving window should be large enough to include at least two major ridges and/or valleys otherwise the results would simply represent the slope gradient (Evans, 1972). Thus, we selected a moving window of 9km for all morphometric maps.

## 4. Results

### *4.1. Topographic profiles*

#### *4.1.1. Eger graben and Erzgebirge mountains*

NNW-trending swath profiles 1 to 3 (Fig. 4 and 5) allow to compare the along strike variations of main tectonic and topographic features across the Eger graben and Erzgebirge range.

In each profile the Eger graben is well defined by topographic scarps. The difference in elevation between the northern and southern rims of the graben is well marked in the east (almost 500 m in profile 3) but decreases westward (~200m in profile 1). We also observe an eastward widening of the Eger graben from ~10km (Sokolov Basin in profile 1) to ~25km in the Most basin (profile 2) and finally ~35km in the easternmost region (profile 3 in Fig. 5). The graben floor is heterogeneous. In profile 1 it is concave and the Eger river is clearly entrenched as indicated by the curve of minimum topography while in profile 2 it is flat and slightly tilted to the south. In profile 3 the graben is almost completely filled by the Böhmische Mittelgebirge volcanic field.

The southern rim of the Eger graben consists in elevated plateaus which extend up to 50 km from the Southern Boundary fault system and are limited to the SE by the Central Bohemian shear zone. The flat portions of landscapes observed in each profiles (noted "KNES" in profile 1 and "RHS" in profiles 2 and 3) may represent in fact the remnants of a single regional paleosurface. The mean elevation of the Rakovník High remains relatively constant (~300m NW of Prag to ~500m north of Plzeň). The Kaiservald plateau appears to be tilted along both the Southern Boundary fault system and the Mariánské-Lázně fault as the highest elevations (~900m) are found at the junction between the eastern rim of the Cheb half-graben and the southern rim of the Eger graben.

The northern rim of the Eger graben consists in the Erzgebirge range which displays significant along strike variations. In topographic profiles the Erzgebirge range appears as a block tilted toward the north-west. The SE flank of the range is marked by a sharp topographic scarp associated to the Krušné Hory fault in profiles 2 and 3. In profile 1 the southern flank of the Erzgebirge range is complicated by a topographic high (referred as "Nejdek High" in Fig. 5). This topographic high may correspond to a tectonic block which may be separated from the rest of the Erzgebirge range by a secondary fault (see the

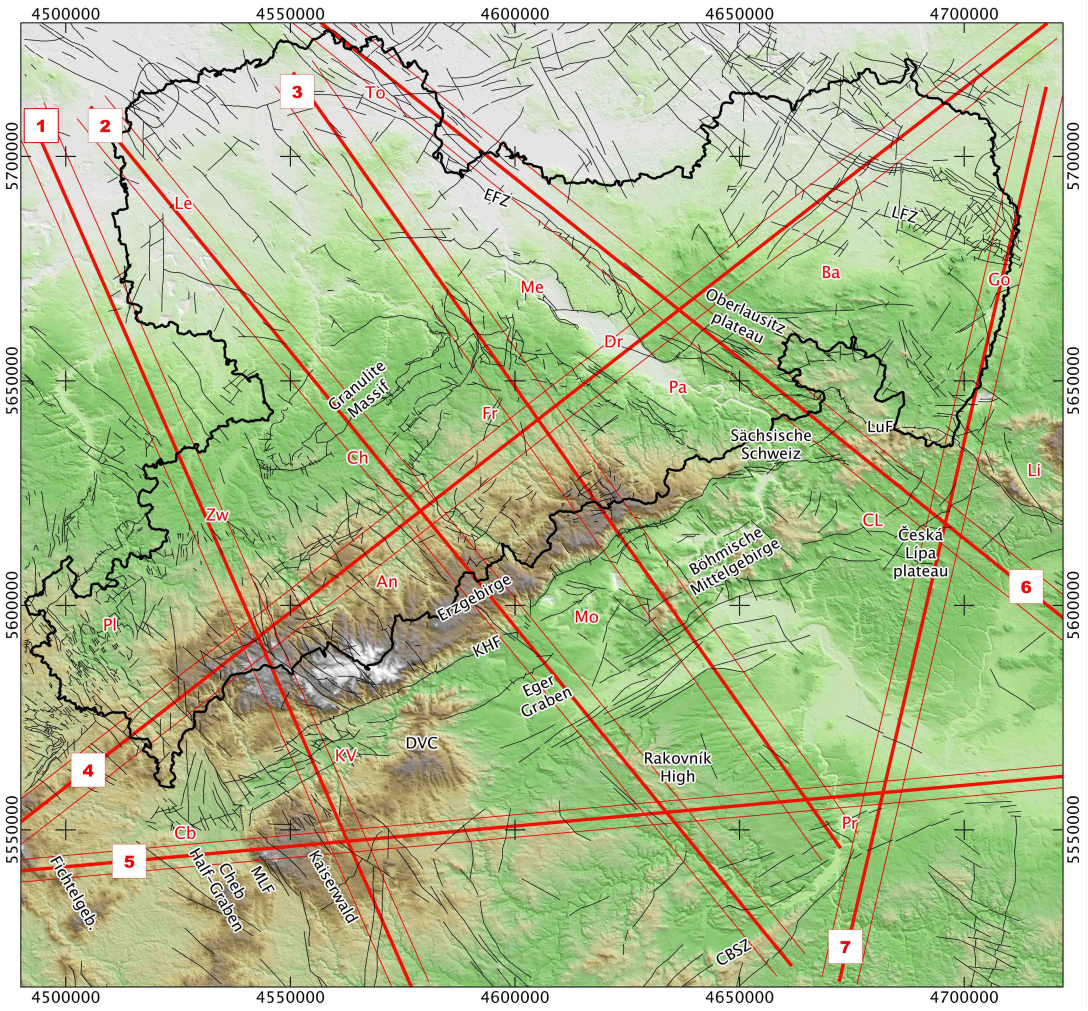


Fig. 4 – *Locations of regional swath topographic profiles (in red). Main structures: CBSZ - Central Bohemian Shear Zone, DVC - Doupov Volcanic Complex, EFZ - Elbe fault zone, KHF - Krušné hory fault, LFZ - Lauzitzer fault zone, LuF - Lusatian fault, MLF, Mariánské-Lázně fault. Red letters indicate main cities: By - Bayreuth , Zw - Zwickau , Ch - Chemnitz , Fr - Freiberg , Dr - Dresden , Pl - Plauen , Le - Leipzig , Go - Görlitz , Ba - Bautzen , Me - Meißen , Pa - Pirna , To - Torgau , An - Annaberg , Je - Jena , Pz - Plzeň , CL - Česká Lípa , Pr - Praha , Mo - Most , Li - Liberec , Cb - Cheb , KV - Karlovy Vary.*

inferred "Nejdek Fault" in profile 1). All profiles display a recognizable surface on top of the Erzgebirge range (noted "UPS" in Fig. 5). The NW part of the Erzgebirge range vary strongly from East to West. The easternmost section (profile 3 in Fig. 5) displays a gentle, slightly concave and continuous surface extending up to 80km from the Krušné Hory fault. The connection with the Nordsachsen lowlands to the North is barely marked. The central area (profile 2 in Fig. 5) presents a similar shape but we can define a topographic high (Marianberg High) with distinct flat portions and higher incisions (see the difference between maximum and minimum elevations) and a lower topography (Chemnitz-Plauen low) which connects further north with the Nordsachsen lowlands. In the westernmost section (profile 1 in Fig. 5) the NW flank of the Erzgebirge displays a more concave shape with a strongly incised topography (Eibenstock High) and a flat topography (Chemnitz-Plauen low). The concave shape of the range is disrupted by a flat surface with an elevation similar to the Nejdek High and Kaiservald plateau. All these surfaces may represent in fact a single regional surface. In this profile the Chemnitz-Plauen surface is well defined and is slightly elevated with respect to the Nordsachsen lowlands.

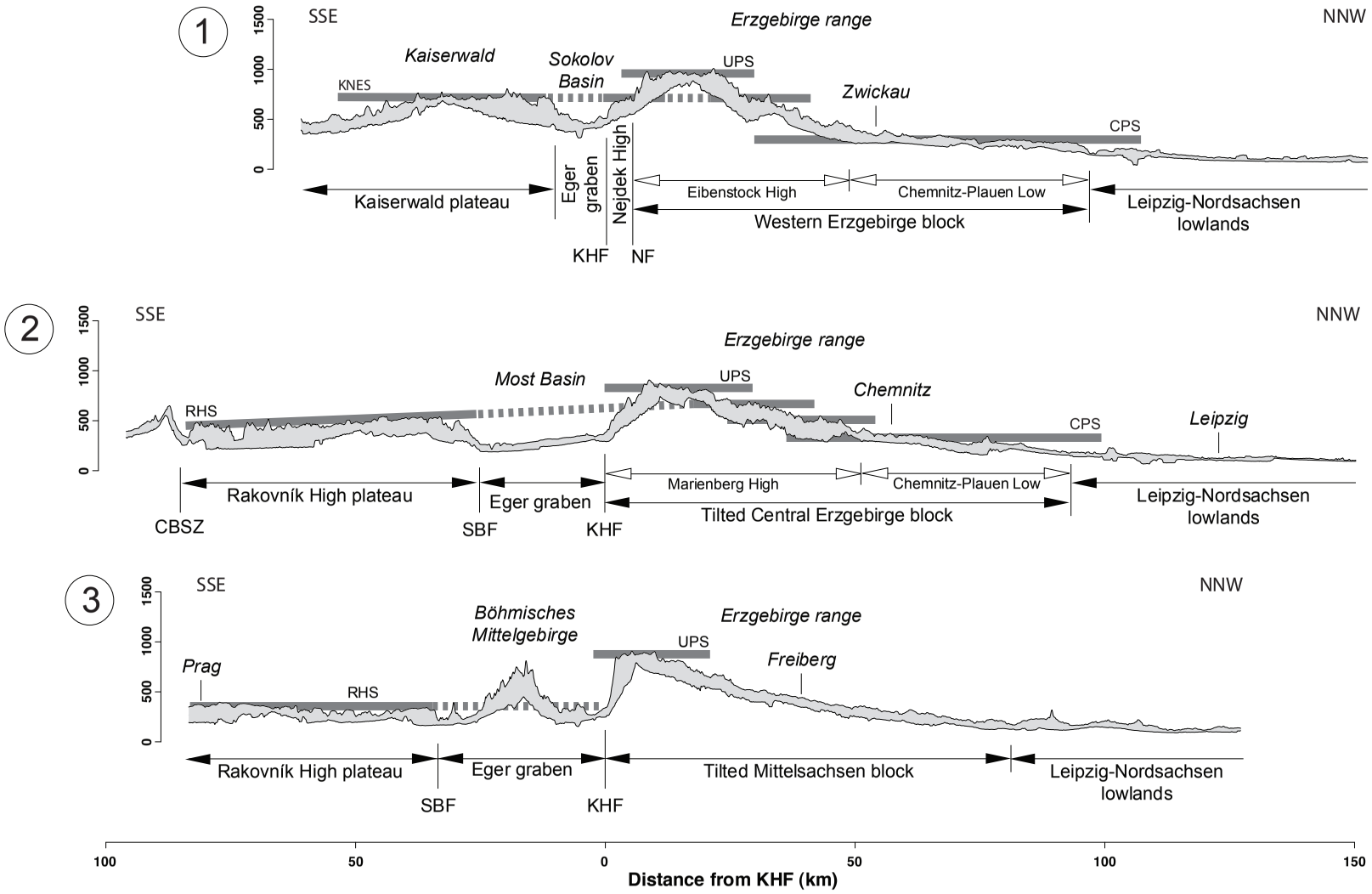


Fig. 5 – *Topographic swath profiles along the Erzgebirge-Eger graben system. See locations in Fig. 4. All profiles have the same horizontal and vertical scales with a vertical exageration of 20. Bold grey lines indicate inferred paleosurfaces. CPS - Chemnitz-Plauen surface, KNES - Kaiserwald, Nejdek and Eibenstock surfaces (possibly the same), RHS - Rakovník High surface, UPS - Uppermost surface. Main structures: CBSZ - Central Bohemian Shear Zone, KHF - Krušné hory fault, SBF - Southern Boundary fault, NF - inferred Nejdek fault.*

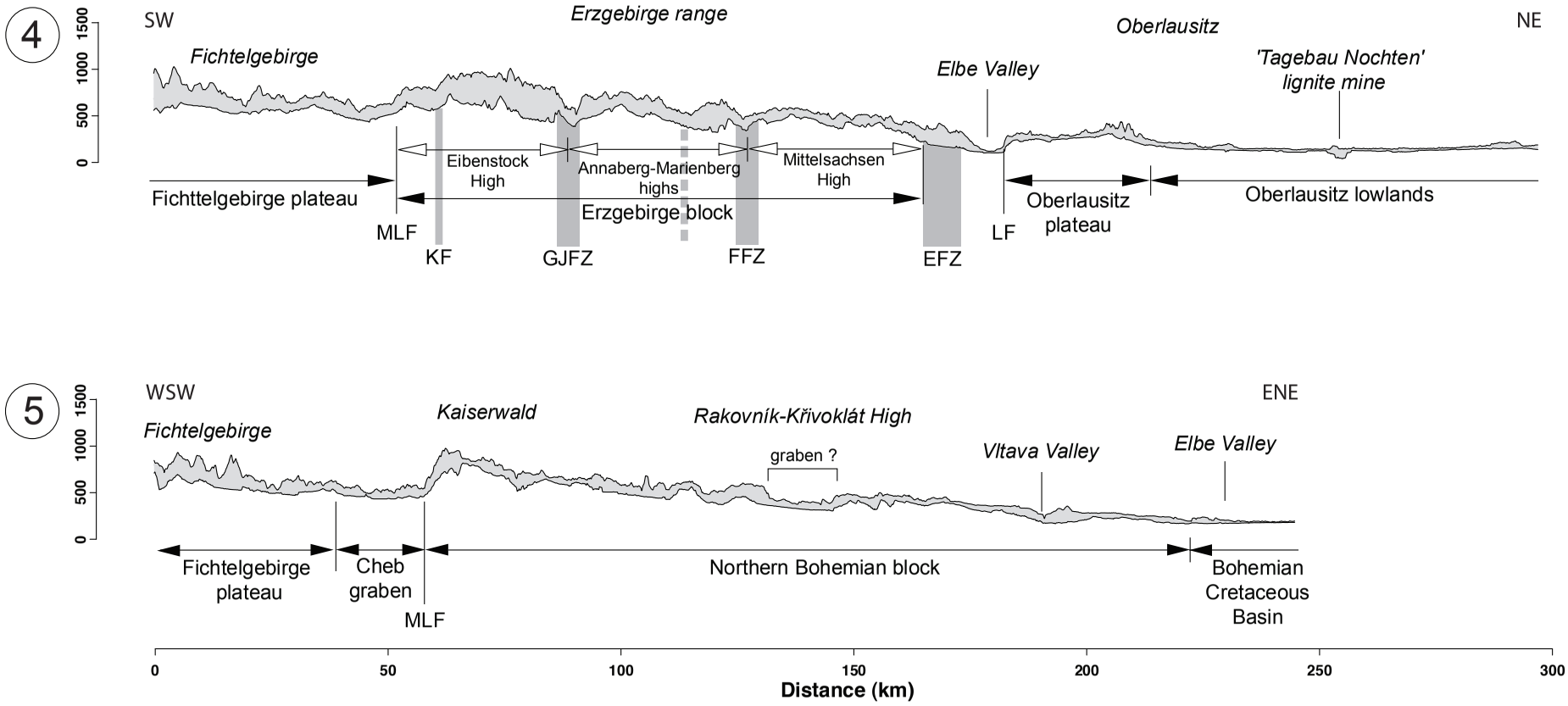


Fig. 6 – *Topographic swath profiles across the Mariánské-Lázně fault and Elbe Valley. See locations in Fig. 4. All profiles have the same horizontal and vertical scales with a vertical exageration of 20. Main structures: EFZ - Elbe fault zone, FFZ - Flöha fault zone, GJFZ - Gera-Jáchymov fault zone, KF - Klingenthal fault, LF - Lusatian fault, MLF - Mariánské-Lázně fault.*

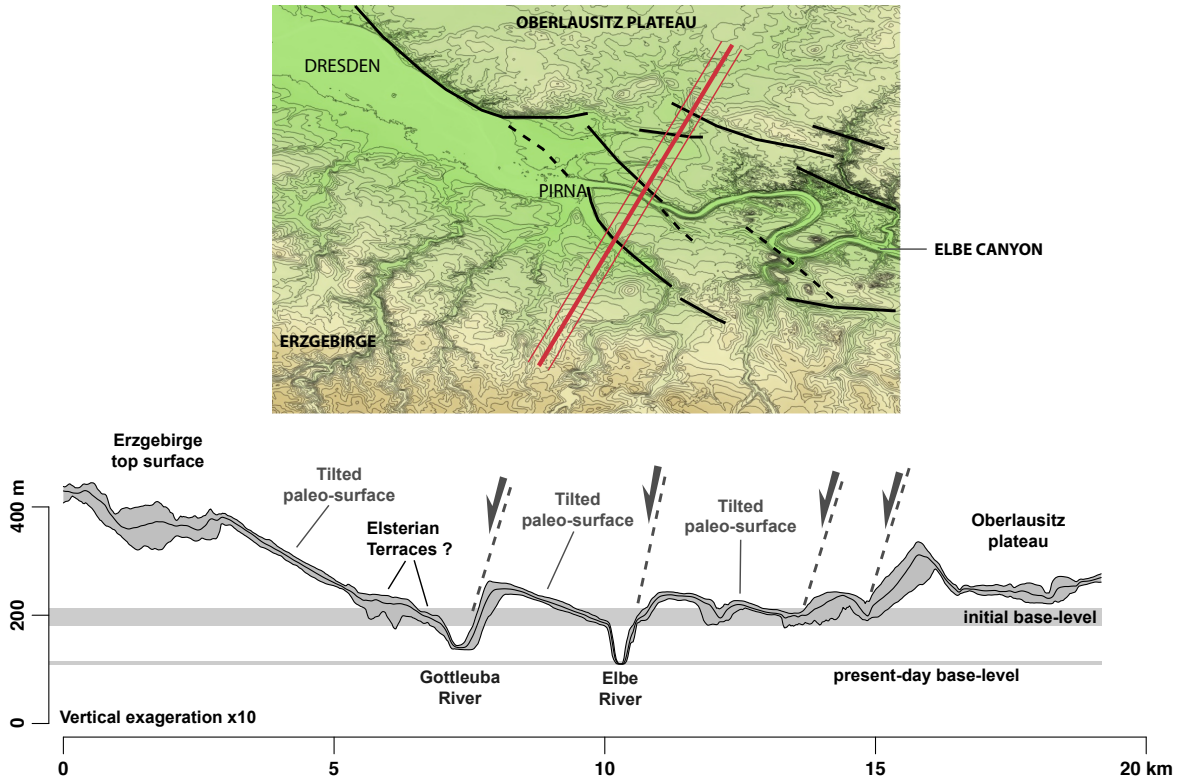


Fig. 7 – *Topographic swath profile showing tilted blocks and inferred normal faults across the Elbe valley east of Pirna (western end of the Elbe canyon).*

### *4.1.2. Mariánské-Lázně fault system and Elbe valley*

Profiles 4 and 5 (Fig. 6, location in Fig. 4) are transverse to previous profiles. They show the main topographic features between the Mariánské-Lázně fault system and the Elbe valley for the Erzgebirge range (profile 4) and the Bohemian plateaus (Kaiserwald and Rakovník High, profile 5).

Both profiles show a similar trend. West of the Mariánské-Lázně fault system (Fichtelgebirge and Cheb basin) the topography is relatively constant with elevations above ~500m. The Mariánské-Lázně fault is marked by a ~500m high topographic scarp in profile 5. The depression related to the Cheb half-graben is poorly marked. In profile 4 the western edge of the Erzgebirge block is affected by two major faults (Mariánské-Lázně and Klingenthal faults).

Areas located between the Mariánské-Lázně fault system and the Elbe valley appear to be gently tilted toward the East. In profile 5 the main trend is slighly concave with a stronger tilt close to the Mariánské-Lázně fault (Kaiserwald) and then a more gentle tilt within the Rakovník High. In profile 4 the main trend is disrupted by deep river incisions corresponding to major NW-trending structures (e.g., Gera-Jáchymov and Flöha fault zones) and by the incision of the Elbe river between the Elbe fault zone and the Lusatian Fault. The Lusatian fault itself is bounded to the East by the 30km wide Oberlausitz plateau. The difference between minimum and maximum elevations suggests a strong incision by the drainage network in the Fichtelgebirge range and Eibenstock High (western Erzgebirge). By contrast, the central part of the Mittelsachsen High and the Oberlausitz plateau appear less incised.

Fig. 7 displays a topographic profile between the Erzgebirge range and the Oberlausitz plateau. In areas surrounding Pirna several surfaces are well identified by spaced topographic contours. The topographic

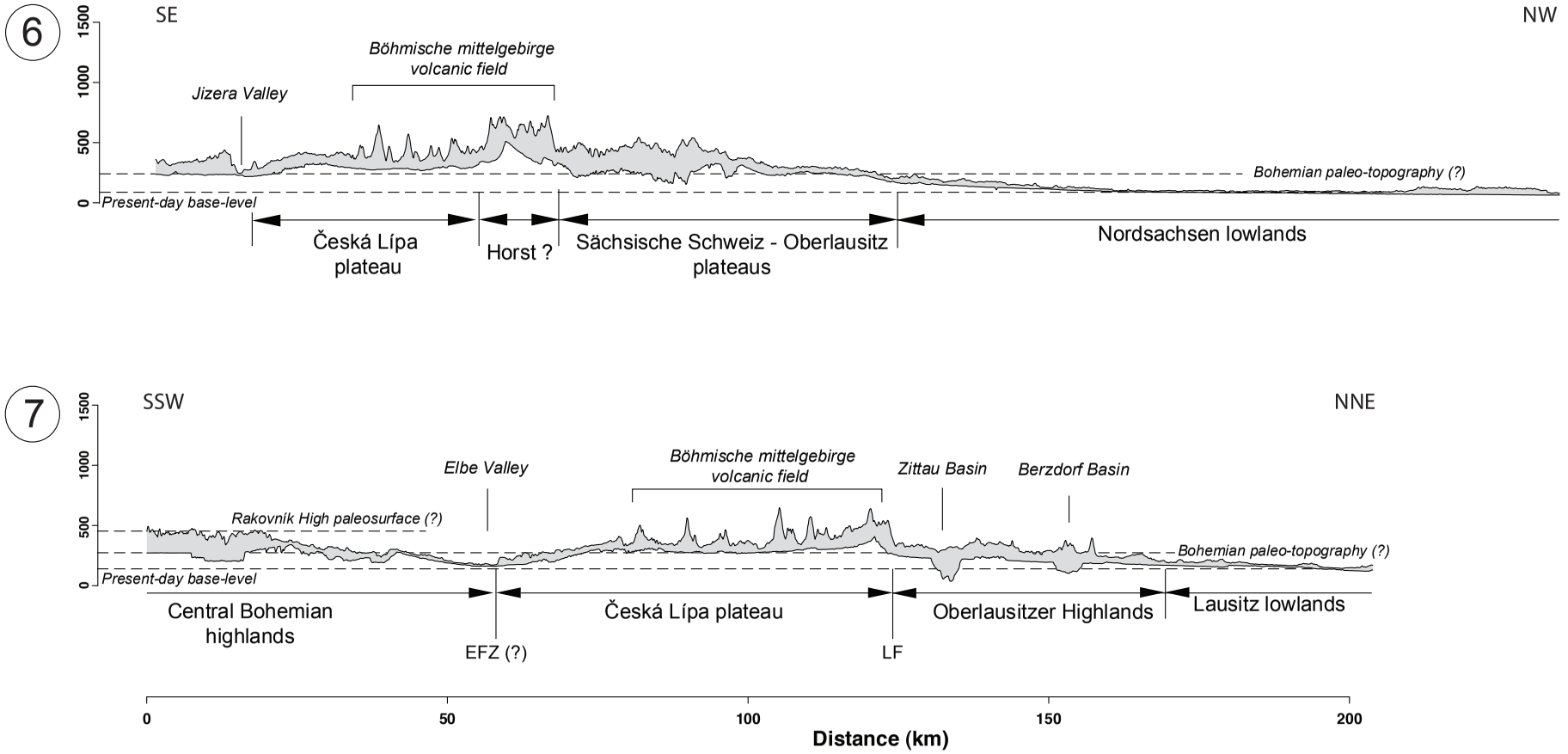


Fig. 8 – *Topographic swath profiles across the Lusatian region. See locations in Fig. 4. All profiles have the same horizontal and vertical scales with a vertical exageration of 20. Main structures: EFZ - Elbe fault zone, LF - Lusatian Fault.*

profile in Fig. 7 suggests that most of these surfaces may in fact represent a single one which is tilted along inferred NW- to E-trending normal faults. We also observe two main levels of incisions by the rivers. The highest one is probably related to a relict base-level while the lower one (reached by the Gottleuba and Elbe rivers) represent the present-day base-level.

#### *4.1.3. Česká Lípa plateau and Lusatian Highlands*

Profiles 6 and 7 (Fig. 8, location in Fig. 4) are located in the eastern regions (Lusatian highlands and Česká Lípa plateau). If we except volcanic centers, both profiles show similar elevations (ranging between 250 and 350m) for the Česká Lípa plateau south of the Lusatian Fault and for Oberlausitz plateau and Lusatian Highlands located north of the Lusatian Fault. These three units possibly formed a paleo-topographic high. The curves for minimum elevations suggest a relict base-level which is now located 100 to 150 m above the present day base-level corresponding to the Nordsachsen and Lausitz lowlands. The paleo-topography is disrupted by an elevated portion of the Böhmische Mittelgebirge (perhaps related to a horst-like structure) in profile 6 and by a scarp related to the Lusatian Fault in profile 7.

East of the Česká Lípa plateau the Elbe river has incised this paleo-topography and has almost the same elevation than the Nordsachsen lowlands (profile 7 in Fig. 8). The base-level of rivers located in the Česká Lípa plateau corresponds to the one located in the Central Bohemian Highlands (see minimum elevations in profile 7). However, rivers in Central Bohemian Highlands have incised a paleosurface (referred as "Rakovník High paleosurface" in profile 7) which can be observed in maximum elevations.

### *4.2. Morphometric maps and analysis of surfaces*

#### *4.2.1. Topographic position index*

The topographic position index (TPI, Fig. 9) provides a map of major topographic scarps and incisions by the drainage network. It also allows to characterize the topographic expression of main faults and to compare incisions between different drainage systems.

The observed pattern in TPI values is clearly controlled by the structural setting. Low TPI values associated to valleys show four preferential directions: ~N050°(related to the Eger graben and Central Bohemian shear zone), N135°to N155°(related to several mapped lineaments such as the Mariánské-Lázně, Flöha or Gera-Jáchymov fault zones), N350°to N010°(mainly defined by linear rivers in the central part of the Erzgebirge range) and N080°to N100°(defined by local alignement of rivers in the western part of the Ergebirge and Oberlausitz/Česká Lípa plateaus). The Krušné Hory fault scarp located along the northern border of the Eger graben is particularly well defined by the juxtaposition of extremely high (>150) and low (< -150) TPI values. The southern rim of the Eger graben is well delimited within the Sokolov depression while its topographic expression is clearly attenuated in the Most depression. The Mariánské-Lázně fault scarp is also well defined. It delimitates the Kaiserwald plateau and the Erzgebirge range to the west and its trace can be followed to the SE of Plauen.

The intensity of negative TPI values reflects both the geometry of the valleys and the degree of incision of the surrounding topography by the drainage network. The Elbe river and its tributaries are deeply entrenched (TPI $\leq$ -100) in the areas encompassing the Sächsische Schweiz and the Böhmisches Mittelgebirge. Most of the Elbe river downstream of Meißen and upstream of the Böhmisches Mittelgebirge show moderate incision (TPI values between 0 and -50). The drainage network upstream from Prag

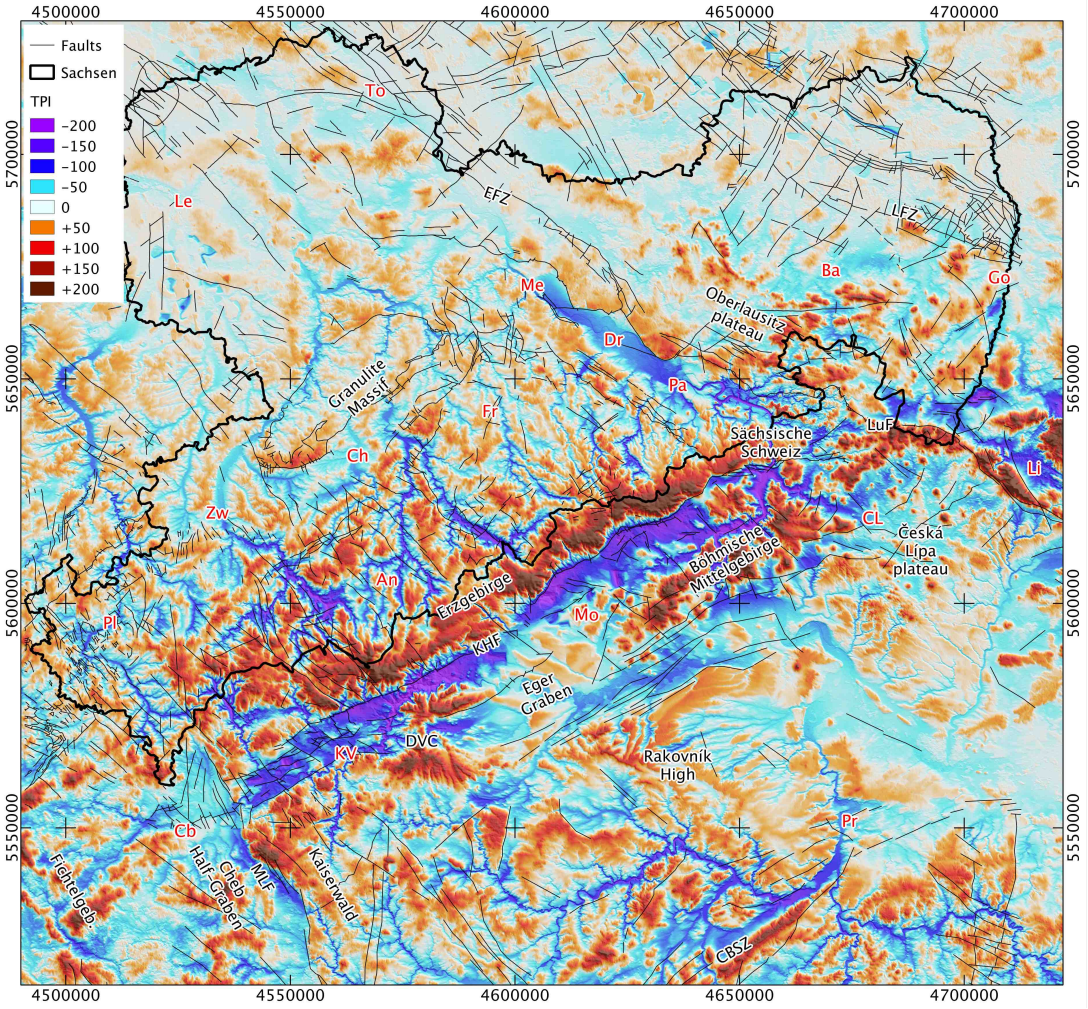


Fig. 9 – *Topographic position index (see explanations in section 3.1.) calculated using a 100 pixels (~9 km) moving window. See Fig. 4 for structures and cities abbreviations.*

(Berounka, Vltava and Sázava rivers) and Karlovy Vary (Teplá river) are also deeply entrenched as suggested by narrow valleys and TPI values lower than -100. The upper part of the Mulde drainage system in the Erzgebirge is deeply entrenched between the the Mariánské-Lázně and Flöha fault zones. By contrast rivers in the eastern Erzgebirge (between the Flöha fault zone and the Elbe valley) display lower (Freiberger Mulde) or moderate (tributaries of the Elbe) incisions.

### *4.2.2. Hypsometry*

The distribution of hypsometry in Saxony and NW Czech Republic (Fig. 10) closely follows two main structural trends associated to the ENE-trending Eger graben system and to the NW- to NNW-trending faults of the Mariánské-Lázně and Elbe fault systems.

The Eger graben is well outlined by low HI values (<0.35). Two main areas can be identified. The first one is approximately 70 km long and 30 km wide and encompasses the Most depression and the SW part of the Böhmisches Mittelgebirge (Northern Bohemian Uplands). Lowest HI values are located along the two flank of the Eger graben and mainly reflect the contrast between the Eger and Bílina rivers valleys and the rims of the Eger graben. In the central part of the Eger graben HI values increase up to 0.45. It is related to the moderate incision of graben floor deposits by the tributaries of the Eger river (e.g., Chomutovka river) and to the incisions of the Böhmisches Mittelgebirge. The second area corresponds to

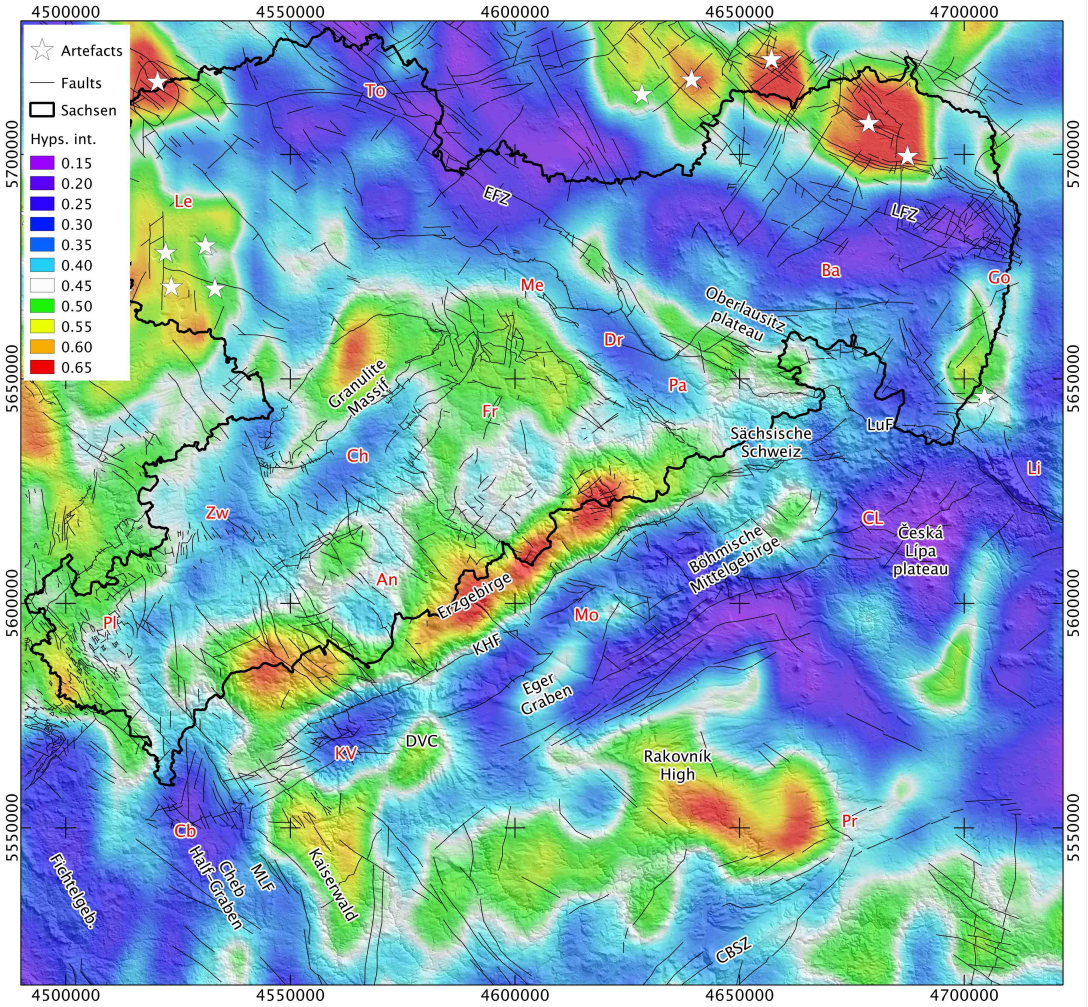


Fig. 10 – *Hypsometric integral (see explanations in section 3.1.) calculated using a 100 pixels (~9 km) moving window. See Fig. 4 for structures and cities abbreviations.*

---

the 40 km long and only 11 km wide Sokolov basin which is wedged between the Erzgebirge to the north, the Kaiserwald to the south and the Neogene Doupov volcanic complex to the east.

The rims of the Eger graben are marked by high HI values (>0.50). The southern rim is characterized by irregular and discontinuous hypsometric highs: from east to west the Rakovník-Křivoklátsko high (the largest one) located to the west of Prag, the Jecenice high located to the north of Plzeň and the Kaiserwald high located to the south of Karlovy Vary. These hypsometric highs correspond to a topography of deeply incised plateaus. Main rivers (e.g., Teplá, Střela, Rakovnický potok) crossing these areas are deeply entrenched with an average incision of ~100m with respect to surrounding plateaus (Fig. 9).

The hypsometric high corresponding to the northern rim of the Eger graben (Erzgebirge) is particularly well marked as it form a narrow and almost continuous band between 12.5°E and 14°E. High HI values (>0.5) are related to the topographic scarp formed by the Krušné Hory fault and to the relative flat top of the range which is deeply incised by entrenched rivers (Fig. 9). However, the hypsometric high located at the SW end of the Erzgebirge (north of the Sokolov depression) is located well afar from the Krušné Hory fault. This can be explained by the fact that the main elavation is produced not by the Krušné Hory fault but by the inferred E-trending Nejdek fault (see profile 1 in Fig. 5). Hypsometric highs are also disrupted along NNE- and NW-trending discontinuities possibly related to a structural control. For instance, the Marienberg hypsometric high (located to the east of Annaberg) is clearly delimited by the NW-trending

Flöha fracture zone to the east an by a NNE-trending hypsometric low to the west. This NNE-trending hypsometric low (Annaberg low) is associated to several parallel N-trending rivers and valleys and may be of tectonic origin.

Two hypsometric lows potentially related to ENE- to NE-trending structures are also highlighted. The first one is marked by a 80 km long and 10 to 15 km wide band of low HI values extending between Plauen and Chemnitz. It may correspond to a topographic contrast between the northern rim of the Erzgebirge and its relatively flat foreland. The second one is located south of the Berounka river between Plzeň and Prag, along the Central Bohemian Shear Zone.

The ENE to NE zonation of the central part of the area is disrupted to the SW by the Cheb half-graben and to the NE by the Elbe Fault Zone. The Mariánské-Lázně Fault Zone which marks the NE limit of the Cheb half-graben separate an area with low HI values corresponding to the Cheb and Bor-Domažlice basins from the Erzgebirge and Kaiserwald hypsometric highs. The Elbe valley is marked by an hypsometric low between Meißen and Pirna. In this area, the Elbe valley is bounded to the south by an hypsometric high which encompass the Granulite Massif and the area between Freiberg and Meißen. These two areas correspond to a gentle topography moderatly incised by rivers (50 to 60m, Fig. 9). The hypsometric high located along the northern flank of the Elbe valley is aligned in a NW direction. It corresponds to the western border of the Oberlausitz plateau which is separated from the Elbe valley by the NW-trending Lauzitzer fault.

Hypsometric integral values in northen saxony are low and reflect a gentle topography with moderate incisions (Fig. 9). All the hypsometric highs marked by stars in Fig. 10 (region of Lepzig, north of Bautzen and south of Görlitz) are artefacts resulting from mining activities.

#### *4.2.3. Surface roughness*

Surface roughness (Fig. 11) appears to be strongly influenced by river incisions. Extreme values (> 1.01) are concentrated along two main areas. The first one corresponds to the Elbe canyon (the portion of the Elbe river between Bad Schandau and Ústí nad Labem) and reflects high incision by the tributaries of the Elbe river in this area. The second SR peak is located between the Doupov volcanic complex and the western part of the Erzgebirge range. This area corresponds to the highest portion of the Erzgebirge range with elevations above 1200m. To the south (along the Eger graben fault scarp) the Eger river is jammed between the Erzgebirge range and the Doupov volcanic complex and forms a deeply entrenched canyon (Fig. 9). High SR values in this area result thus from the topographic contrast between the elevated part of the Erzgebirge range (up to 1200m) and the narrow Eger valley (~300m). In a similar way incisions along the Weiße Elster (north of Plauen), Teplá (south of Karlovy Vary) and Moldau-Berounka rivers and their tributaries (SW of Prag) produced relatively high SR values (1.004 to 1.008).

SR values along the Erzgebirge display a complex pattern. This pattern is influenced by river incisions but also reveals a potential structural control. We can define three main regions delimited from east to west by the Elbe fault zone, the Flöha fault zone, the Gera-Jáchymov fault zone and the Mariánské-Lázně fault system. Each of these fault zones mark a discontinuity in the surface roughness map. We also note a substantial decrease in SR values from SW to NE. The western region between the Gera-Jáchymov and the Mariánské-Lázně fault zones show high SR values (1.008 to 1.010) related to incisions along the upper segments of the Zwickauer Mulde and the Svatava (Fig. 9). The central area between the Flöha and Gera-Jáchymov fault zone show moderate values (~1.006) related to the Preßnitz river and its tributaries.

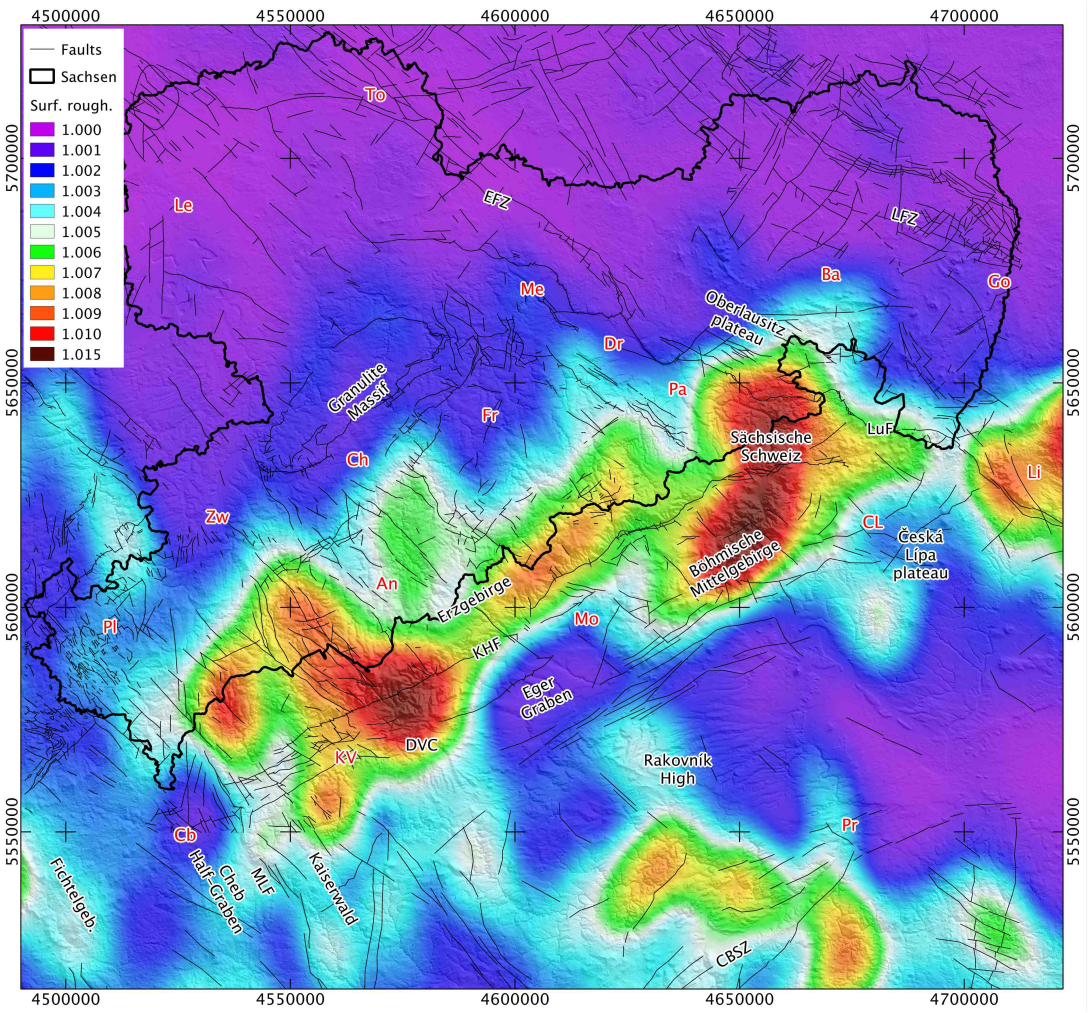


Fig. 11 – *Surface roughness (see explanations in section 3.1.) calculated using a 100 pixels (~9 km) moving window. See Fig. 4 for structures and cities abbreviations.*

Finally east of the Flöha fault zone most of the high SR values are located along the southern rim of the Erzgebirge and can be explained by the topography of the Erzgebirge range rather than a strong incision by the tributaries of the Mulde river (Fig. 9).

Most of the areas located in northern Saxony display low SR values indicating a gentle topography with moderate incisions (SR<1.003, Granulite Massif, area between Freiberg and Meißen) or flat areas (SR<1.001, northern Oberlausitz, regions of Leipzig, Torgau and Bautzen). In NW Czech Republic the Most depression and Bohemian Cretaceous Basin are well outlined by extremely low SR values (<1.001).

### *4.2.4. Surface index*

The surface index (SI, Fig. 12) classify the landscape using both hypsometric integral and surface roughness and allows thus to observe more clearly the pattern of preserved and eroded regions (see section 3.1. for more details).

Most of the areas located in northern Saxony appear as a steady-state topography. As indicated by SI values between -0.05 and 0.05, these areas are extremely flat and poorly incised by the drainage network. For instance, there is no effects of the Elbe river on SI values downstream Meißen.

By contrast, the Erzgebirge mountains are locally deeply incised by the drainage network. Positive SI values correspond to flat or tilted surfaces observed in Fig. 5. These areas can be considered as the

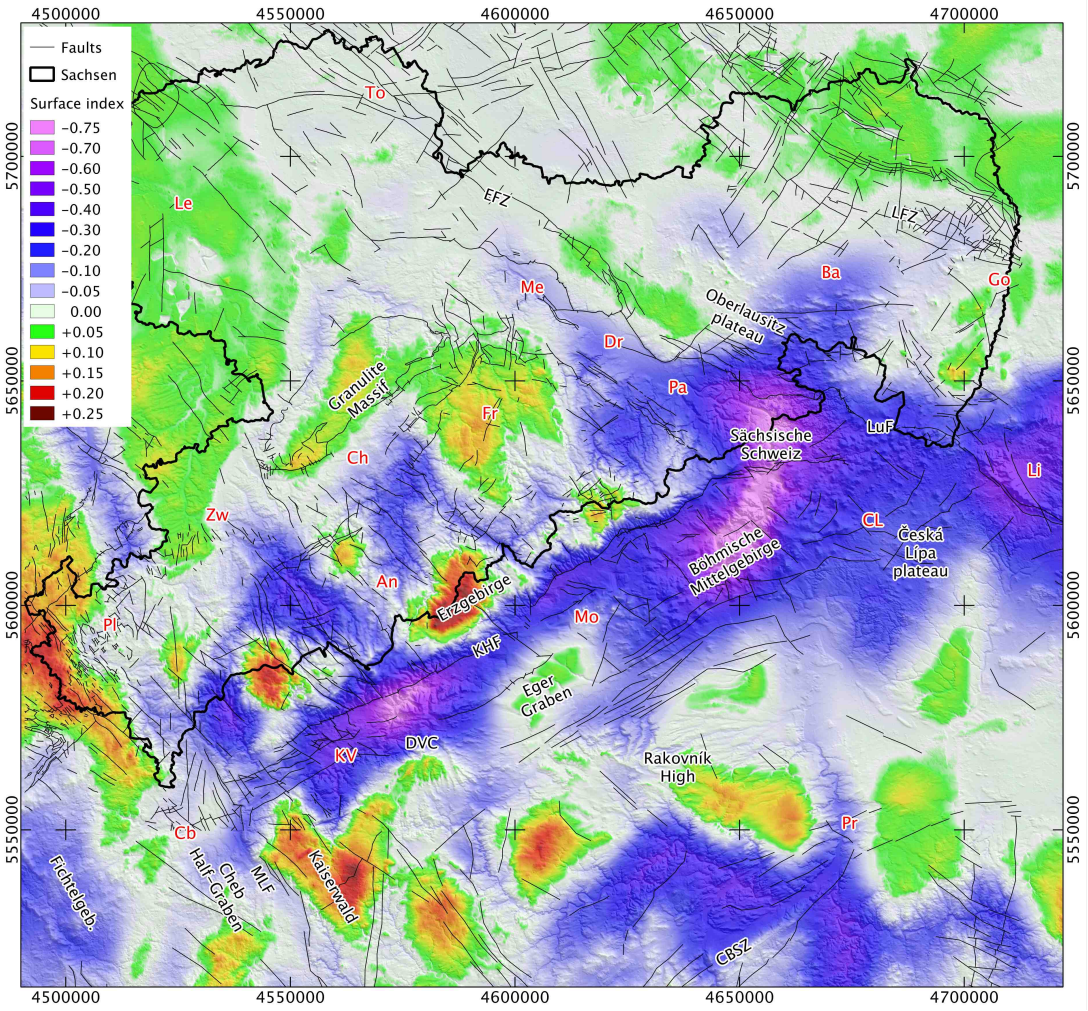


Fig. 12 – *Surface index (classification of landscapes using hypsometric integral and surface roughness, see explanations in section 3.1.). Structures and cities abbreviations are provided in Fig. 4.*

relicts of an initially flat landscape which is now significantly elevated above the present-day regional base-level. The uppermost paleosurface ("UPS" in Fig. 5) is represented by small patches of positive SI values located along the border between Saxony and Czech Republic. The higher topographic position of this surface is marked by SI values above 0.2, especially in Marienberg and Eibenstock highs. The Chemnitz-Plauen low as well as the tilted surface in Freiberg area are represented by lower values (between 0 and 0.15). These surfaces are also relatively well preserved but located at a lower elevation. Negative SI values reveals strong incisions of these surfaces by the drainage network. These incisions result from a disequilibrium in topography related to a base-level change. SI values suggest a stronger incision of the Erzgebirge region south of a line between Plauen and Dresden. These strong incisions results from the sharp topographic contrast between the uppermost paleosurface and the Chemnitz-Plauen surface (Fig. 5). Areas located north of the Plauen-Dresden line are less incised as the difference in elevation between the Chemnitz-Plauen surface and the present-day steady-state topography is less important.

Areas located within the Eger rift are dominated by erosional processes as indicated by negative SI values. The canyon of the Elbe across the Böhmisches Mittelgebirge and the entrenched portion of the Eger river between the Sokolov depression and the Most basin correspond to extremely deep incisions. The Most basin is the only area within the Eger rift which displays a relatively well preserved surface. On the southern rim of the Eger rift several surfaces identified by positive SI values are also well preserved

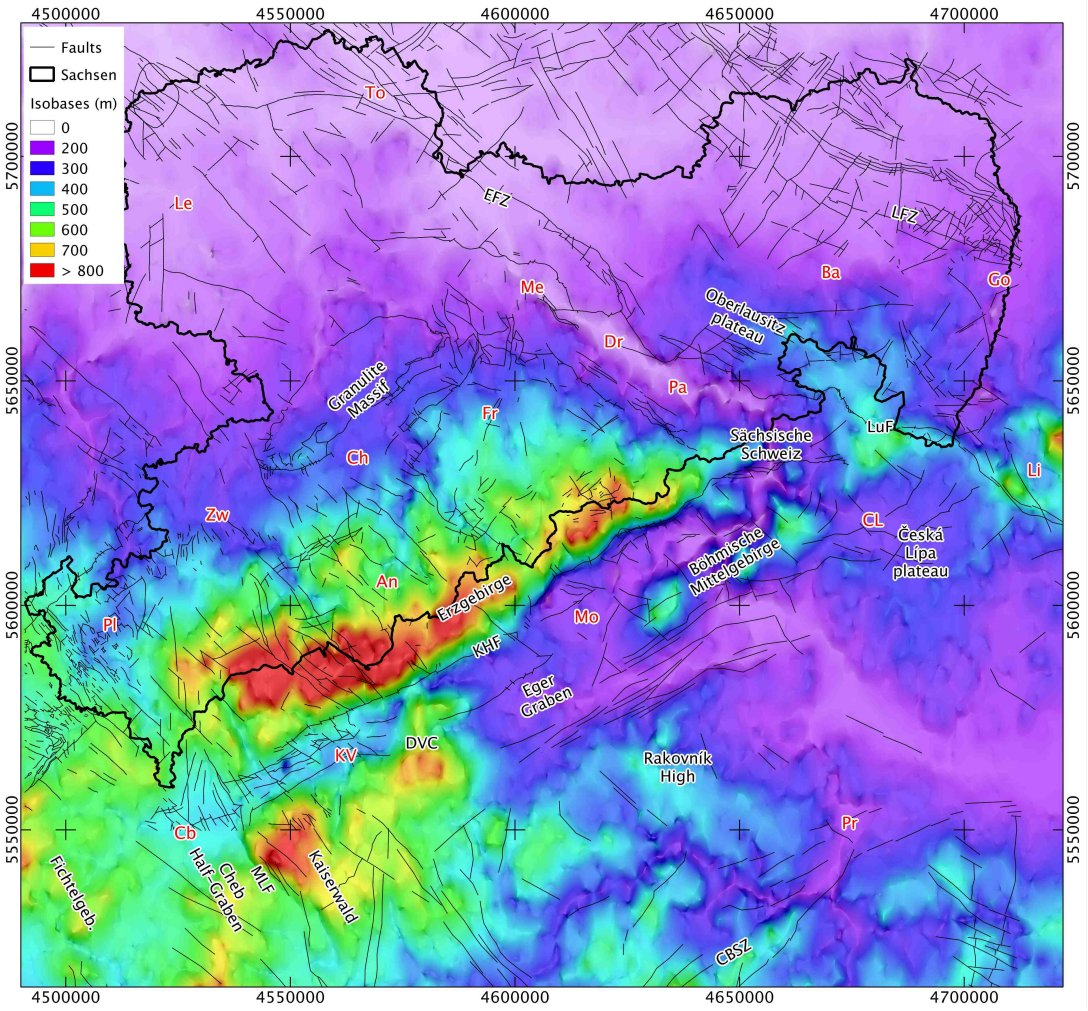


Fig. 13 – *Isobases from rivers (interpolation of streams height using natural neighbour method, Sibson, 1981). See Fig. 4 for structures and cities abbreviations.*

(see Rakovnik and Kaiserwald surfaces in Fig. 5). These surfaces are heavily eroded to the south by the Berounka and Vltava drainage systems.

## *4.3. Analysis of the drainage network*

### *4.3.1. Isobases from rivers*

Isobases (Fig. 13, interpolation of streams and rivers heights) provide an overview of the base-level for the main rivers in Saxony and NW Czech Republic. The isobasic surface is strongly affected by the Eger graben. There is a sharp contrast between the Eger graben floor in the Most depression and the Erzgebirge range. The southern flank of the Sokolov depression (Kaiserwald area) and the Mariánské-Lázně fault system also affect the isobase surface. The rest of the isobase surface displays several flat areas roughly corresponding to two successive base-levels. The first one is the present day base-level (elevations < 150m) and correspond to the areas located in northern Saxony (Nordsachsen and Oberlausitz lowlands) and along the Elbe river (violet colors in Fig. 13). The second one is what we suggest to be an older base-level occupying a higher position (between 250 and 400m in Fig. 13) with respect to the present day one. It is largely preserved in the eastern regions of the Central Bohemian Highland (e.g., Rakovník High) as well as in the areas corresponding to the Ceská Lípa plateau and Lusatian highlands. A few remnants of this base level are preserved along the northern flank of the Erzgebirge mountains, along an axis going

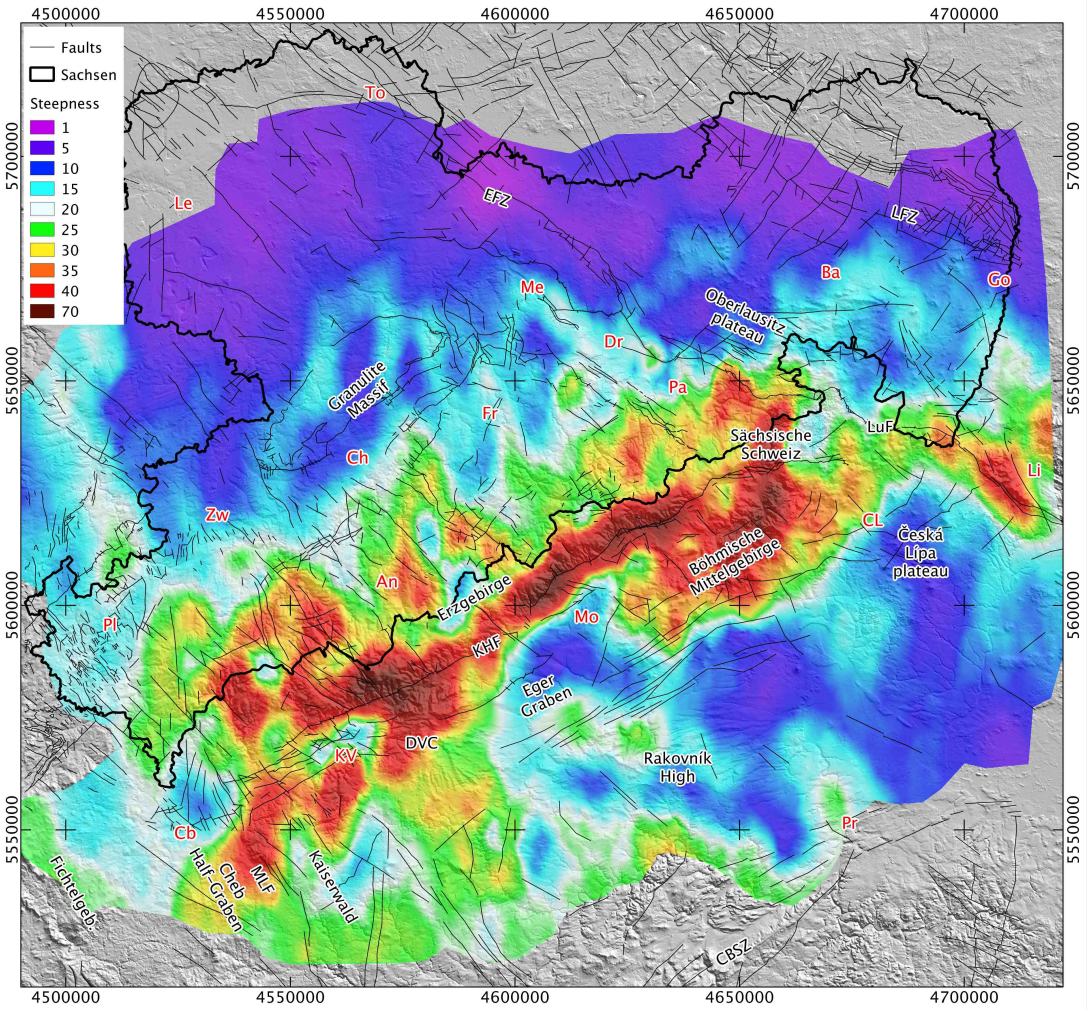


Fig. 14 – *Interpolated map of steepness indices ($k_{sn}$, see section3.3.). See Fig. 4 for structures and cities abbreviations.*

from Plauen to Freiberg. The area located west of the Mariánské-Lázně fault system (Fichtelgebirge and Cheb depression) form an homogenous base-level at ~500m. Finally, the highest isobases values are found along the Krušné Hory fault and in the Kaiservald area and can be associated with identified paleo-surfaces (see "Uppermost paleosurface" and "Kaiserwald-Nejdek-Eibenstock surface" in Fig. 5)

The areas corresponding to the transition between two base levels are marked by an higher incision by the rivers (and by an increase in surface roughness values as described in previous section) as the rivers adjust to the present-day base level. For example the lower part of the Vltava-Berounka river system is strongly entrenched between Plzeň (which is located in the upper base-level surface) and the region of Prag (corresponding to the present day base-level). The incision of the Česká Lípa-Lusatian highlands is also well marked in Fig. 11 and correspond to the difference between the present-day base-level already reached by the Elbe river and the relict base level of the surrounding plateaus.

### *4.3.2. Steepness index*

We manually extracted $k_{sn}$ values from ~17000 segments belonging to more than 3000 streams and rivers. Stream segments containing individual $k_{sn}$ values were converted to points. Fig. 14 displays the result of the interpolation using an inverse distance weighting scheme.

Highest $k_{sn}$ values are mainly distributed along the Eger graben. Peak values ($\geq$70) are found along the Krušné Hory fault scarp and in tributaries of the Elbe river located in Sächsische Schweiz and

Böhmisches Mittelgebirge. These peak values reflect fast incisions which are associated either to high uplift rates along the Krušné Hory fault or to a rapid fall of the regional base-level.

The $k_{sn}$ values reflect the complexity of the tilted areas located between the Krušné Hory fault and the Chemnitz-Plauen low (see Fig. 5). Low $k_{sn}$ values in Marienberg High and Velký močál area (on top of the Eibenstock block) are associated to the paleo-surfaces observed in swath profiles 1 to 3 (Fig. 5). These low $k_{sn}$ values are found in the uppermost segments of river profiles and suggest that relict base-levels corresponding to an antecedant flat and low topography are still locally preserved. Lower segments of main rivers (e.g., Zwickauer Mulde, Zschopau, Flöha) and their tributaries display higher $k_{sn}$ values (25 to 50) which indicate a disequilibrium in river profiles and relatively strong incisions within the central and western portions of the Erzgebirge mountains. By contrast most of the areas located between the Flöha fault zone and the Elbe valley (referred as Mittelsachsen block in Fig. 5) show lower $k_{sn}$ values. It suggests that the initial topography of this region is still largelly preserved. $k_{sn}$ values along the Freiberger Mulde and its tributaries does not exceed 25 and reflect lower incisions than in central and western Erzgebirge mountains. On the other hand, tributaries of the Elbe river (east of the Weißeritz river) show greater values (up to 40) and reflect thus a strong disequilibrium possibly resulting from the capture of these rivers by the Elbe drainage system.

Most of the areas located north of the Erzgebirge mountains display $k_{sn}$ values lower than 25. Values below 10 mainly found in Nordsachsen and Oberlausitz lowlands indicate extremely flat areas with low incisions by the drainage network. Flat areas associated to low $k_{sn}$ values are also found in the foreland of the Erzgebirge (e.g., Oberlausitz plateau, Chemnitz-Plauen low). However, $k_{sn}$ values between 15 and 20 found along main tributaries of the Mulde and Weiße Elster rivers suggest that these flat surfaces are located slightly above the present day base-level and are now being gently eroded by the drainage network.

Areas located south of the Most depression and Böhmisches Mittelgebirge display low $k_{sn}$ values which also indicate flat areas with low incisions by the drainage network. T he Česká Lípa plateau as well as the Bohemian Creataceous Basin and Rakovník High are highlighted by extremely low values ($\leq$10) which make a strong contrast with the Böhmisches Mittelgebirge and Lusatian fault areas. However, as for the Oberlausitz plateau and Chemnitz-Plauen area, $k_{sn}$ values between 15 and 20 found around the Česká Lípa plateau and Rakovník High suggest that these surfaces are not in equilibrium with the present-day base-level.

Finally, areas located south of the Sokolov depression and Doupov Volcanic Complex display mainly high $k_{sn}$ values (25 to 40). As in the Erzgebirge low $k_{sn}$ values (<20) are found locally and indicate relict base-levels corresponding to an antecedant flat and low topography. However, higher $k_{sn}$ values along main rivers (e.g., Teplá) clearly indicate that this antecedent topography is well above the present-day regional base-level and that it is now being eroded. A flat area located between the Mariánské-Lázně fault system and the Fichtelgebirge range and partly corresponding to the Cheb depression is highlighted by low $k_{sn}$ values (<20). This flat region is possibly continuous with the Chemnitz-Plauen low topography observed on the northern flank of the Erzgebirge mountains.

#### *4.3.3. River longitudinal profiles*

We analyzed the profiles of the main tributaries of the Elbe river in the Erzgebirge and Sächsische Schweiz areas. Representative river profiles and analyses for major rivers are displayed in appendices I

(tributaries of the Elbe river) and II (rivers in the Erzgebirge range). River profiles and relict base-levels interpretation is summarized in Fig. 15. The geometry of river profiles within the considered area is not uniform. Indeed, each domain defined using swath topographic profiles (Fig. 5) and geomorphic maps (Fig. 10 to 14) is associated to a specific geometry: (1) Eastern Elbe valley (Oberlausitz plateau and Sächsische Schweiz), (2) Western Elbe valley, (3) Mittelsachsen block, (4) Central Erzgebirge block and (5) Western Erzgebirge block.

*1/ Eastern Elbe valley:*

This region is characterized by a flat topographic surface in the north (Oberlausitz plateau) and by the more mountainous Sächsische Schweiz landscape in the south. Both areas are deeply incised along the Elbe river canyon. Although these two areas seem to be different from a geomorphological point of view, their river profiles show significant similarities. Most of the tributaries located on the eastern side of the Elbe river are characterized by a smooth concave upper segment corresponding to a relict base-level (noted "b.l.1" in Fig. A1.2 to A1.7). Best-fitting concave curves suggest that this base-level is located approximately between 100 and 135m above the present-day base-level of the Elbe river (see the offsets between the best-fitting curves and the actual rivers profiles in Fig. A1.2 to A1.7). The elevation of this relict base-level seems to decrease toward the north perhaps as the result of a regional tilt.

The relict base-level observed in upper parts of the rivers is connected to the Elbe river by steeper segments (for example "b.l.2" and "b.l.3" in Fig. A1.3). These transient segments are characterized by higher $k_{sn}$ values (30 to 50) than the upper part of the rivers ($\leq$15). These abnormally steep segments are also associated to peaks in stream length-gradient values (SL index higher than 250 in Fig. A1.2 to A1.7).

*2/ Western Elbe valley:*

The second region corresponds roughly to the areas located between the Weißeritz river to the West and the Elbe river to the East and between the Krušné-Hory fault to the South and Dresden to the North (profiles in Fig. A1.8 to A1.11). We identified a relict base-level with an elevation of 100m to 150m (noted "b.l.1" in Fig. A1.8 to A1.10). This base-level is similar to the one found in Oberlausitz plateau and Sächsische Schweiz areas. However, $k_{sn}$ values associated to this base-level are relatively high for the Biela ($k_{sn}$=44 in Fig. 1.8) and Gottleuba ($k_{sn}$=40 in Fig. 1.10) rivers. These values may reflect a disequilibrium resulting from the tilting of the Erzgebirge mountain. The same base-level is unaffected and possibly still in its initial position close to the Elbe river (see the Struppenbach stream profile in Fig. A1.9) as suggested by a $k_{sn}$ value of 12.

The Weißeritz river (Fig. A1.11) displays three main segments (noted "b.l.1" to "b.l.3") separated by knickpoints. Knickpoints can be easily identified by peak values in both SL and SA indices. These segments show high $k_{sn}$ values and may also reflect a disequilibrium resulting from the tilting of the Erzgebirge mountain. Base-levels 1 and 2 may be equivalent to those found in other rivers such as the Kirnitzsch (Fig. A1.2) or the Sebnitz (Fig. A1.3). However, reconstructions of these base-levels for the Weißeritz river may be inaccurate as the curves intercept the river profile. The base-level 3 is the highest one and roughly corresponds to the uppermost surface observed in swath profile 3 (Fig. 5). Reconstruction of this base-level suggests an offset of ~400m with respect to the present-day base-level of the Elbe river.

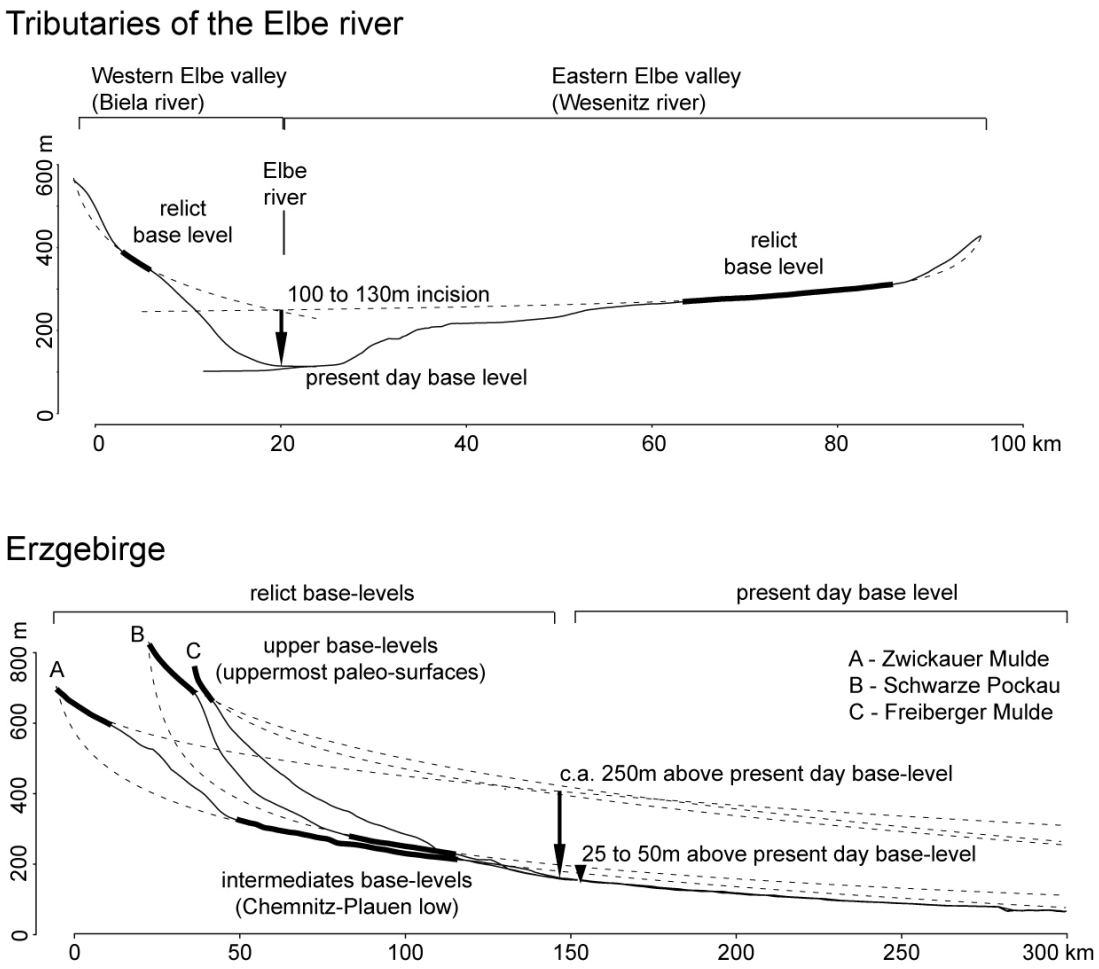


Fig. 15 – *Summary of interpreted relict base-levels in the Elbe valley and Erzgebirge range. Bold lines highlight relict base-levels. Dashed lines show the reconstructed profile based on corresponding relict base-level.*

---

Downstream tributaries of the Elbe river (Triebisch river in Fig. 1.12 and Ketzerbach stream in Fig. A1.13) also display an upper relict base-level noted "b.l.1". However, reconstructed profiles suggest a minor offset ($\leq$15m) between this relict base-level and the present-day base-level of the Elbe river. SL indices associated to knickpoints as well as $k_{sn}$ values gradually decrease toward the north. This area corresponds to the northernmost extend of the tilted Erzgebirge block.

*3/ Mittlesachsen block:*

The Mittlesachsen block is incised by two main rivers: the Freiberger Mulde (Fig. A2.1) and the Flöha (Fig. A2.3). The profiles of these two rivers are similar. Both profiles display an uppermost relict base-level (noted "b.l.1"), intermediate relict base-levels (noted "b.l.2" and "b.l.3") and a lower base level (noted "b.l.4") corresponding to the present-day regional base level (Nordsachsen lowlands). Relict base-level 1 roughly corresponds to the uppermost surface observed in swath profile 3 (Fig. 5). Low $k_{sn}$ values (~20) suggest that this part of the drainage system is still in steady-state although it is elevated between 700 and 800m. Reconstructed profiles suggest an offset of ~200m with respect to the present-day base-level. Intermediate base-levels display slightly higher $k_{sn}$ values (25 to 35) which may indicate a transient stage. These segments are separated from the lowermost base-level by a prominent knickpoint highlighted by a sharp peak in SL index. According to reconstructed profiles this knickpoint is associated to an incision of ~30m between the base-levels 3 and 4.

*4/ Central Erzgebirge (Marienberg block):*

The Schwarze Pockau (upstream segment in Fig. A2.4) is a tributary of the Flöha river located within the Marienberg high (see swath profile 2 in Fig. 5). It displays an upper relict base-level (noted "b.l.1"in Fig. 2.4) similar to the one found in the Freiberger Mulde (Fig. A2.1) and Flöha (Fig. A2.3) rivers. However, it is separated from lower base-levels by a steeper segment ($k_{sn}$=52).

The Zschopau (Fig. A2.6) and Jöhstädter Schwarzwasser (Fig. A2.5) river profiles are similar to the eastern tributaries of the Freiberger Mulde river. However, their uppermost segments are steeper ($k_{sn}\geq$30). These higher $k_{sn}$ values suggest that the corresponding portions of the drainage network are not in steady-state and reconstructions of relict base-levels may thus be inaccurate. For instance, reconstruction for the Jöhstädter Schwarzwasser uppermost base-level (noted "b.l.1" in Fig. A2.5) suggest an offset of only ~150m while it is over 300m for other profiles. This is mainly due to abnormally high steepness of this segment. The Zschopau (Fig. A2.6) and Jöhstädter Schwarzwasser (Fig. A2.5) display an intermediate base-level (noted "b.l.2" in Fig. A2.5) corresponding to the Chemnitz-Plowen low (swath profile 2 in Fig. 5). This intermediate base-level is separated from the present-day lower base-level (noted "b.l.3" in Fig. A2.5) by a knickpoint associated to a minor incision (~50m).

The Zwönitz (Fig. A2.8) and Würschnitz (Fig. A2.9) rivers are tributaries of the Zwickauer Mulde. The Zwönitz river displays an uppermost base-level (noted "b.l.1" in Fig. A2.8) corresponding to a relict surface (Annaberg High). This base-level is separated from an intermediate base-level (noted "b.l.2" in Fig. A2.8) by a smooth knickpoint. Reconstructions of profiles show an offset of less than 25m between both base-levels. The intermediate base-level is also observed in Zschopau and Jöhstädter Schwarzwasser profiles ("b.l.2" in Fig. A2.5) and corresponds to the Chemnitz-Plowen low (swath profile 2 in Fig. 5). The intermediate base-level is separated from the present day base-level (noted "b.l.3" in Fig. A2.8) by a well marked knickpoint ($k_{sn}$=52 and SLindex>400 in Fig. 2.8). According to reconstructed profiles in Fig. 2.8, this knickpoint is associated to an incision of 50 to 75m. The Würschnitz river profile (Fig. A2.9) is similar but it does not display the uppermost base-level observed in the Zwönitz river.

*5/ Western Erzgebirge (Eibenstock block):*

The western Erzgebirge is mainly incised by the tributaries of the Zwickauer Mulde and Weiße Elster rivers (Fig. A2.10 to A2.14). The Zwickauer Mulde (Fig. A2.11) and Schwarzwasser (Fig. A2.10) river profiles show three main base-levels. The highest segment in Schwarzwasser profile (noted "b.l.1." in Fig. A2.10) corresponds to the uppermost paleosurface observed in swath profile 1 (Fig. 5). This segment displays a very low $k_{sn}$ value which suggest that this part of the drainage network was part of an initially flat and low topography. According to the reconstructed profile this relict base-level is now located at ~500m above the present day base-level. The highest segment for the Zwickauer Mulde river (noted "b.l.1." in Fig. A2.11) is located at a lower elevation and corresponds to the Nejdek-Eibenstock surface in Fig. 5. In both profiles base-levels 2 and 3 correspond respectively to the Chemnitz-Plauen low and to the Leipzig-Nordsachsen lowlands (present-day local base level) in swath profile 1 (Fig. 5). They are separated from the upper base-levels by very steep segments characterized by SL index values between 200 and 600 and by $k_{sn}$ values of ~60. Base-levels 2 and 3 are themselves separated by a knickpoint associated to an incision of ~30m. A similar amount of incision can be found in the Pleiße (Fig. A2.12) and Göltzsch (Fig. A2.13) rivers.

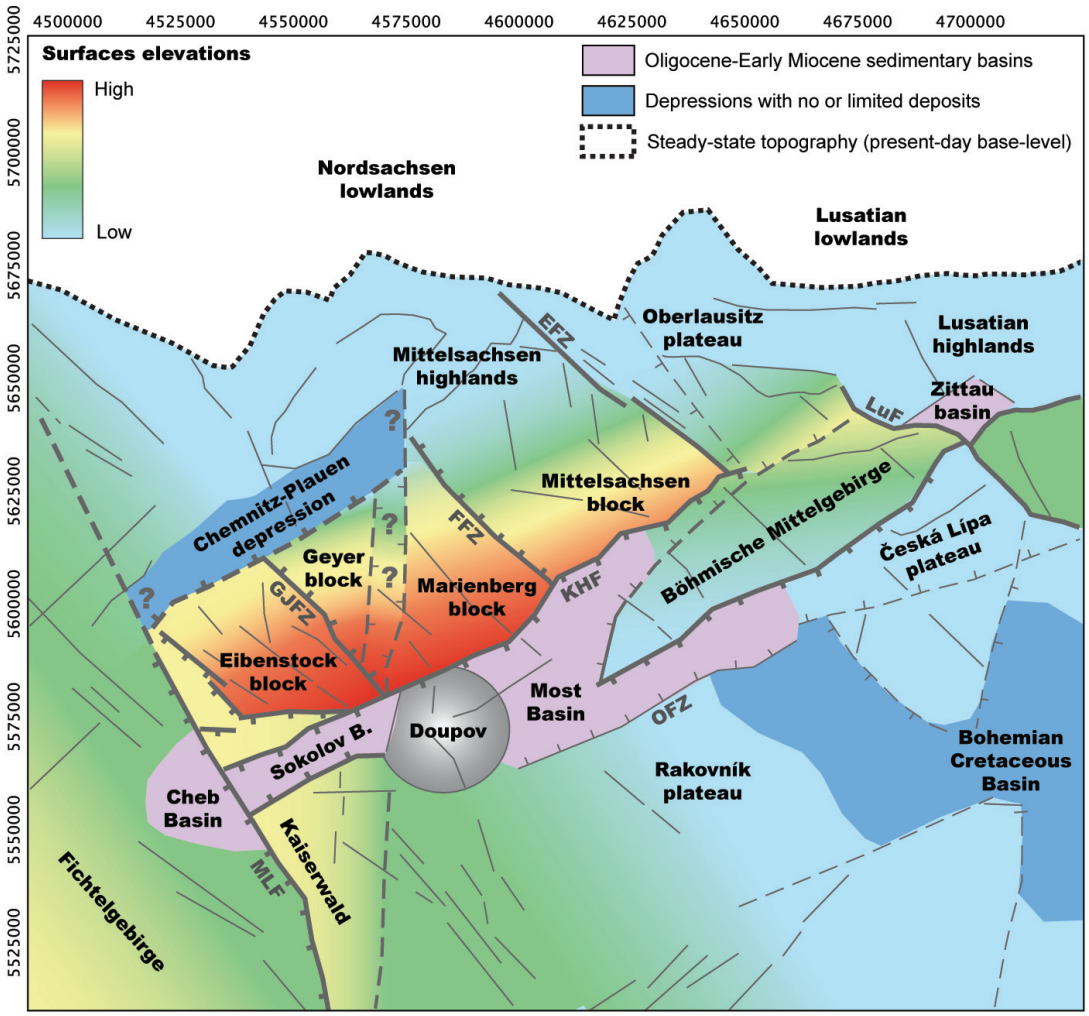


Fig. 16 – *Interpretative structural diagram of the Eger rift and Erzgebirge range showing main discontinuities from geomorphic indices. Faults abbreviations: EFZ - Elbe fault zone, FFZ - Flöha fault zone, GJFZ - Gera-Jáchymov fault zone, KHF - Krušné Hory fault, LuF - Lusatian fault, MLF - Mariánské-Lázně fault, OFZ - Eger fault zone.*

## 5. Discussion

The topography of Saxony and NW Czech Republic appears to be geomorphically young. Our topographic profiles (Fig. 5 to 8) as well as geomorphic maps (Fig. 9 to 12) show that large portions of the landscape consist of relatively well preserved surfaces. These surfaces are mainly characterized by a low amplitude topography and a low degree of incision by the drainage network. These surfaces are also associated to well defined relict base-levels in river profiles. Most of these relict base-levels display low $k_{sn}$values ($\leq$20) which may indicate that the associated portions of landscapes were located at a much lower elevation. In addition, our geomorphic maps show a strong structural control on the landscape (Fig. 16). Geomorphic domains corresponding to the NE-trending Eger graben and its northern and southern rims can be clearly identified. Our results also reveal a strong fabric in geomorphic maps and rivers corresponding to NW-trending lineaments (Mariánské-Lázn˘e, Gera-Jáchymov, Flöha, Elbe lineaments). These lineaments divide the Erzgebirge tilted block in three main compartments with different erosional and thus evolutionary stages. The drainage network is also strongly affected by N-trending lineaments in the central part of the Erzgebirge.

Although located at different elevations, observed surfaces and base-levels may be assimilated to relicts of the "etchplain" described by Czudek & Demek (1970). During Paleogene times, regional peneplains

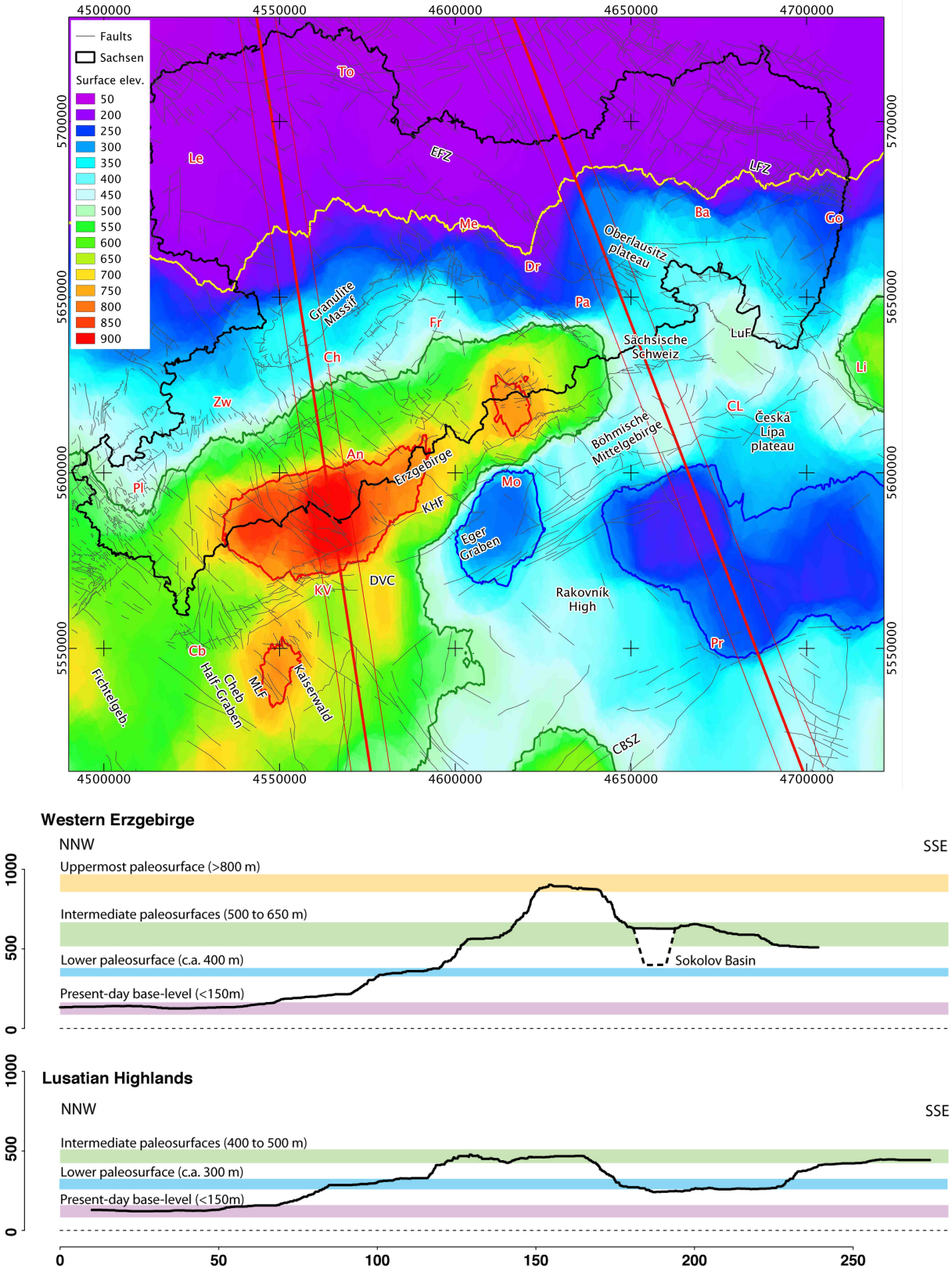


Fig. 17 – *Elevations of main surfaces in Saxony and NW Czech Republic. We interpolated flat (i.e. not incised by rivers) portions of landscapes highlighted by TPI values close to 0 (Fig. 9) or positive SI values (Fig. 12). The result is a simplified topography without major incisions. Main topographic "steps" are shown in profiles below. See Fig. 4 for structures and cities abbreviations.*

developped under tropical conditions. These peneplains marked a period of tectonic stagnation throughout the Bohemian massif. Then, during Oligocene and Neogene, the layer of tropical regolith was stripped of (Demek, 2004). The basal surface of weathering (referred as "etchplain") was modelled by a drainage network flowing from the main drainage divide located in central regions of the Bohemian massif (south of Plzeň and Prag) to a sea covering northernmost parts of Saxony (Malkovský, 1979; Suhr, 2003). The resulting irregular surface was then affected by tectonics events and forms now the uppermost surface of uplifted blocks (Migoń, 1997, 2008).

Relicts of the Paleogene etchplain can be used as a proxy for base-levels changes. We made an attempt to reconstruct the present day geometry of this surface. We sampled elevations from portions of landscapes that were assumed to be preserved surfaces. We mainly used the poorly eroded and relatively flat areas highlighted by positive SI values in Fig. 12. We also sampled elevations corresponding to positive TPI values (Fig. 9) in strongly incised areas (Böhmisches Mittelgebirge and Sächsische Schweiz). Sampled elevations were interpolated using an inverse distance weighting scheme. The result in Fig. 17 is an approximation of topographic surfaces as they would be without the incision by the drainage network.

Profiles in Fig. 17 show that surfaces occupy four mains levels in the regional landscape. The highest one is observed only along the northern rim of the Eger graben. Intermediate surfaces are located between 500 and 650m in Erzgebirge range-Kaiserwald plateau and between 400 and 500m in the Lusatian Highlands. Lower surfaces are located between ~400m (Chemnitz-Plauen low) and ~300m (Oberlausitz plateau). Finally, areas located in northern Saxony display a relatively flat landscape which correponds to the present day steady-state topography.

Topographic profiles as well as the distribution of surfaces indicate that the main event of deformation is related to the uplift and tilting of the Erzgebirge block along the Krušné Hory fault. According to Suhr (2003), uplift started in the SW Erzgebirge during the Aquitanian and then propagated toward the NE during the Burdigalian. This is consistent with mapped geomorphic indices (see for example Fig. 12) which show higher erosion in the western part of the Erzbebirge range. The eastern part is less eroded and appears thus to be younger. The uplift of the observed uppermost surface (Fig. 5) probably began during this Early Miocene event. Our observations suggest that the limit between the Eibenstock block and the Nejdek surface may correspond to an E-trending fault (Nejdek fault). Rajchl et al. (2009) proposed a NNE- to N- oriented extension between the end of Eocene and early Miocene. This initial deformation involved *en échelon* E- to ENE-trending faults. The difference between the uppermost surface and the Kaiserwald-Nejdek surface in swath profile 1 (Fig. 5) suggests a displacement of at least 300m along the Nejdek fault.

The Eger rift system was reorganized during the Middle Miocene and E-trending faults were overprinted by a more recent NE-trending normal fault system (Rajchl et al., 2009). NE-trending faults delimited several blocks. Both northern and southern rims of the Eger graben as well as parts of the Böhmisches Mittelgebirge and Lusatian Highlands were uplifted a few hundred meters (100 to 300m ?). Areas located within the graben as well as the areas between the Böhmisches Mittelgebirge and the Central Bohemian Shear Zone remained at low elevations.

The lowest set of surfaces is associated to the most recent evolution of the region. These surfaces are associated to well defined relict base-levels in analyzed river profiles. The difference between the relict base-levels and the present day base-level of the Elbe river is approximately 150 m for the Sokolov

basin (Eger river), 100 m for the tributaries of the Vltava, 100 to 130 m for the tributaries of the Elbe river (Böhmisches Mittelgebirge, Sächsische Schweiz, Oberlausitz plateau) and 40 to 60 m for the tributaries of the Mulde River. These base-levels seem to be related to the more recent evolution of the Elbe drainage system as some of them seems to be correlated with the upper part of the Pleistocene Vltava and Elbe terrace sequences (Tyráček, 2001; Tyráček et al., 2004). Higher terraces in the Elbe valley are Cromerian (465 to 850 ka) or Elsterian (418 to 465 ka) and are located at ~100m above the present-day base-level of the Elbe river (Eissmann, 2002). We propose to correlate observed relict base-levels to these terraces. Assuming that the bulk of the post-Cromerian or post-Elsterian incision of 100 to 150m is related to uplift, it would correspond to a maximum uplift rate of 0.17 to 0.35 mm/yr.

Uplift in the Erzgebirge seems to be mainly associated to a tilt along the axis of the Krušné Hory fault. However, regional-scale uplift may also be possibly associated to an E- to NE-trending tilt. Swath profiles in Fig. 6 illustrate well this regional tilt east of the Mariánské-Lázně fault system. Regional tilting is possibly related to the reactivation of NW-trending lineaments (Mariánské-Lázně, Gera-Jáchymov, Flöha, Elbe lineaments) as normal faults under the present-day NW- to NNW-trending compression (Müller et al., 1997; Jarosinski, 2006). Earthquake swarms (e.g., Fischer & Horálek, 2005; Babuška et al., 2007), $CO_2$-emanation (Bräuer et al., 2003) as well as geomorphological and geological studies (e.g., Peterek et al., 2011) provide evidences for active magmatism and ongoing tectonic activity along the Mariánské-Lázně fault system.

## 6. Conclusions

We analyzed the landscapes of Saxony and NW Czech Republic and their response to tectonics using a combination of different geomorphic indices. Our results indicate that large portions of the landscape consist in well preserved topographic surfaces. These surfaces are important features as they can provide a complete record of the evolution of the Eger rift area. In addition, the limits and incisions of these surfaces can reveal the structural control of major lineaments.

The NE-trending Eger graben and its rims can be clearly identified in geomorphic maps. Areas located south (Kaiserwald and Rakovník High) consist in a large plateau. Whithin this domain observed surfaces suggest a regional tilt toward the east, possibly related to NNW-trending structures such as the Mariánské-Lázně fault system. The Erzgebirge block to the north is mainly tilted along the Krušné Hory fault. Geomorphic indices and topographic profiles show that it is divided in three main compartments by NW-trending lineaments (Mariánské-Lázně, Gera-Jáchymov, Flöha, Elbe lineaments). The drainage network in the central part of the Erzgebirge is also aligned along N-trending lineaments. Alongstrike changes in incisions suggest that the uplift of the Erzgebirge block was initiated along the western block and then propagated toward the east. Areas located east of the Elbe fault zone form a plateau. Well preserved surfaces and relict base-levels in river-profiles suggest a Pleistocene 100 to 150m base-level change along the Elbe river.

## Acknowledgements

The authors greatly thank the Sächsisches Landesamt für Umwelt, Landwirtschaft und Geologie for providing useful 20m resolution data, geological data (including mapped faults for Saxony) and

discussions. The authors also thank Leomaris Domínguez-González for her precious help during the extraction of river profiles.

## References

Adamovic, J., & Coubal, M. (1999). Intrusive geometries and Cenozoic stress history of the northern part of the Bohemian Massif. *GeoLines*, *9*, 5–14.

Ascione, A., Cinque, A., Miccadei, E., Villani, F., & Berti, C. (2008). The Plio-Quaternary uplift of the Apennine chain: new data from the analysis of topography and river valleys in Central Italy. *Geomorphology*, *102*, 105–118.

Babuška, V., Plomerová, J., & Fischer, T. (2007). Intraplate seismicity in the western Bohemian Massif (central Europe): A possible correlation with a paleoplate junction. *Journal of Geodynamics*, *44*, 149–159.

Bräuer, K., Kämpf, H., Strauch, G., & Weise, S. M. (2003). Isotopic evidence ($^3$He/$^4$He, $^{13}C_{CO2}$) of fluid-triggered intraplate seismicity. *Journal of Geophysical Research: Solid Earth*, *108*, doi: 10.1029/2002JB002077.

Burbank, D. W., & Anderson, R. S. (2001). *Tectonic Geomorphology*. Cambridge: Blackwell Science.

Cajz, V., & Valečka, J. (2010). Tectonic setting of the Ohře/Eger Graben between the central part of the České středohoří Mts. and the Most Basin, a regional study. *Journal of Geosciences*, *55*, 201–215.

Cajz, V., Vokurka, K., Balogh, K., Lang, M., & Ulrych, J. (1999). The České středohoří Mts.: volcanostratigraphy and geochemistry. *Geolines*, *9*, 21–28.

Chen, Y. C., Sung, Q., & Cheng, K. Y. (2003). Along-strike variations of morphotectonic features in the Western Foothills of Taiwan: tectonic implications based on stream-gradient and hypsometric analysis. *Geomorphology*, *56*, 109–137.

Cheng, K.-Y., Hung, J.-H., Chang, H.-C., Tsai, H., & Sung, Q.-C. (2012). Scale independence of basin hypsometry and steady state topography. *Geomorphology*, *171-172*, 1–11.

Czudek, T., & Demek, J. (1970). Některé problémy interpretace povrchových tvarů České vysočiny. *Zprávy Geografického ústavu ČSAV*, *7*, 9–28.

Delcaillau, B., Deffontaines, B., Floissac, L., Angelier, J., Deramond, J., Souquet, P., Chu, H. T., & Lee, J. F. (1998). Morphotectonic evidence from lateral propagation of an active frontal fold; Pakuashan anticline, foothills of Taiwan. *Geomorphology*, *24*, 263–290.

Demek, J. (2004). Etchplain, rock pediments and morphostructural analysis of the Bohemian Massif (Czech Republic). In D. Drbohlav, J. Kalvoda, & V. Voûenìlek (Eds.), *Czech Geography at the Dawn of the Millenium* (pp. 69–81). Palacky University in Olomouc, Olomouc.

Duncan, C., Masek, J., & Fielding, E. (2003). How steep are the Himalaya? Characteristics and implications of along-strike topographic variations. *Geology*, *31*, 75–78.

Duvall, A., Kirby, E., & Burbank, D. (2004). Tectonic and lithologic controls on bedrock channel profiles and processes in coastal California. *J. Geophys. Res.*, *109*, F03002, doi:10.1029/2003JF000086.

Dèzes, P., Schmid, S. M., & Ziegler, P. A. (2004). Evolution of the European Cenozoic Rift System: interaction of the Alpine and Pyrenean orogens with their foreland lithosphere. *Tectonophysics*, *31*, 1–33.

Eissmann, L. (2002). Quaternary geology of eastern Germany (Saxony, Saxon–Anhalt, South Brandenburg, Thüringia), type area of the Elsterian and Saalian Stages in Europe. *Quaternary Science Reviews*, *21*, 1275–1346.

Evans, I. S. (1972). General geomorphometry derivatives of altitude and descriptive statistics. In R. J. Chorley (Ed.), *Spatial Analysis in Geomorphology* (pp. 17–90). London: Harper and Row.

Fairfield, J., & Leymarie, P. (1991). Drainage networks from grid digital elevation models. *Water Resources Research*, *27*, 709–717.

Fischer, T., & Horálek, J. (2005). Slip-generated patterns of swarm microearthquakes from West Bohemia/Vogtland (central Europe): evidence of their triggering mechanism? *Journal of Geophysical Research*, *110*, 1–14.

Font, M., Amorese, D., & Lagarde, J. L. (2010). DEM and GIS analysis of the stream gradient index to evaluate effects of tectonics: The Normandy intraplate area (NW France). *Geomorphology*, *119*, 172–180.

Frischbutter, A., & Schwab, G. (1995). Karte der rezenten vertikalen Krustenbewegungen in der Umrahmung der Ostsee-Depression. Ein Beitrag zu IGCP.Projekt Nr. 346 “Neogeodynamica Baltica”. *Brandenburgische Geowissenschaftliche Beiträge*, *2*, 59–67.

Golts, S., & Rosenthal, E. (1993). A morphotectonic map of the northern Arava in Israel, derived from isobase lines. *Geomorphology*, *7*, 305–315.

Grenerczy, G., Sella, G., Stein, S., & A., K. (2005). Tectonic implications of the GPS velocity field in the northern Adriatic region. *Geophysical Research Letters*, *32*, doi:10.1029/2005GL022947.

Grohmann, C. H. (2004). Morphometric analysis in geographic information systems: applications of free software GRASS and R. *Computers & Geosciences*, *30*, 1055–1067.

Grohmann, C. H., Riccomini, C., & Alves, F. M. (2007). SRTM-based morphotectonic analysis of the Pocos de Caldas Alkaline Massif, southeastern Brazil. *Computers & Geosciences*, *33*, 10–19.

Grohmann, C. H., Riccomini, C., & Chamani, M. A. C. (2011). Regional scale analysis of landform configuration with base-level (isobase) maps. *Hydrology and Earth System Sciences*, *15*, 1493–1504.

Guzzetti, F., & Reichenbach, P. (1994). Towards a definition of topographic divisions for Italy. *Geomorphology*, *11*, 57–74.

Hack, J. T. (1957). Studies of longitudinal stream profiles in Virginia and Maryland. *U.S. Geological Survey Professional Paper*, *294*, 45–97.

Hack, J. T. (1973). Stream profile analysis and stream–gradient index. *J. Res. U.S. Geol. Survey*, *30*, 421–429.

Isacks, B. L. (1992). Long term land surface processes: erosion, tectonics and climate history in mountain belts. In P. Mather (Ed.), *TERRA-1: Understanding the Terrestrial Environment* (pp. 21–36). London: Taylor and Francis.

Jarosinski, M. (2006). Recent tectonic stress field investigations in Poland: a state of the art. *Geological Quarterly*, *50*, 303–321.

Jarvis, A., Reuter, H. I., Nelson, A., & Guevara, E. (2008). Hole-filled seamless SRTM data V4. *International Centre for Tropical Agriculture (CIAT)*, *http://srtm.csi.cgiar.org*.

Jenness, J. (2006). Topographic Position Index (tpi_jen.avx) extension for ArcView 3.x, v. 1.3a. *Jenness Enterprises*, *available at: http://www.jennessent.com/arcview/tpi.htm*.

Jones, R. (2002). Algorithms for using a DEM for mapping catchment areas of stream sediment samples. *Computers & Geosciences*, *28*, 1051–1060.

Keller, E. A., & Pinter, N. (1996). *Active tectonics : earthquakes, uplift, and landscape*. Englewood Cliffs, N.J.: Prentice Hall.

Kirby, E., & Whipple, K. X. (2001). Quantifying differential rock–uplift rates via stream profile analysis. *Geology*, *29*, 415–418.

Kirby, E., & Whipple, K. X. (2012). Expression of active tectonics in erosional landscapes. *Journal of Structural Geology*, *44*, 54–75.

Malkovský, M. (1975). Palaeogeography of the Miocene of the Bohemian Massif. *Věstník Ústředního ústavu geologického*, *50*, 27–31.

Malkovský, M. (1979). *Tektogeneze Platformn ího Pokryvu Ceskéo Masívu. Yvdal Ustrední ustav geologicky*. Praha.

Malkovský, M. (1987). The Mesozoic and Tertiary basins of the Bohemian Massif and their evolution. *Tectonophysics*, *137*, 31–42.

Masek, J. G., Isacks, B. L., Gubbels, T. L., & Fielding, E. J. (1994). Erosion and tectonics at the margins of continental plateaus. *Journal of Geophysical Research*, *99*, doi: 10.1029/94JB00461.

Mather, A. E. (2000). Adjustment of a drainage network to capture induced base-level change. *Geomorphology*, *34*, 271–289.

Mather, A. E., Harvey, A. M., & Stokes, M. (2000). Quantifying long-term catchment changes of alluvial fan systems. *Geological Society of America Bulletin*, *112*, 1825–1833.

Migoń, P. (1997). Tertiary etchsurfaces in the Sudetes Mountains, SW Poland: a contribution to the pre-Quaternary morphology of Central Europe. In M. Widdowson (Ed.), *Palaeosurfaces: recognition, reconstruction, and*

*palaeoenvironmental interpretation, Geological Society Special Publication, 120* (pp. 187–202). London.

Migoń, P. (2008). Main features of geomorphology of the Sudetes re-assessed in the light of digital elevation model. *Geografie Sborník České Geografické Společnosti*, *113*, 400–416.

Müller, B., Wehrle, V., Zeyen, H., & Fuchs, K. (1997). Short-scale variations of tectonic regimes in the western European stress province north of the Alps and Pyrenees. *Tectonophysics*, *275*, 199–219.

Ohmori, H. (1993). Changes in the hypsometric curve through mountain building resulting from concurrent tectonics and denudation. *Geomorphology*, *8*, 263–277.

Pawlewicz, M. J., Steinshouer, D. W., & Gautier, D. L. (1997). Map Showing Geology, Oil and Gas Fields, and Geologic Provinces of Europe including Turkey. *U.S. Geological Survey*, *Open File Report 97-470I*, available at http://pubs.usgs.gov/of/1997/ofr–97–470/OF97–470I/.

Pearce, S. A., Pazzaglia, F. J., & Eppes, M. C. (2004). Ephemeral stream response to growing folds. *Geological Society of America Bulletin*, *116*, 1223–1239.

Pedrera, A., Pérez-Peña, J. V., Galindo-Zaldívar, J., Azañón, J. M., & Azor, A. (2009). Testing the sensitivity of geomorphic indices in areas of low-rate active folding (eastern Betic Cordillera, Spain). *Geomorphology*, *105*, 218–231.

Pérez-Peña, J. V., Azañón, J. M., Booth-Rea, G., Azor, A., & Delgado, J. (2009). Differentiating geology and tectonics using a spatial autocorrelation technique for the hypsometric integral. *Journal of Geophysical Research*, *114*, F02018, doi:10.1029/2008JF001092.

Peterek, A., Reuther, C. D., & Schunk, R. (2011). Neotectonic evolution of the Cheb Basin (Northwestern Bohemia, Czech Republic) and ist implications for the late Pliocene to Recent crustal deformation in the western part of the Eger Rift. *Zeitschrift für Geologische Wissenschaften*, *39*, 335–365.

Pike, R. J., & Wilson, S. E. (1971). Elevation relief ratio, hypsometric integral, and geomorphic area-altitude analysis. *Geological Society of America Bulletin*, *82*, 1079–1084.

Ponza, A., Pazzaglia, F. J., & Picotti, V. (2010). Thrust-fold activity at the mountain front of the Northern Apennines (Italy) from quantitative landscape analysis. *Geomorphology*, *123*, 211–231.

Rajchl, M., Uličný, D., Grygar, R., & Mach, K. (2009). Evolution of basin architecture in an incipient continental rift: the Cenozoic Most Basin, Eger Graben (Central Europe). *Basin Research*, *21*, 269–294.

Schenk, V., Cacon, S., Bosy, J., Kontny, B., Kottauer, P., & Schenkova, Z. (2000). GPS network "SUDETEN" - preliminary results of campaigns 1998–1999. *Rep. Geodesy*, *7*, 25–33.

Schumm, S. A. (1956). Evolution of drainage systems and slopes in badlands at Perth Amboy, New Jersey. *Geological Society of America Bulletin*, *67*, 597–646.

Shahzad, F., & Gloaguen, R. (2011a). TecDEM: A MATLAB based toolbox for tectonic geomorphology, Part 1: Drainage network preprocessing and stream profile analysis. *Computers & Geosciences*, *37*, 250–260.

Shahzad, F., & Gloaguen, R. (2011b). TecDEM: A MATLAB based toolbox for tectonic geomorphology, Part 2: Surface dynamics and basin analysis. *Computers & Geosciences*, *37*, 261–271.

Sibson, R. (1981). A brief description of natural neighbor interpolation. In V. Barnett (Ed.), *Interpreting Multivariate Data* chapter Chapter 2. (pp. 21–36). Chichester: John Wiley.

Snyder, N. P., Whipple, K. X., Tucker, G. E., & Merritts, D. J. (2000). Landscape response to tectonic forcing: digital elevation model analysis of stream profiles in the Mendocino triple junction region, northern California. *Geological Society of America Bulletin*, *112*, 1250–1263.

Strahler, A. N. (1952). Hypsometric (area-altitude) analysis of erosional topography. *Geological Society of America Bulletin*, *63*, 1117–1142.

Strahler, A. N. (1957). Quantitative analysis of watershed geomorphology. *Transactions of the American Geophysical Union*, *8*, 913–920.

Suhr, P. (2003). The Bohemian Massif as a Catchment Area for the NW European Tertiary Basin. *Geolines (Praha)*, *15*, 147–159.

Suk, M. (1984). *Geological history of the territory of the Czech Socialist Republic*. Geol. Survey, Prague: Publ.

House Czechoslovak Academy of Sciences.

Teodoridis, V., & Kvaček, Z. (2006). Complex palaeobotanical research of deposits overlying the main coal seam (Libkovice and Lom Mbs.) in the Most Basin (Czech Republic). *Bulletin of Geosciences*, *81*, 93–113.

Troiani, F., & Della Seta, M. (2008). The use of the Stream Length–Gradient index in morphotectonic analysis of small catchments: A case study from Central Italy. *Geomorphology*, *102*, 159–168.

Tyráček, J. (2001). Upper cenozoic fluvial history in the bohemian massif. *Quaternary International*, *79*, 37–53.

Tyráček, J., Westaway, R., & Bridgland, D. (2004). River terraces of the vltava and labe (elbe) system, czech republic, and their implications for the uplift history of the bohemian massif. *Proceedings of the Geologists' Association*, *115*, 101–124.

Ulrych, J., Pivec, E., Lang, M., Balogh, K., & Kropacek, V. (1999). Cenozoic intraplate volcanic rocks series of the bohemian massif: a review. *GeoLines*, *9*, 123–129.

Weinlich, F., Bräuer, K., Kämpf, H., Strauch, G., Tesař, J., & Weise, S. (2003). Gas Flux and Tectonic Structure in the Western Eger Rift, Karlovy Vary – Oberpfalz and Oberfranken, Bavaria. *Geolines*, *15*, 181–187.

Weiss, A. D. (2001). Topographic Position and Landforms Analysis. *Poster presentation. ESRI User Conference, San Diego, CA*, *available at: http://www.jennessent.com/downloads/tpi-poster-tnc_18x22.pdf*.

Westaway, R. (2002). Long-term river terrace sequences: evidence for global increases in surface uplift rates in the Late Pliocene and early Middle Pleistocene caused by flow in the lower continental crust induced by surface processes. *Netherlands Journal of Geosciences*, *81*, 305–328.

Whittaker, A. C., Attal, M., Cowie, P. A., Tucker, G. E., & Roberts, G. (2008). Decoding temporal and spatial patterns of fault uplift using transient river long profiles. *Geomorphology*, *100*, 506–526.

Wobus, C., Whipple, K. X., Kirby, E., Snyder, N., Johnson, J., Spyropolou, K., Crosby, B., & Sheehan, D. (2006). Tectonics from topography: Procedures, promise and pitfalls. *Geological Society of America Special Paper*, *398*, 55–74.

Ziegler, P. A. (1992). European Cenozoic rift system. *Tectonophysics*, *208*, 91–111.

Ziegler, P. A., & Dèzes, P. (2007). Cenozoic uplift of Variscan Massifs in the Alpine foreland: Timing and controlling mechanisms. *Global and Planetary Change*, *58*, 237–269.

## Appendix I.

## Longitudinal profiles for the tributaries of the Elbe.

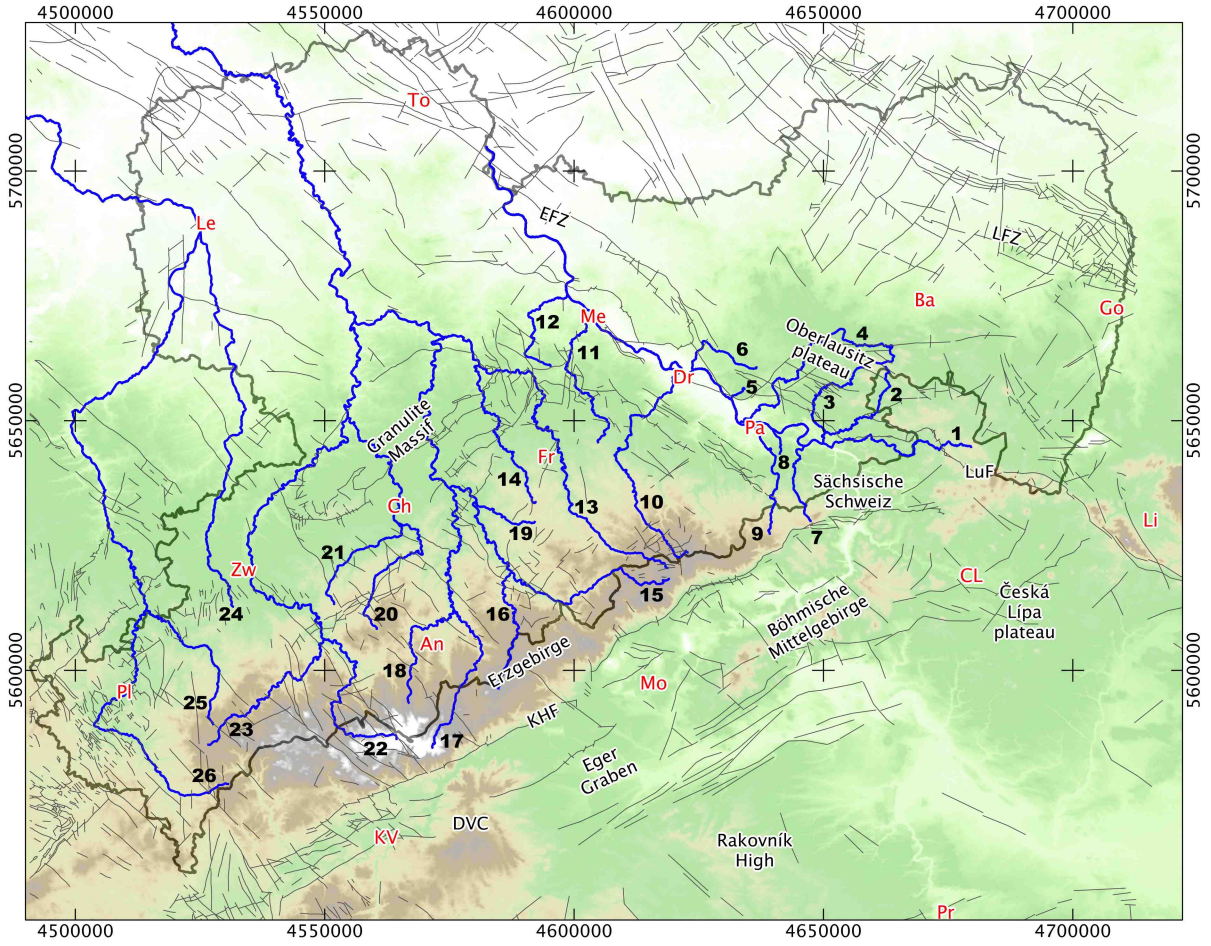


Fig. 1.1 – *Locations of analyzed streams and rivers (blue lines). 1 - Kirnitzsch, 2 - Sebnitz, 3 - Polenz, 4 - Wesenitz, 5 - Friedrichsgrundbach, 6 - Prießnitz, 7 - Biela, 8 - Struppenbach, 9 - Bahra & Gottleuba, 10 - Weißeritz, 11 - Triebisch, 12 - Ketzerbach, 13 - Freiberger Mulde, 14 - Große Striegis, 15 - Flöha, 16 - Schwarze Pockau, 17 - Jöhstädter Schwarzwasser, 18 - Zschopau, 19 - Große Lößnitz, 20 - Zwönitz, 21 - Würschnitz, 22 - Schwarzwasser, 23 - Zwickauer Mulde, 24 - Pleiße, 25 - Göltzsch, 26 - Schwarzbach & Weiße Elster*

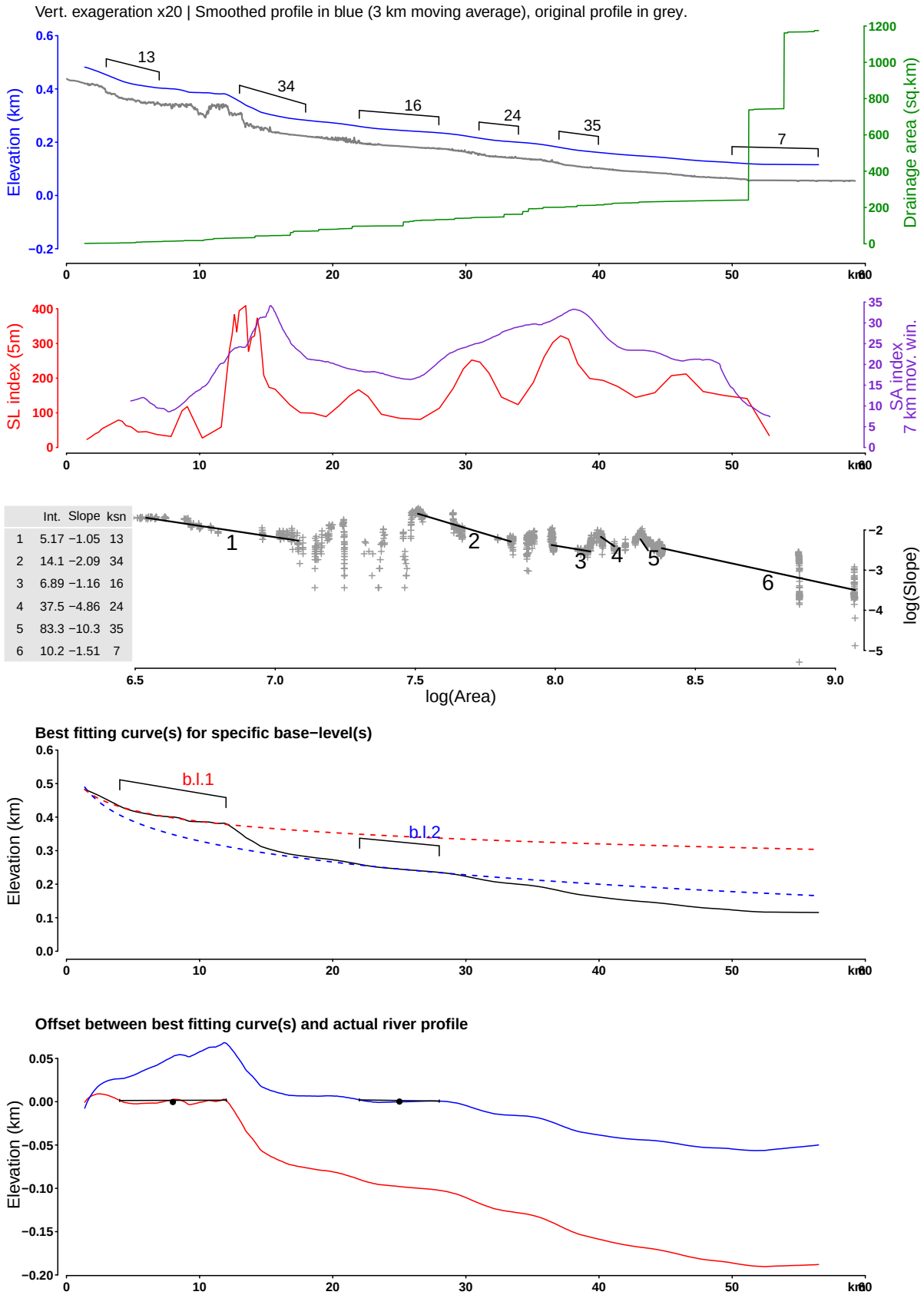


Fig. 1.2 – *Longitudinal profile analysis of the* **Kirnitzsch** *river. See location on Fig. 1.1. From top to bottom: (1) River profile and drainage area. (2) Stream-length gradient (SL) and Slope-Area (SA) indices. Peak values indicate anomalously steep slopes and knickpoints. (3) Regression of normalized steepness indices ($k_{sn}$) on a slope-area plot. $k_{sn}$ values are reported on the river profile. (4) Reconstruction of theoretical river profiles asociated to relict base-levels.*

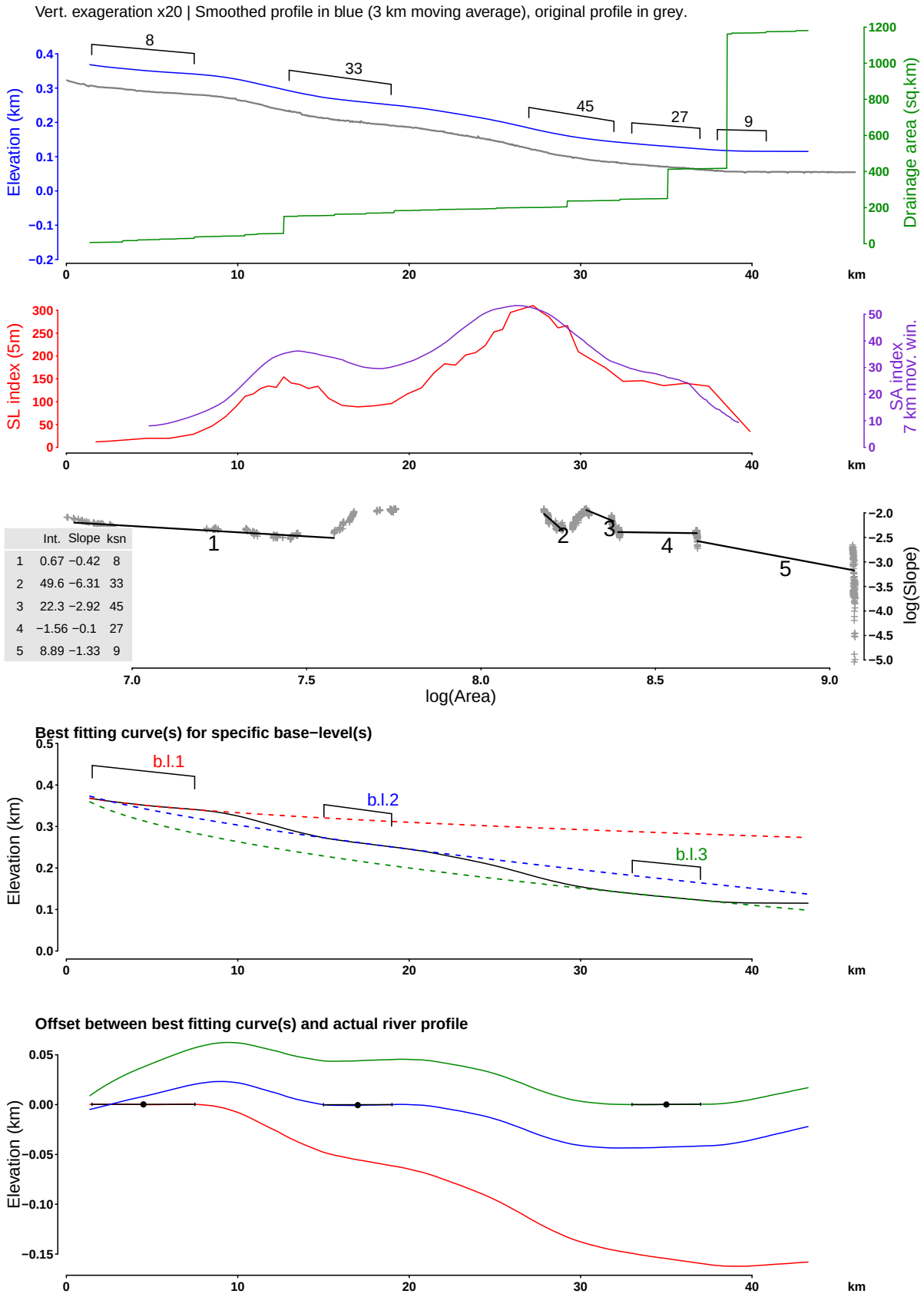


Fig. 1.3 – *Longitudinal profile analysis of the* **Sebnitz** *river. See location on Fig. 1.1. From top to bottom: (1) River profile and drainage area. (2) Stream-length gradient (SL) and Slope-Area (SA) indices. Peak values indicate anomalously steep slopes and knickpoints. (3) Regression of normalized steepness indices ($k_{sn}$) on a slope-area plot. $k_{sn}$ values are reported on the river profile. (4) Reconstruction of theoretical river profiles asociated to relict base-levels.*

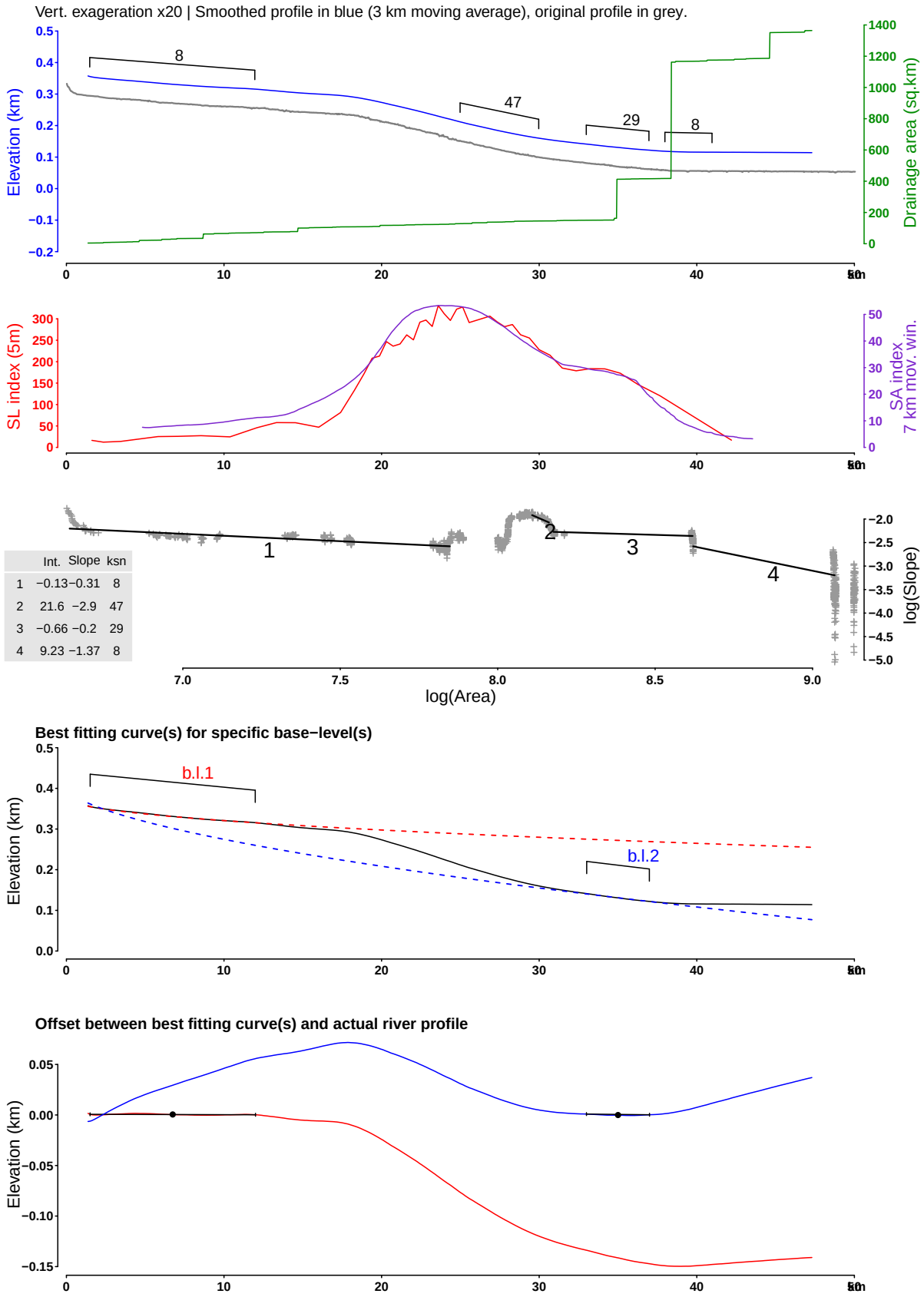


Fig. 1.4 – *Longitudinal profile analysis of the* **Polenz** *river. See location on Fig. 1.1. From top to bottom: (1) River profile and drainage area. (2) Stream-length gradient (SL) and Slope-Area (SA) indices. Peak values indicate anomalously steep slopes and knickpoints. (3) Regression of normalized steepness indices ($k_{sn}$) on a slope-area plot. $k_{sn}$ values are reported on the river profile. (4) Reconstruction of theoretical river profiles asociated to relict base-levels.*

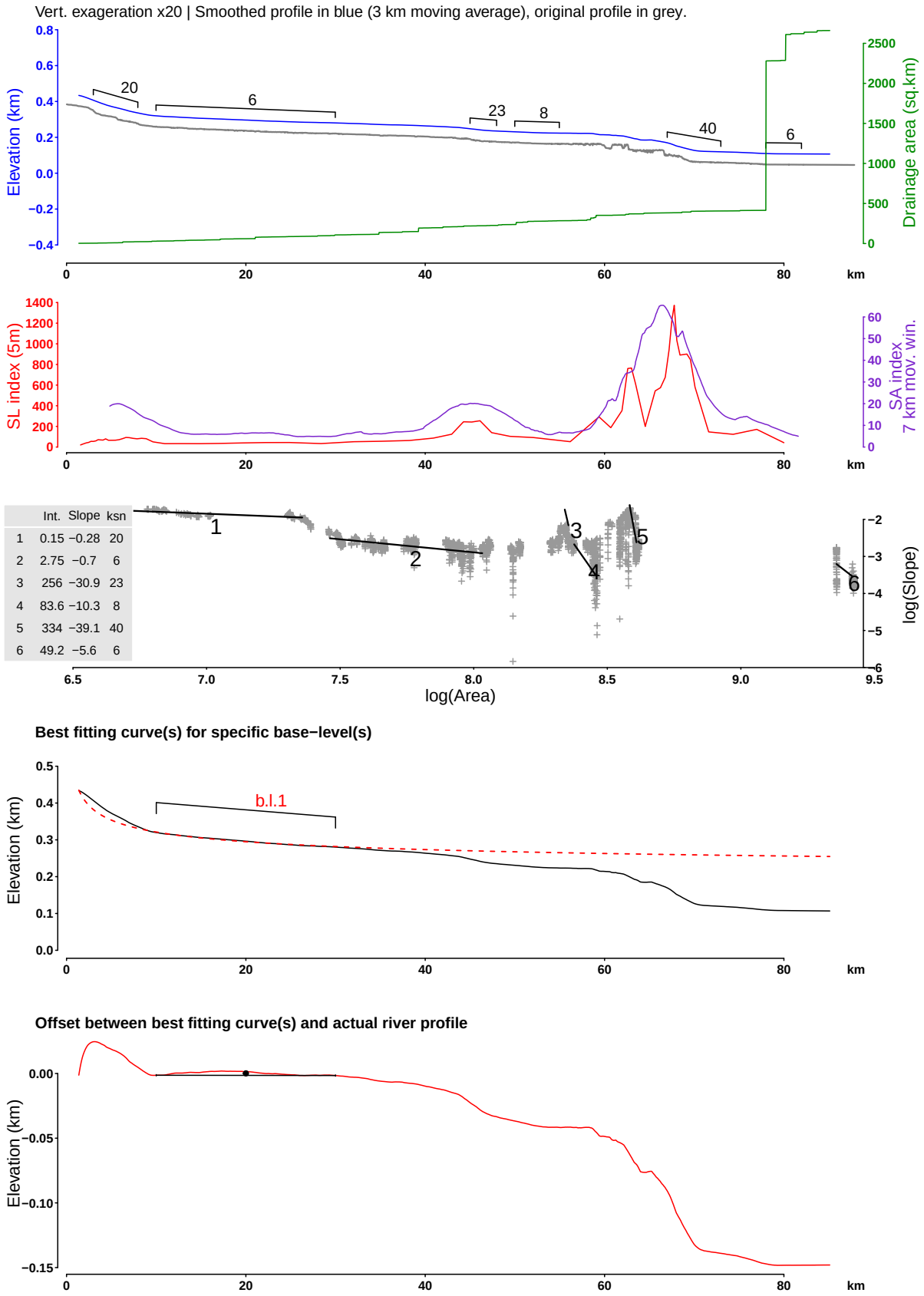


Fig. 1.5 – *Longitudinal profile analysis of the* **Wesenitz** *river. See location on Fig. 1.1. From top to bottom: (1) River profile and drainage area. (2) Stream-length gradient (SL) and Slope-Area (SA) indices. Peak values indicate anomalously steep slopes and knickpoints. (3) Regression of normalized steepness indices ($k_{sn}$) on a slope-area plot. $k_{sn}$ values are reported on the river profile. (4) Reconstruction of theoretical river profiles asociated to relict base-levels.*

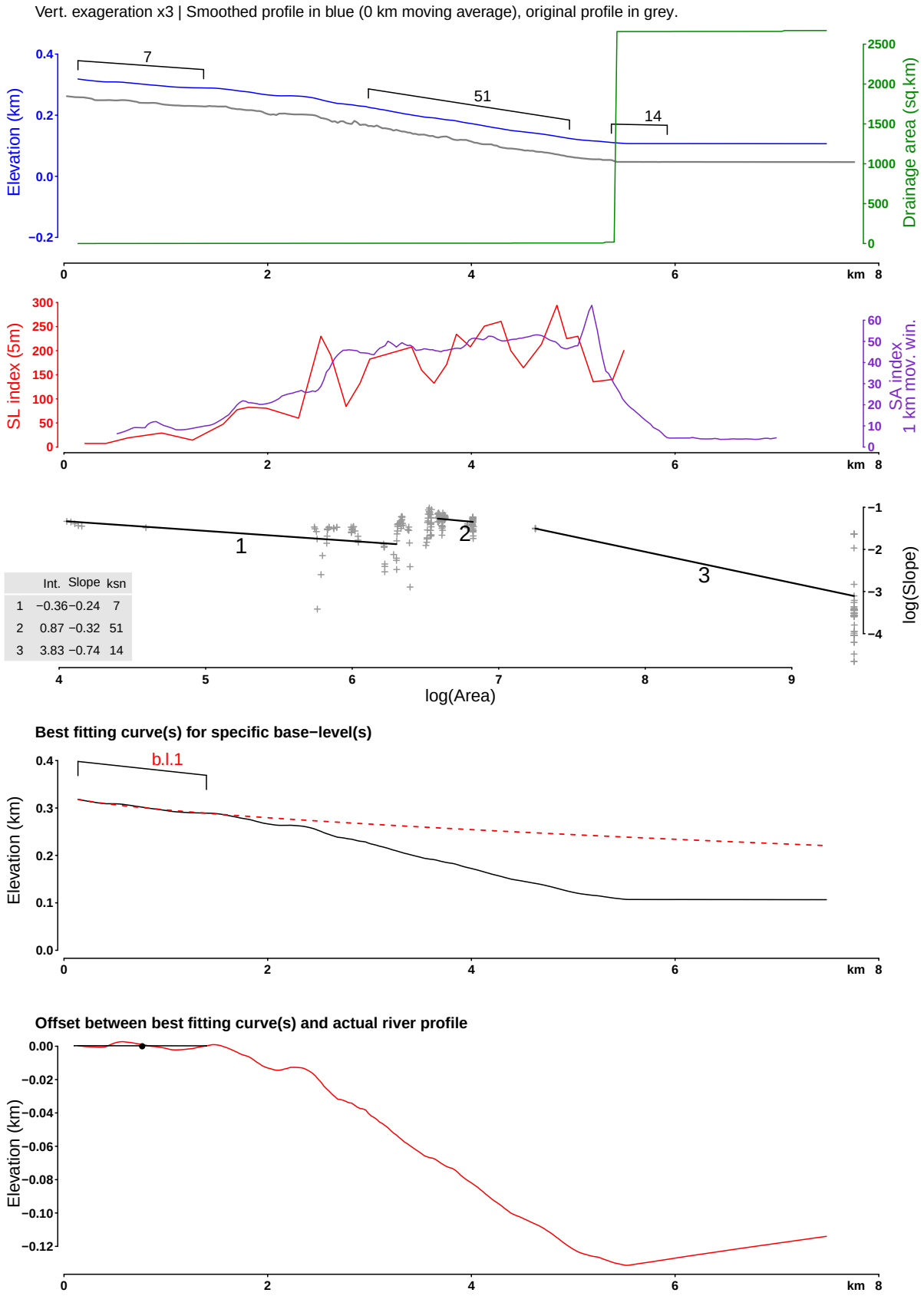


Fig. 1.6 – *Longitudinal profile analysis of the* **Friedrichsgrundbach** *stream. See location on Fig. 1.1. From top to bottom: (1) River profile and drainage area. (2) Stream-length gradient (SL) and Slope-Area (SA) indices. Peak values indicate anomalously steep slopes and knickpoints. (3) Regression of normalized steepness indices ($k_{sn}$) on a slope-area plot. $k_{sn}$ values are reported on the river profile. (4) Reconstruction of theoretical river profiles asociated to relict base-levels.*

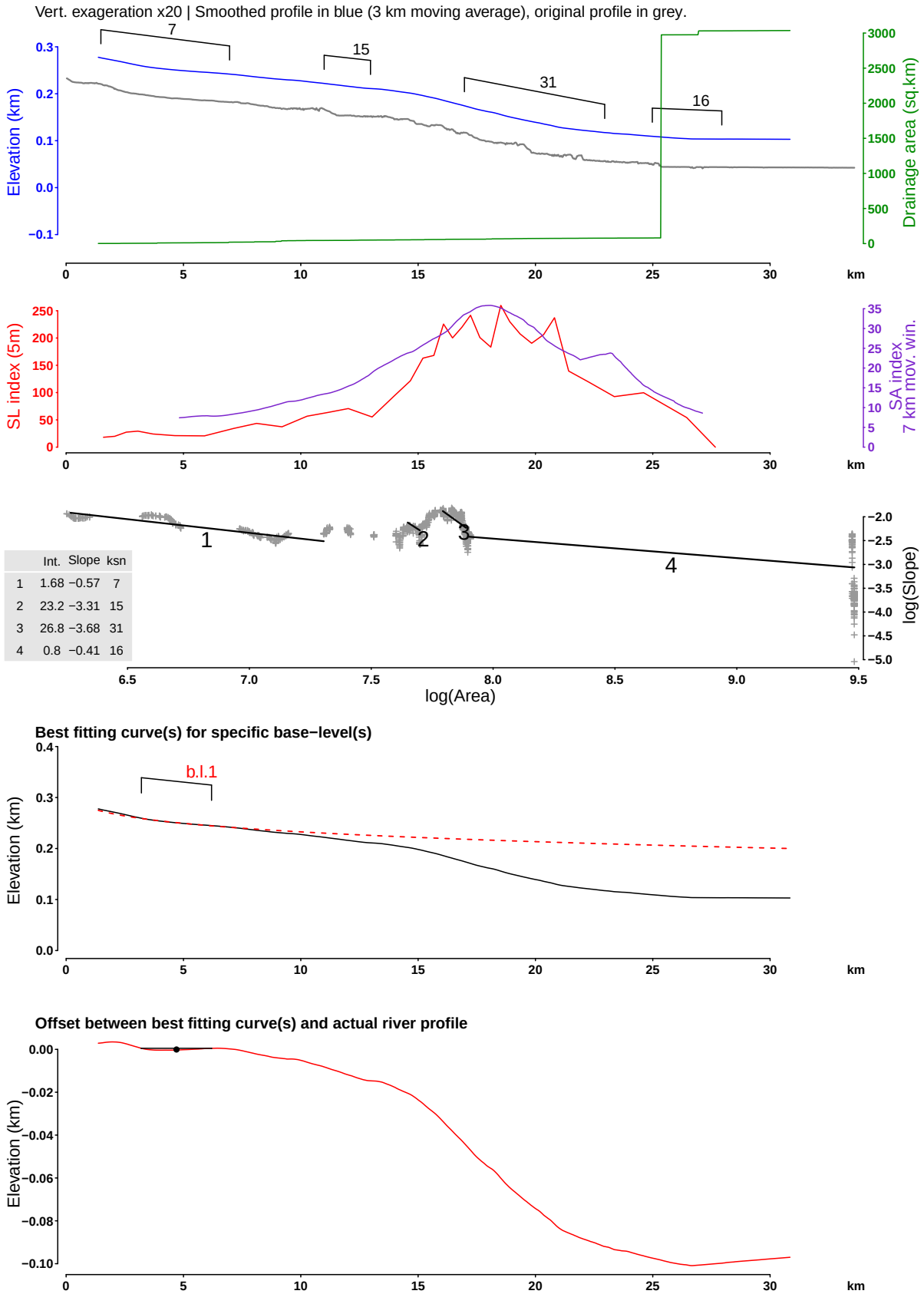


Fig. 1.7 – *Longitudinal profile analysis of the* **Prießnitz** *river. See location on Fig. 1.1. From top to bottom: (1) River profile and drainage area. (2) Stream-length gradient (SL) and Slope-Area (SA) indices. Peak values indicate anomalously steep slopes and knickpoints. (3) Regression of normalized steepness indices ($k_{sn}$) on a slope-area plot. $k_{sn}$ values are reported on the river profile. (4) Reconstruction of theoretical river profiles asociated to relict base-levels.*

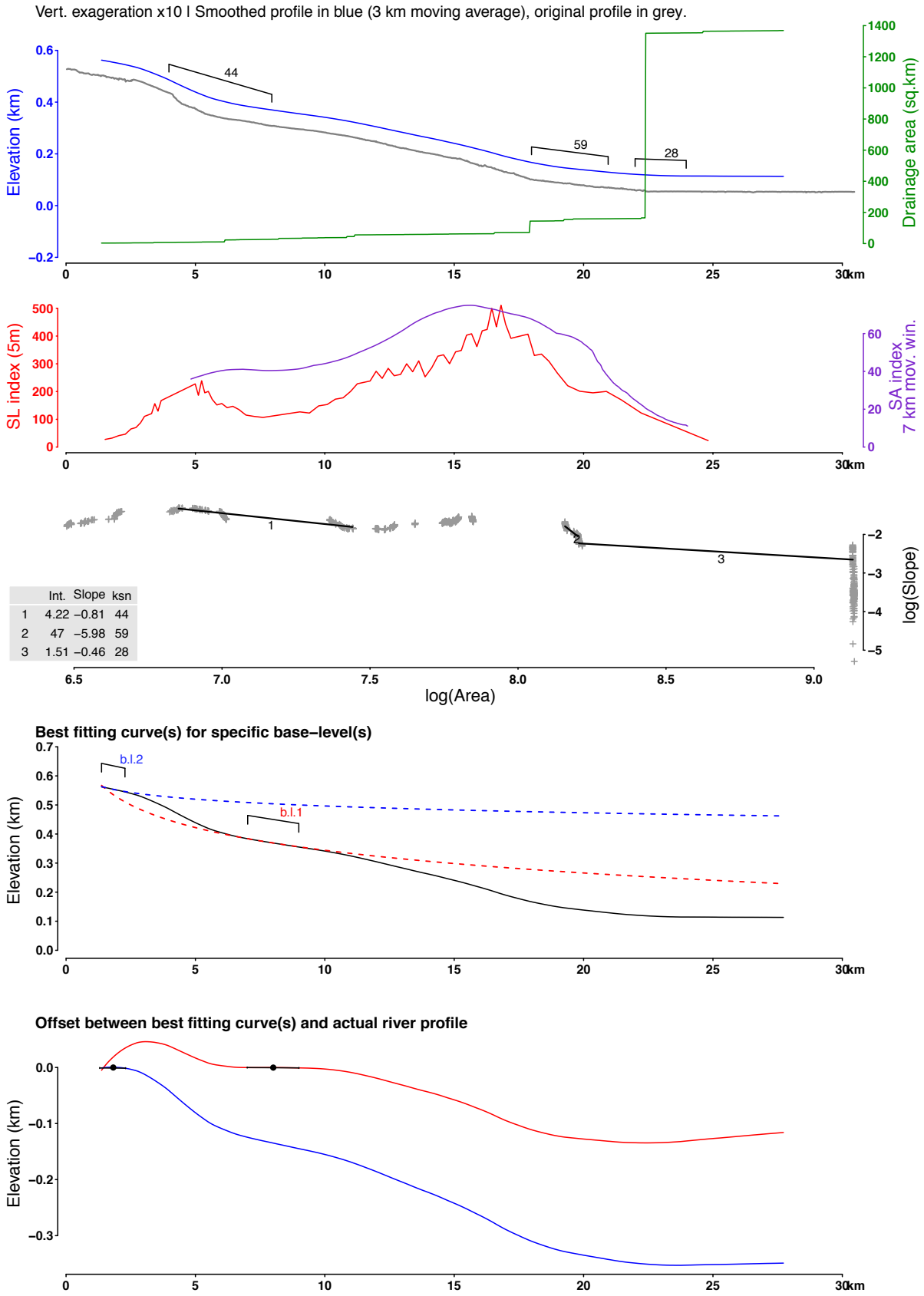


Fig. 1.8 – *Longitudinal profile analysis of the* **Biela** *river. See location on Fig. 1.1. From top to bottom: (1) River profile and drainage area. (2) Stream-length gradient (SL) and Slope-Area (SA) indices. Peak values indicate anomalously steep slopes and knickpoints. (3) Regression of normalized steepness indices ($k_{sn}$) on a slope-area plot. $k_{sn}$ values are reported on the river profile. (4) Reconstruction of theoretical river profiles asociated to relict base-levels.*

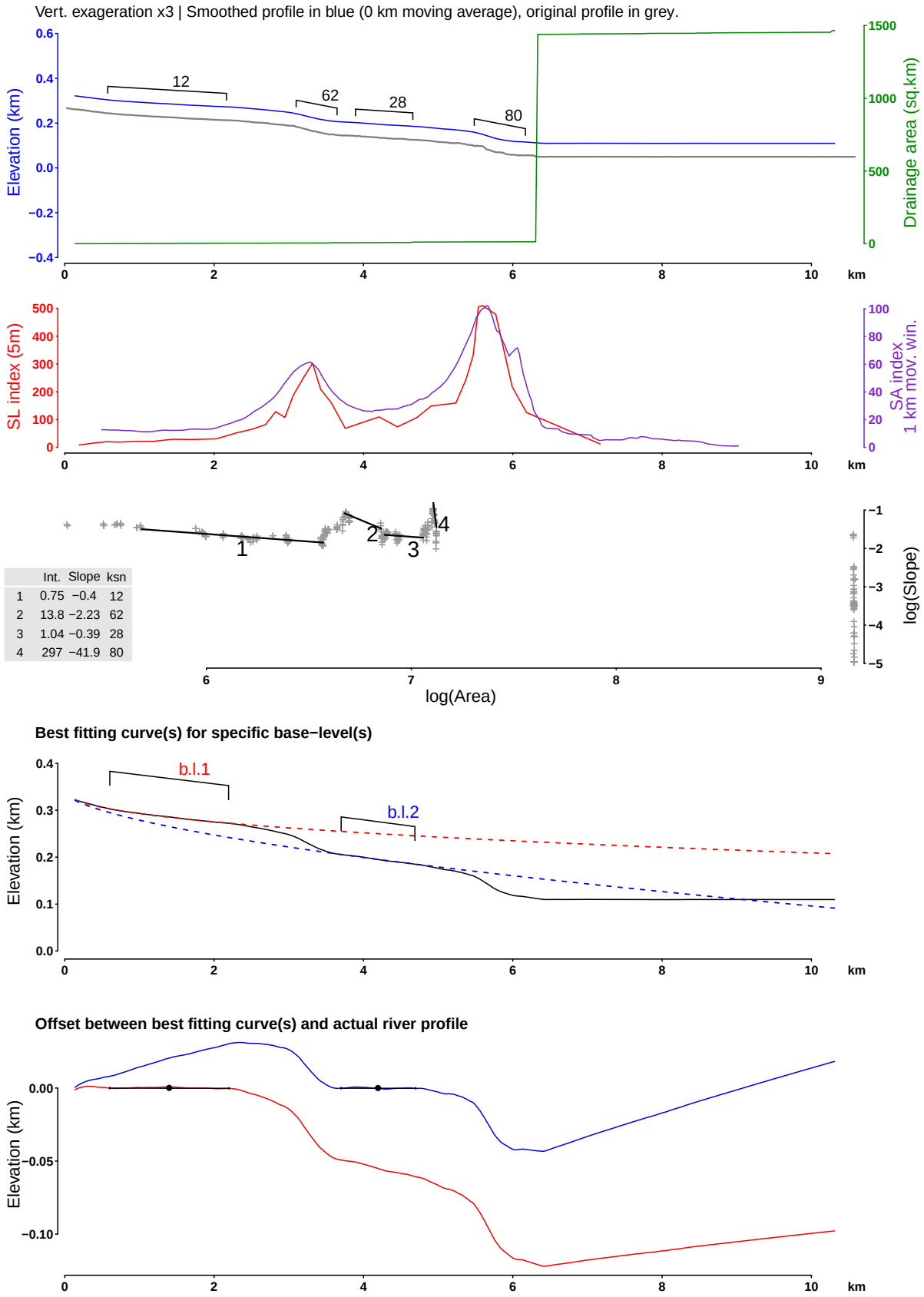


Fig. 1.9 – *Longitudinal profile analysis of the* **Struppenbach** *stream. See location on Fig. 1.1. From top to bottom: (1) River profile and drainage area. (2) Stream-length gradient (SL) and Slope-Area (SA) indices. Peak values indicate anomalously steep slopes and knickpoints. (3) Regression of normalized steepness indices ($k_{sn}$) on a slope-area plot. $k_{sn}$ values are reported on the river profile. (4) Reconstruction of theoretical river profiles asociated to relict base-levels.*

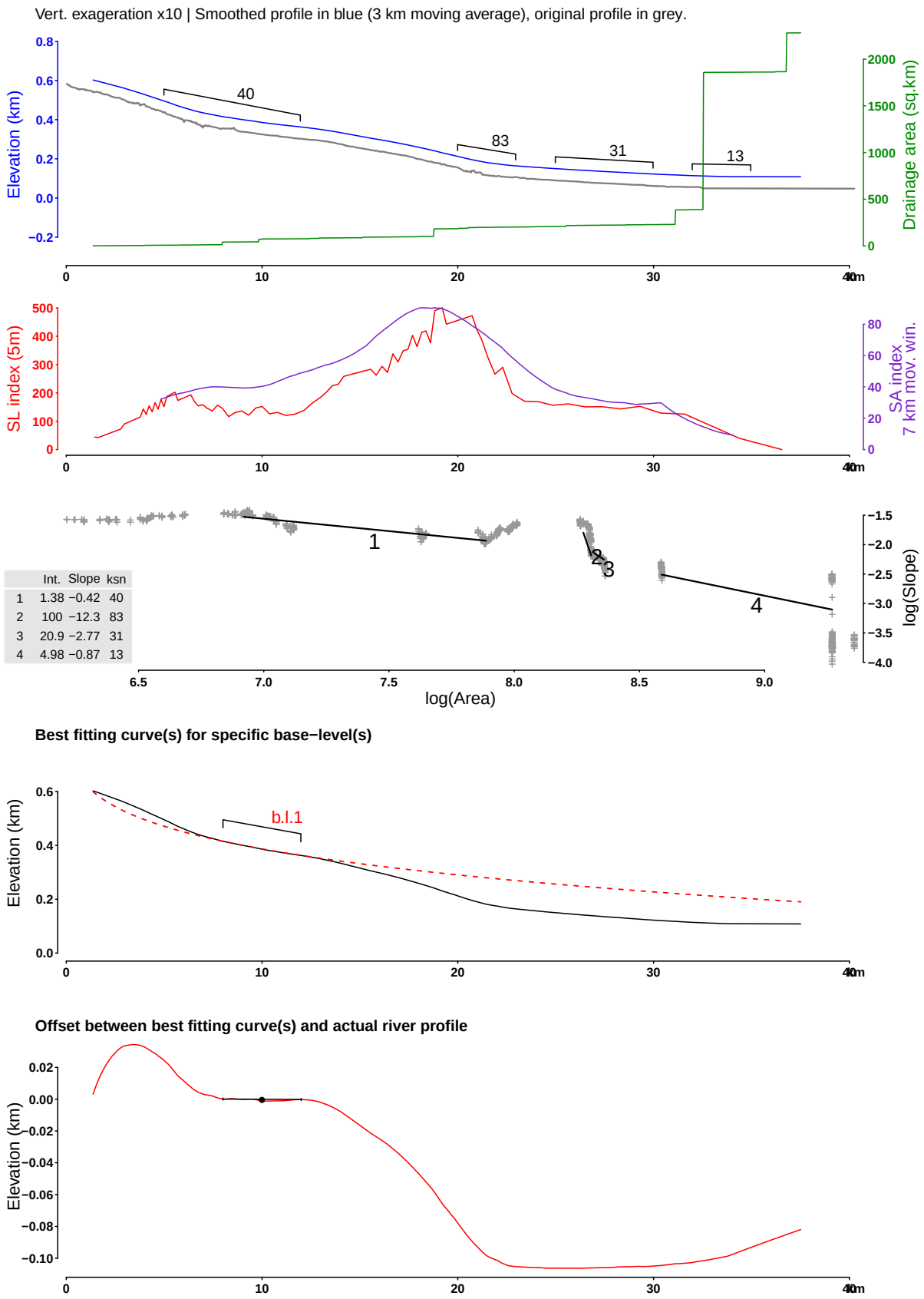


Fig. 1.10 – *Longitudinal profile analysis of the* **Bahra-Gottleuba** *river. See location on Fig. 1.1. From top to bottom: (1) River profile and drainage area. (2) Stream-length gradient (SL) and Slope-Area (SA) indices. Peak values indicate anomalously steep slopes and knickpoints. (3) Regression of normalized steepness indices ($k_{sn}$) on a slope-area plot. $k_{sn}$ values are reported on the river profile. (4) Reconstruction of theoretical river profiles asociated to relict base-levels.*

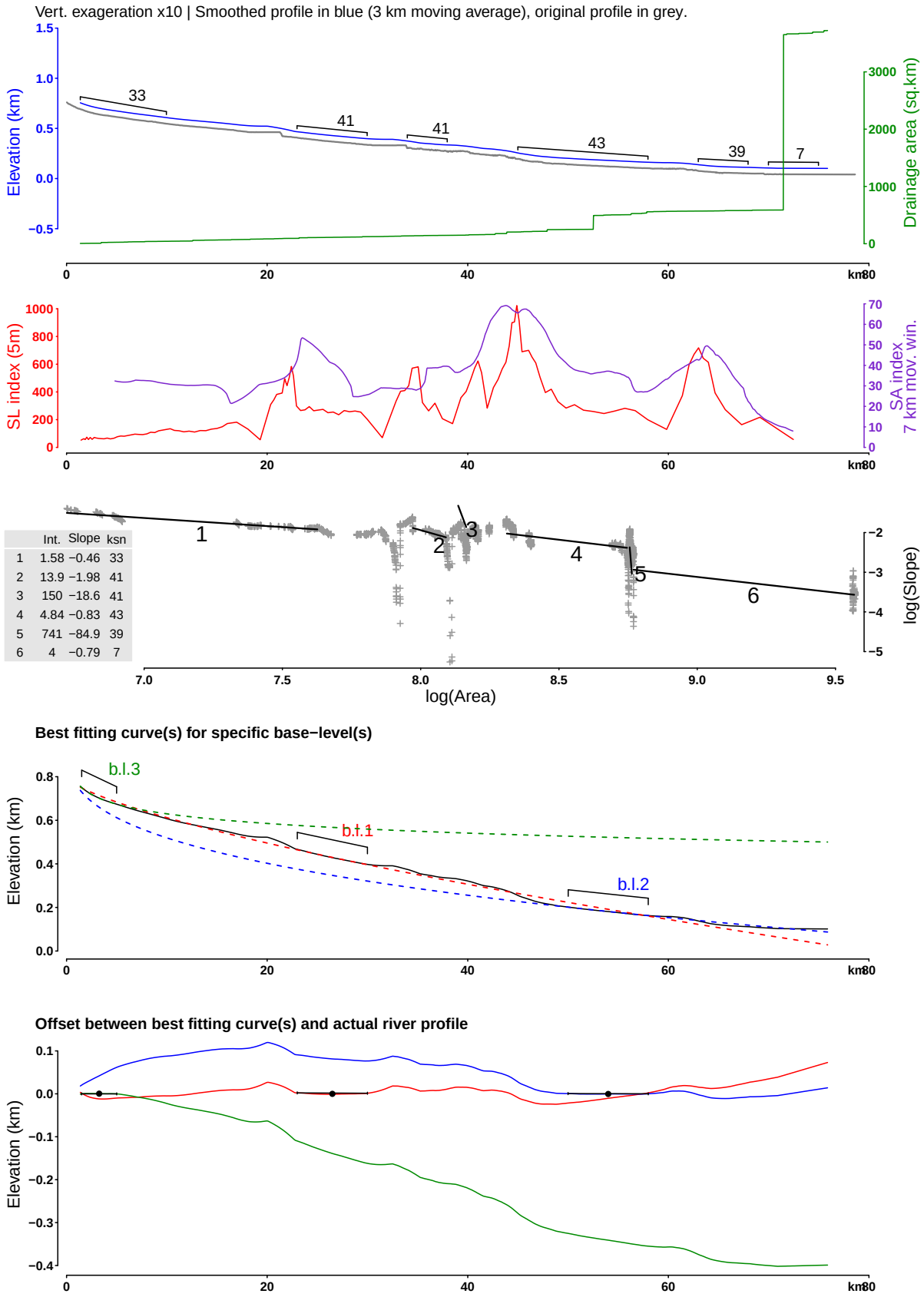


Fig. 1.11 – *Longitudinal profile analysis of the* **Weißeritz** *river. See location on Fig. 1.1. From top to bottom: (1) River profile and drainage area. (2) Stream-length gradient (SL) and Slope-Area (SA) indices. Peak values indicate anomalously steep slopes and knickpoints. (3) Regression of normalized steepness indices ($k_{sn}$) on a slope-area plot. $k_{sn}$ values are reported on the river profile. (4) Reconstruction of theoretical river profiles asociated to relict base-levels.*

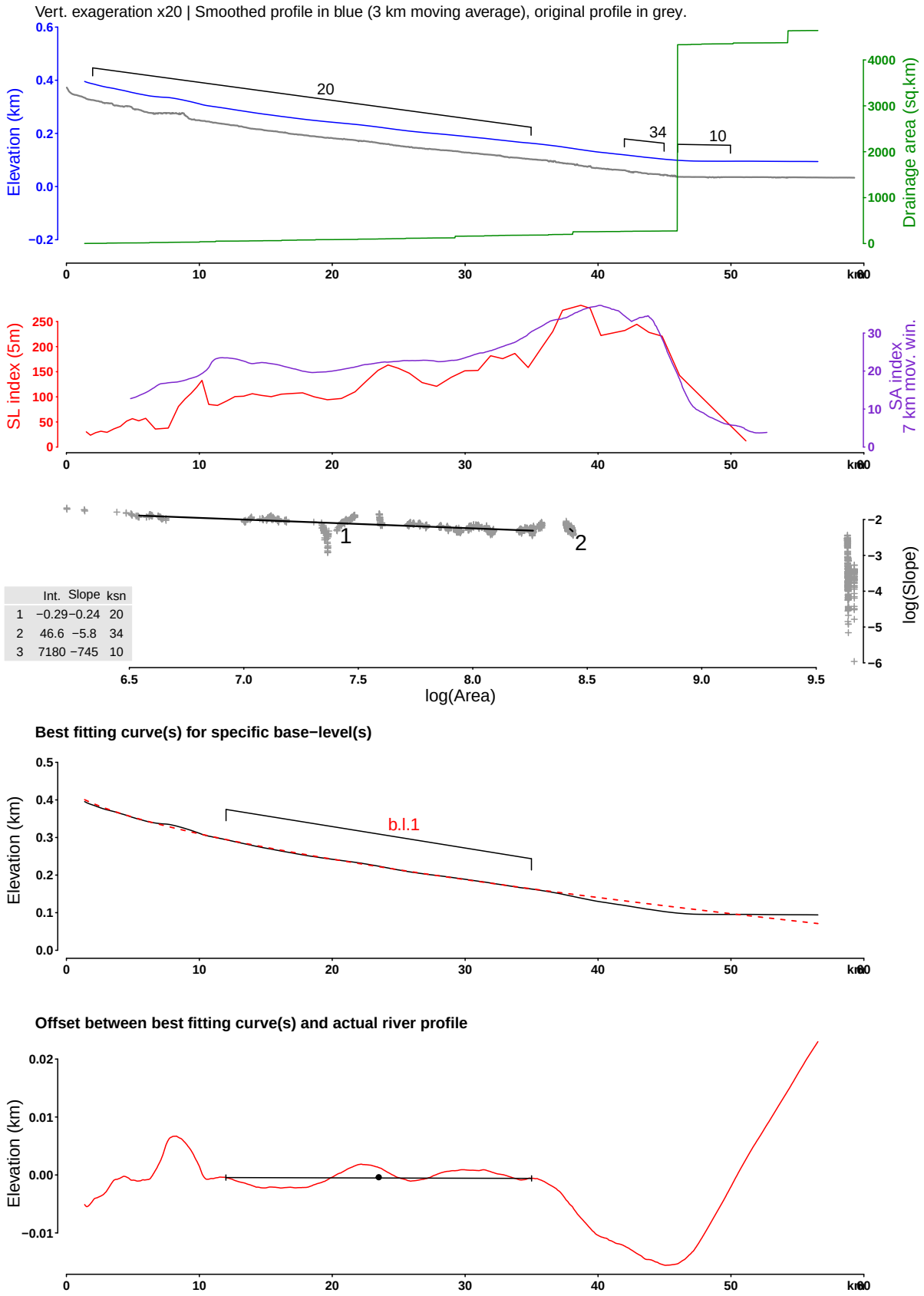


Fig. 1.12 – *Longitudinal profile analysis of the* **Triebisch** *river. See location on Fig. 1.1. From top to bottom: (1) River profile and drainage area. (2) Stream-length gradient (SL) and Slope-Area (SA) indices. Peak values indicate anomalously steep slopes and knickpoints. (3) Regression of normalized steepness indices ($k_{sn}$) on a slope-area plot. $k_{sn}$ values are reported on the river profile. (4) Reconstruction of theoretical river profiles asociated to relict base-levels.*

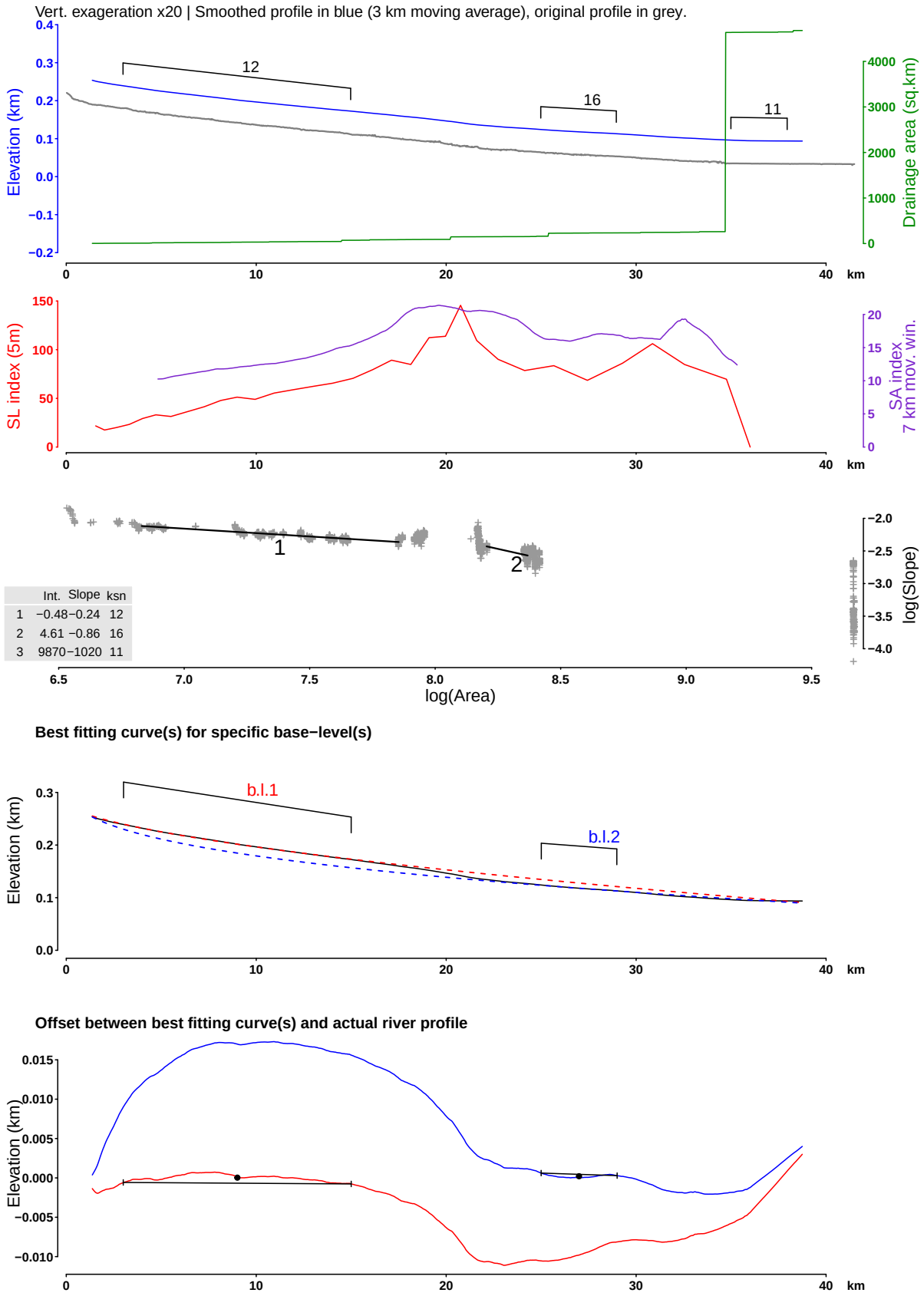


Fig. 1.13 – *Longitudinal profile analysis of the* **Ketzerbach** *river. See location on Fig. 1.1. From top to bottom: (1) River profile and drainage area. (2) Stream-length gradient (SL) and Slope-Area (SA) indices. Peak values indicate anomalously steep slopes and knickpoints. (3) Regression of normalized steepness indices ($k_{sn}$) on a slope-area plot. $k_{sn}$ values are reported on the river profile. (4) Reconstruction of theoretical river profiles asociated to relict base-levels.*

## Appendix II.

## Longitudinal profiles for rivers in the Erzgebirge range.

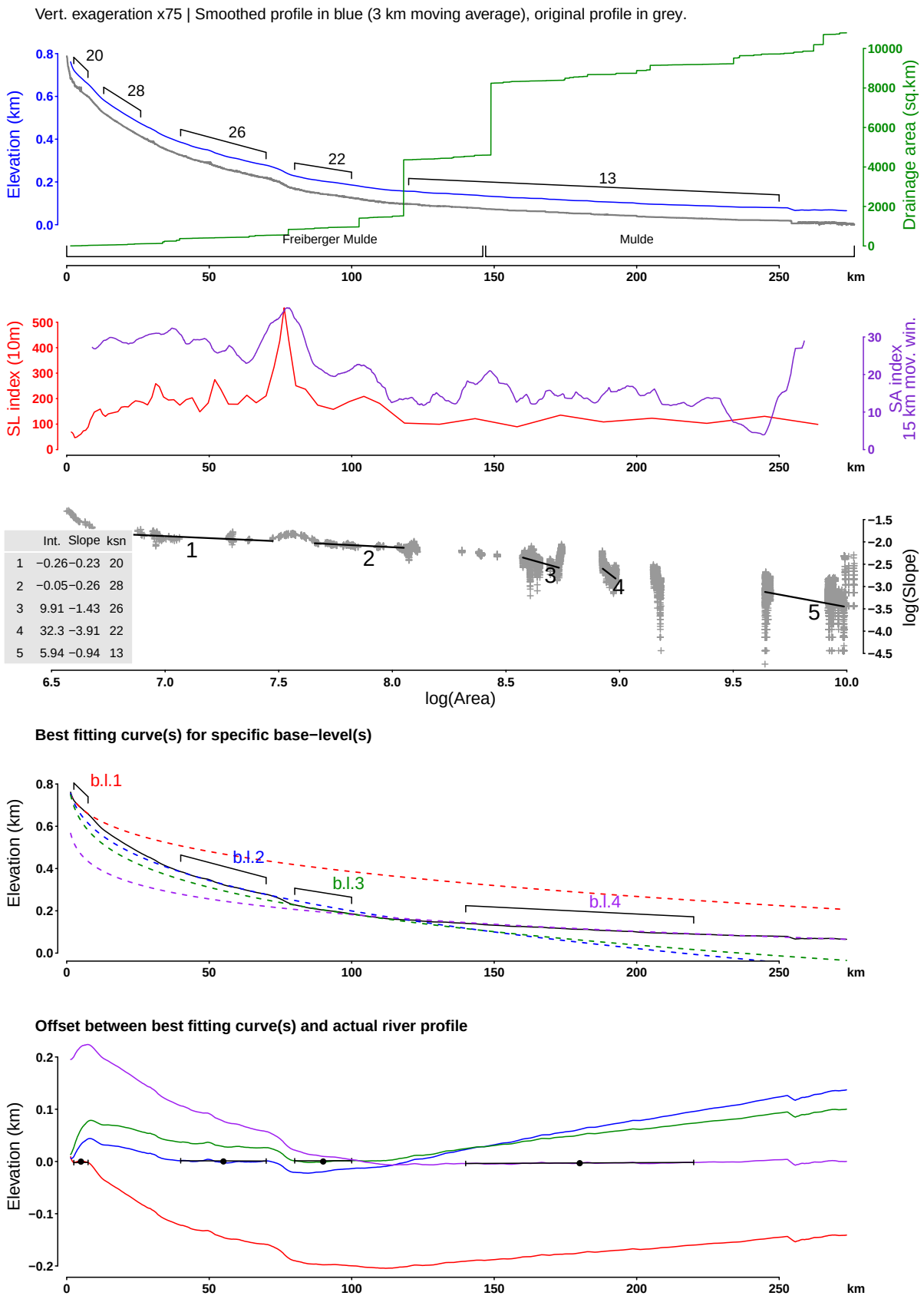


Fig. 2.1 – *Longitudinal profile analysis of the* **Freiberger Mulde** *river. See location on Fig. 1.1. From top to bottom: (1) River profile and drainage area. (2) Stream-length gradient (SL) and Slope-Area (SA) indices. Peak values indicate anomalously steep slopes and knickpoints. (3) Regression of normalized steepness indices ($k_{sn}$) on a slope-area plot. $k_{sn}$ values are reported on the river profile. (4) Reconstruction of theoretical river profiles asociated to relict base-levels.*

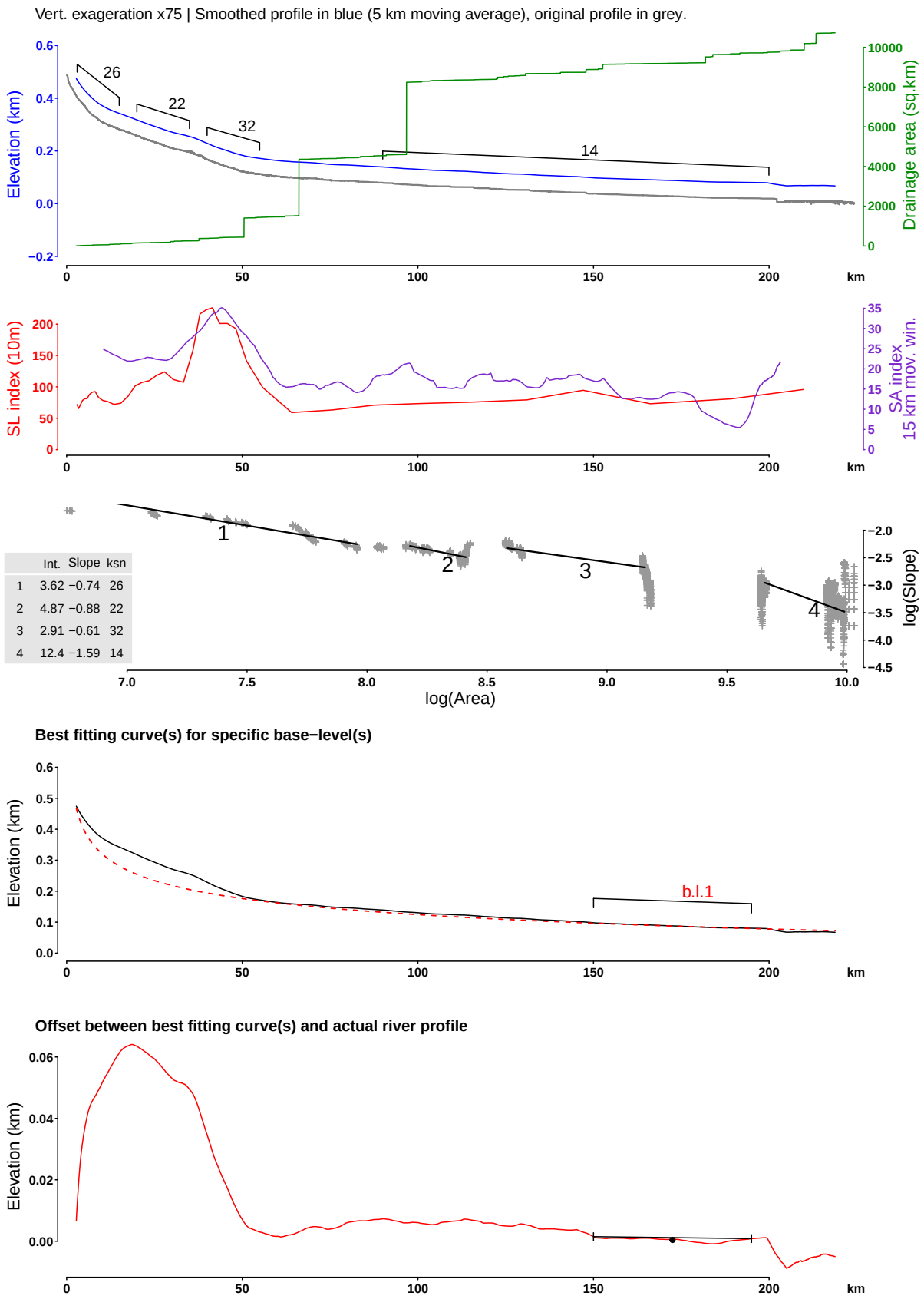


Fig. 2.2 – *Longitudinal profile analysis of the* **Große Striegis** *river. See location on Fig. 1.1. From top to bottom: (1) River profile and drainage area. (2) Stream-length gradient (SL) and Slope-Area (SA) indices. Peak values indicate anomalously steep slopes and knickpoints. (3) Regression of normalized steepness indices ($k_{sn}$) on a slope-area plot. $k_{sn}$ values are reported on the river profile. (4) Reconstruction of theoretical river profiles asociated to relict base-levels.*

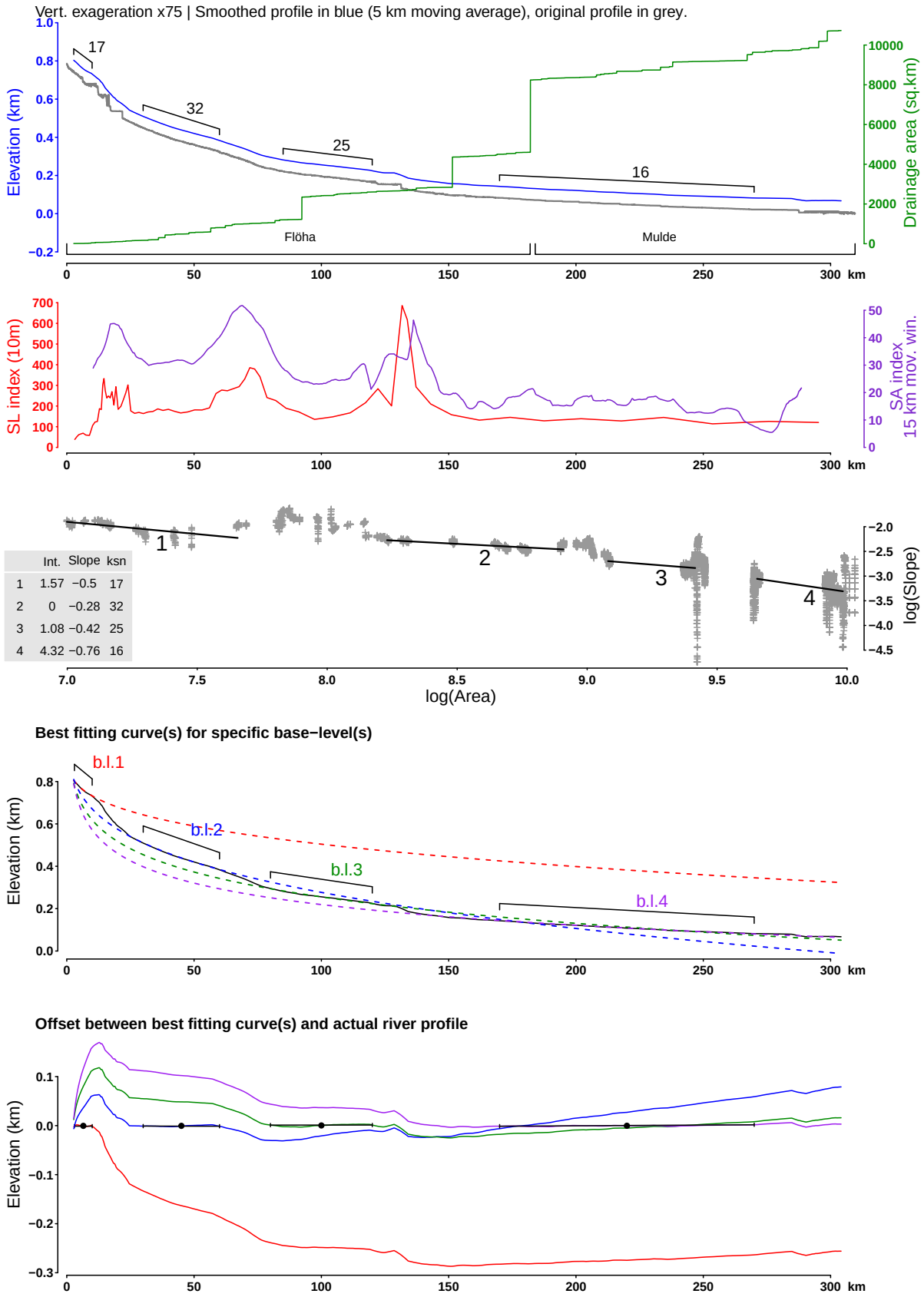


Fig. 2.3 – *Longitudinal profile analysis of the* **Flöha** *river. See location on Fig. 1.1. From top to bottom: (1) River profile and drainage area. (2) Stream-length gradient (SL) and Slope-Area (SA) indices. Peak values indicate anomalously steep slopes and knickpoints. (3) Regression of normalized steepness indices ($k_{sn}$) on a slope-area plot. $k_{sn}$ values are reported on the river profile. (4) Reconstruction of theoretical river profiles asociated to relict base-levels.*

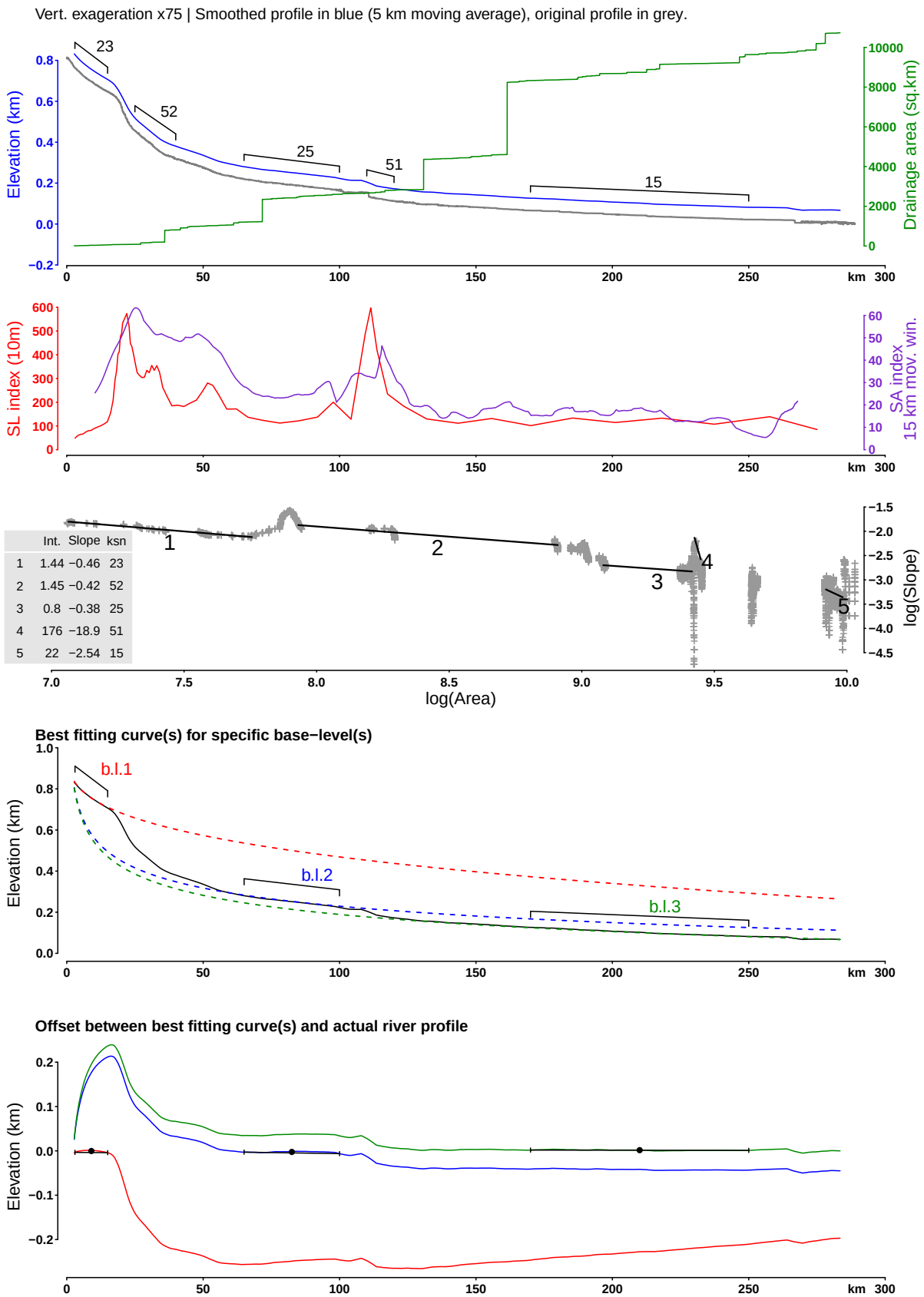


Fig. 2.4 – *Longitudinal profile analysis of the* **Schwarze Pockau** *river. See location on Fig. 1.1. From top to bottom: (1) River profile and drainage area. (2) Stream-length gradient (SL) and Slope-Area (SA) indices. Peak values indicate anomalously steep slopes and knickpoints. (3) Regression of normalized steepness indices ($k_{sn}$) on a slope-area plot. $k_{sn}$ values are reported on the river profile. (4) Reconstruction of theoretical river profiles asociated to relict base-levels.*

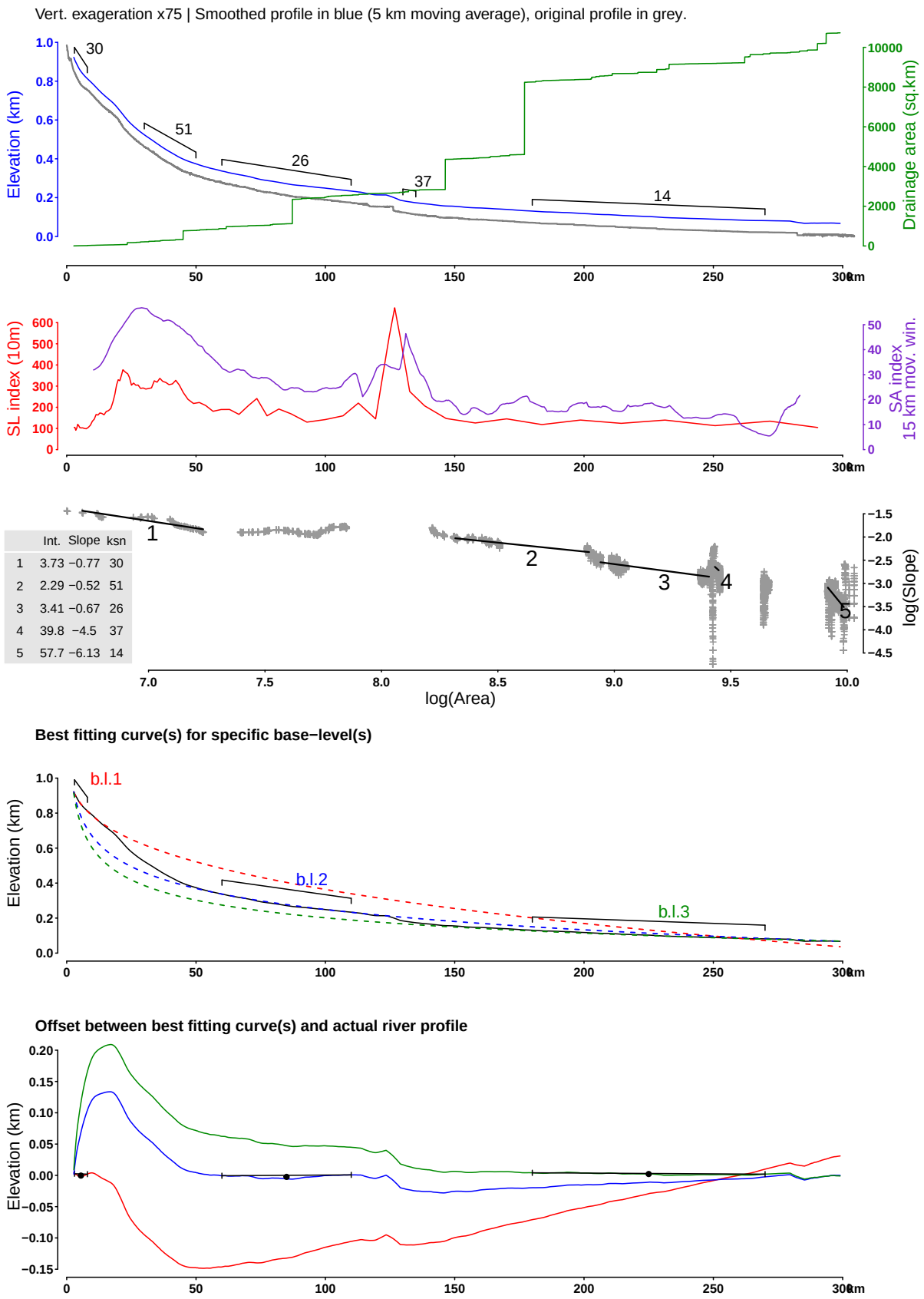


Fig. 2.5 – *Longitudinal profile analysis of the* **Jöhstädter Schwarzwasser** *river. See location on Fig. 1.1. From top to bottom: (1) River profile and drainage area. (2) Stream-length gradient (SL) and Slope-Area (SA) indices. Peak values indicate anomalously steep slopes and knickpoints. (3) Regression of normalized steepness indices ($k_{sn}$) on a slope-area plot. $k_{sn}$ values are reported on the river profile. (4) Reconstruction of theoretical river profiles asociated to relict base-levels.*

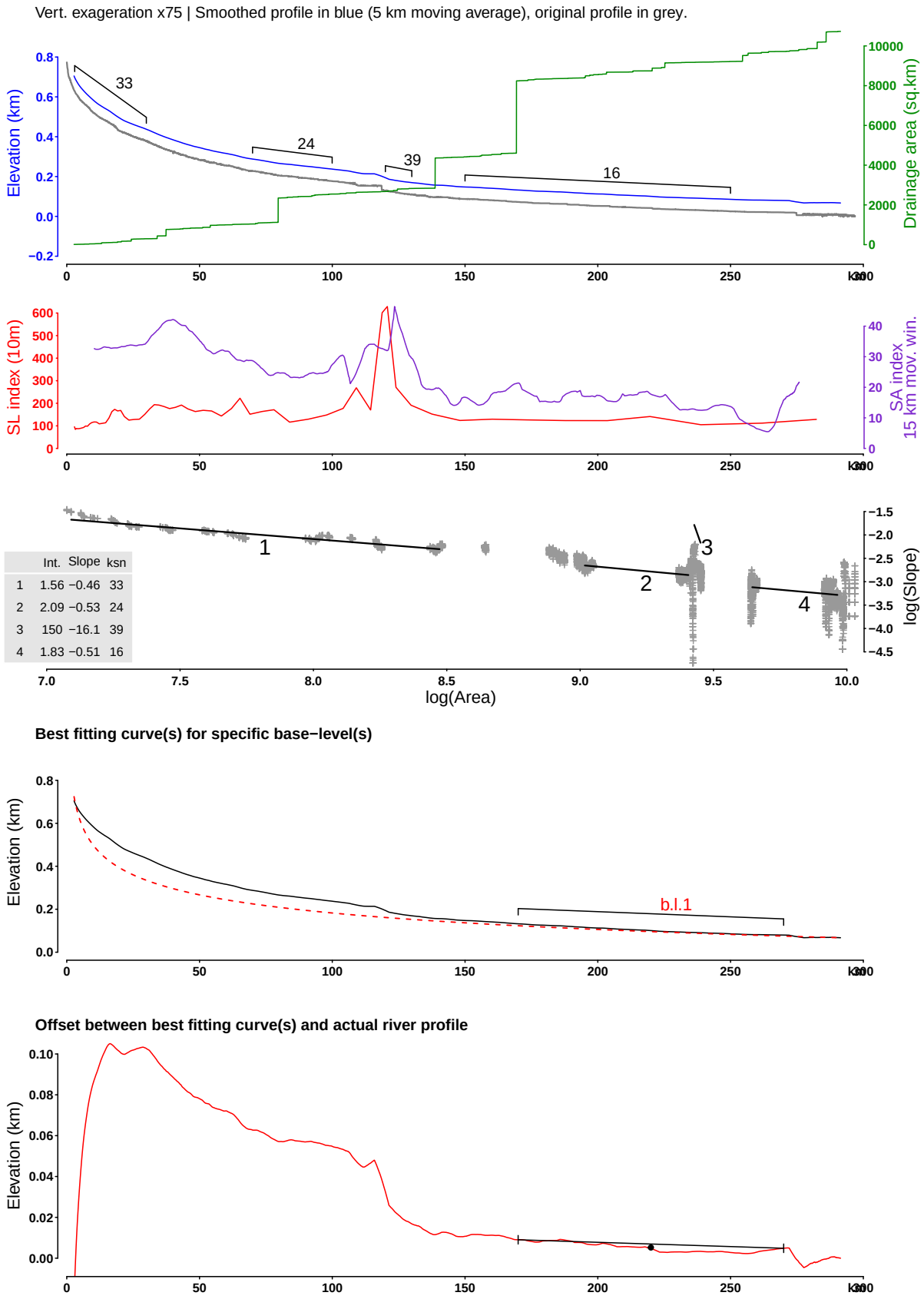


Fig. 2.6 – *Longitudinal profile analysis of the* **Zschopau** *river. See location on Fig. 1.1. From top to bottom: (1) River profile and drainage area. (2) Stream-length gradient (SL) and Slope-Area (SA) indices. Peak values indicate anomalously steep slopes and knickpoints. (3) Regression of normalized steepness indices ($k_{sn}$) on a slope-area plot. $k_{sn}$ values are reported on the river profile. (4) Reconstruction of theoretical river profiles asociated to relict base-levels.*

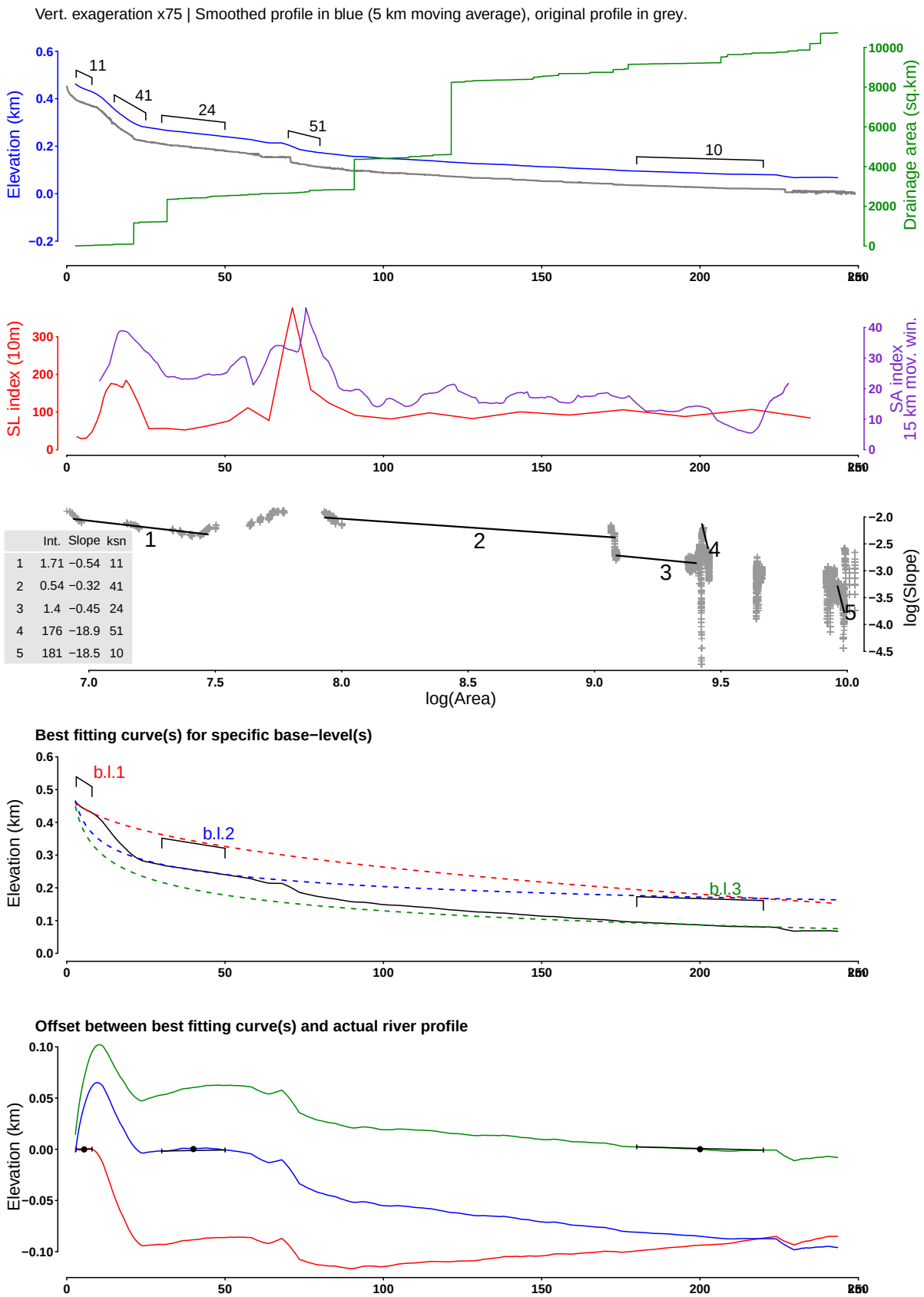


Fig. 2.7 – *Longitudinal profile analysis of the* **Große Lößnitz** *river. See location on Fig. 1.1. From top to bottom: (1) River profile and drainage area. (2) Stream-length gradient (SL) and Slope-Area (SA) indices. Peak values indicate anomalously steep slopes and knickpoints. (3) Regression of normalized steepness indices ($k_{sn}$) on a slope-area plot. $k_{sn}$ values are reported on the river profile. (4) Reconstruction of theoretical river profiles asociated to relict base-levels.*

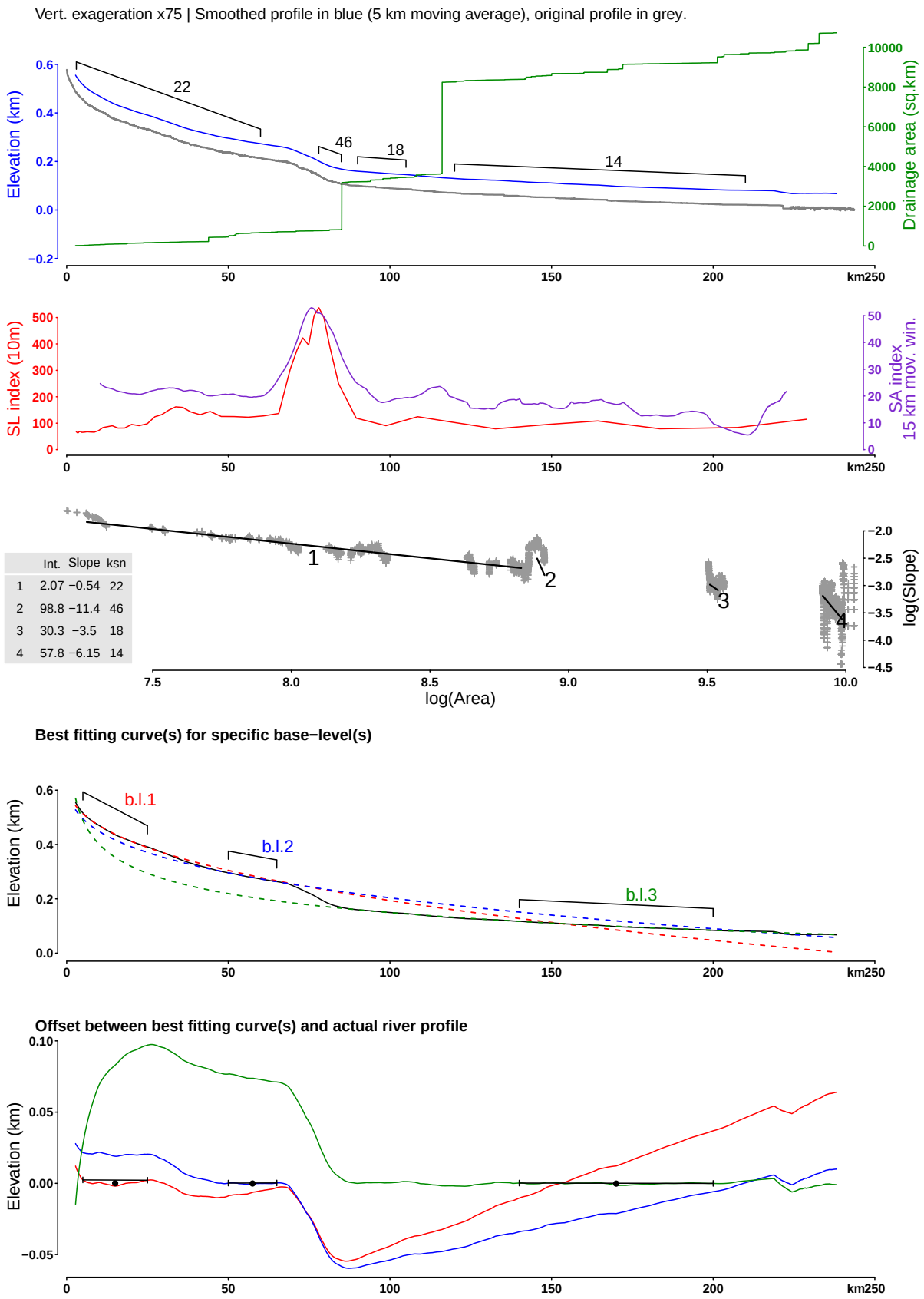


Fig. 2.8 – *Longitudinal profile analysis of the* **Zwönitz** *river. See location on Fig. 1.1. From top to bottom: (1) River profile and drainage area. (2) Stream-length gradient (SL) and Slope-Area (SA) indices. Peak values indicate anomalously steep slopes and knickpoints. (3) Regression of normalized steepness indices ($k_{sn}$) on a slope-area plot. $k_{sn}$ values are reported on the river profile. (4) Reconstruction of theoretical river profiles asociated to relict base-levels.*

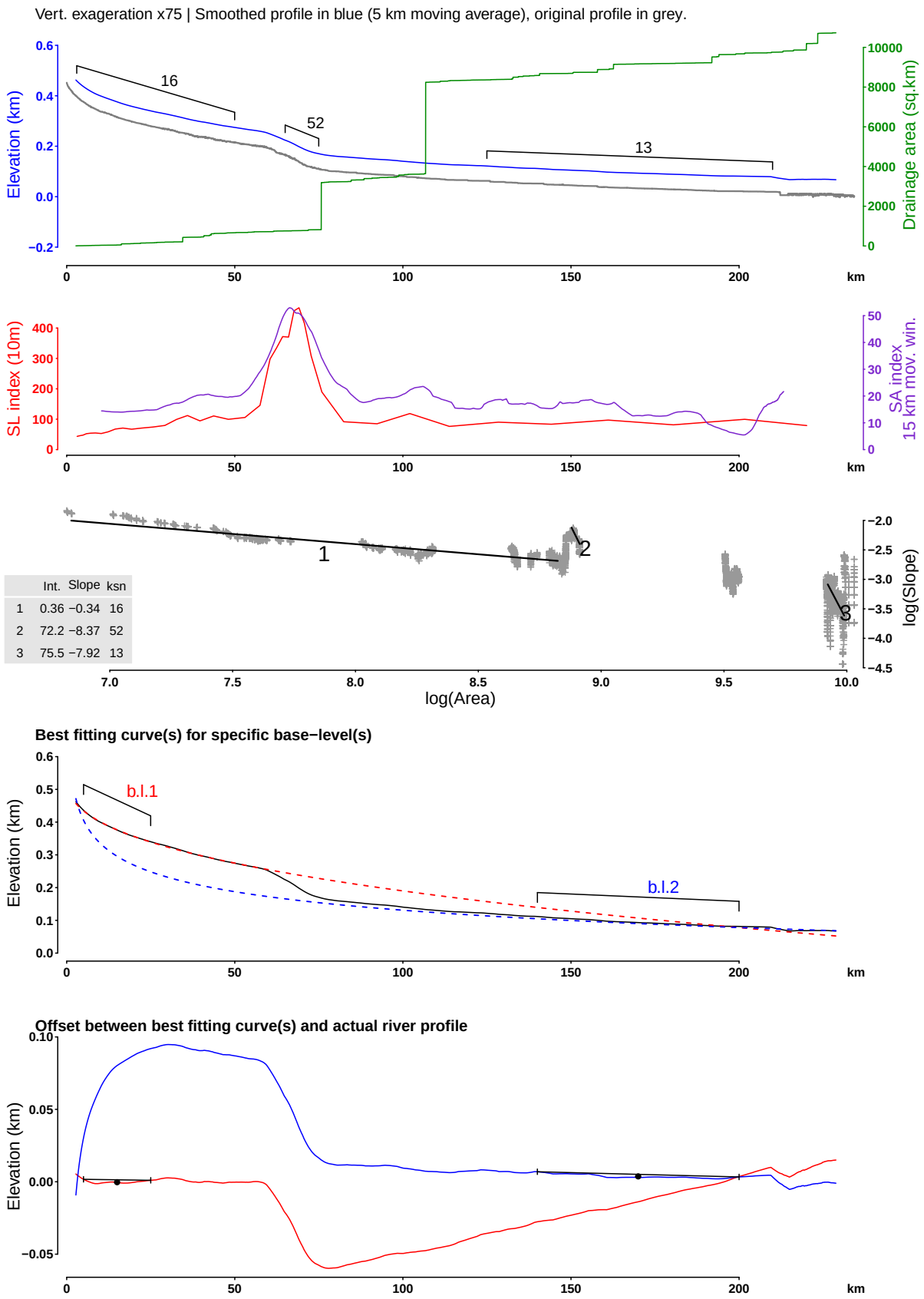


Fig. 2.9 – *Longitudinal profile analysis of the* **Würschnitz** *river. See location on Fig. 1.1. From top to bottom: (1) River profile and drainage area. (2) Stream-length gradient (SL) and Slope-Area (SA) indices. Peak values indicate anomalously steep slopes and knickpoints. (3) Regression of normalized steepness indices ($k_{sn}$) on a slope-area plot. $k_{sn}$ values are reported on the river profile. (4) Reconstruction of theoretical river profiles asociated to relict base-levels.*

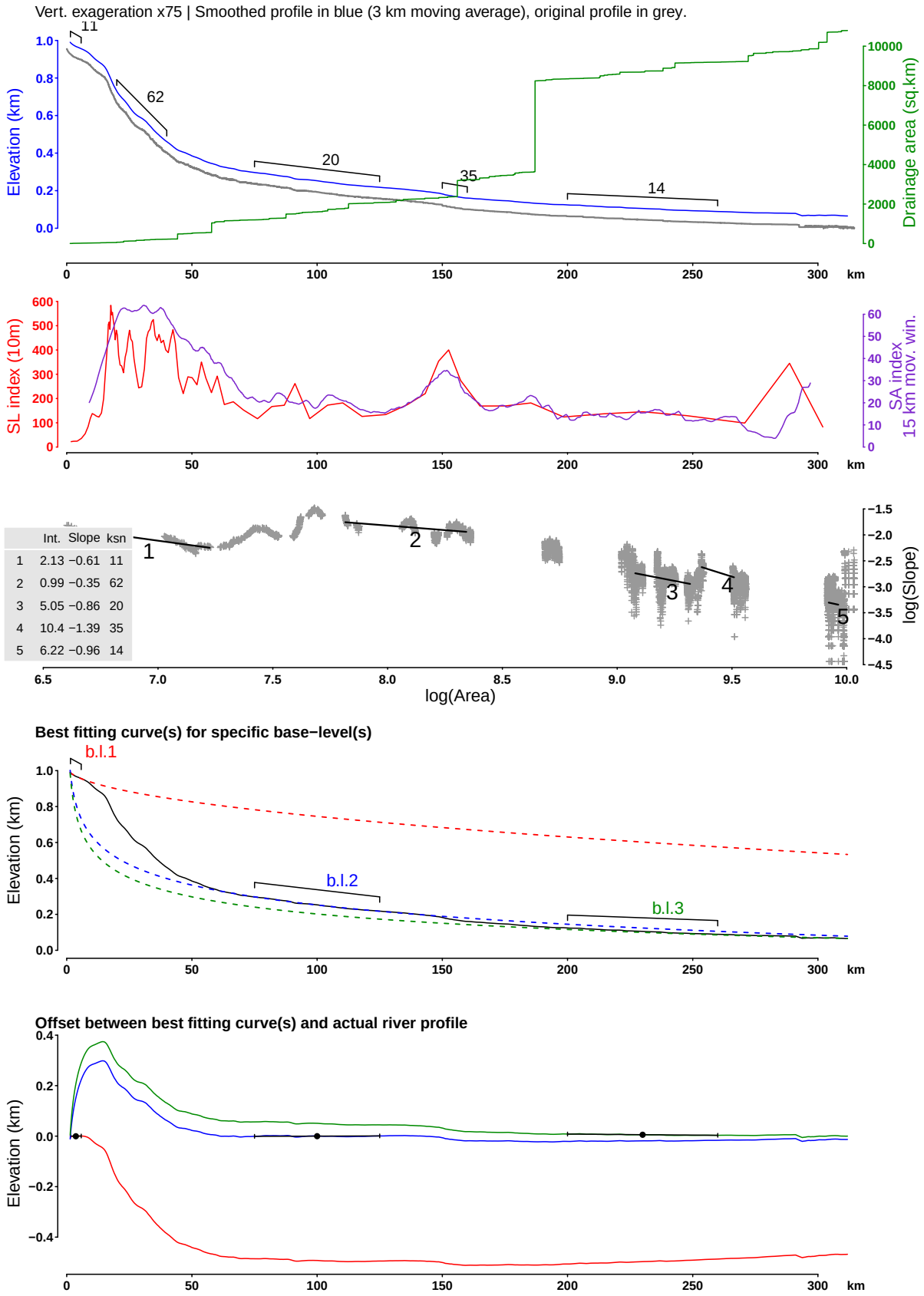


Fig. 2.10 – *Longitudinal profile analysis of the* **Schwarzwasser** *river. See location on Fig. 1.1. From top to bottom: (1) River profile and drainage area. (2) Stream-length gradient (SL) and Slope-Area (SA) indices. Peak values indicate anomalously steep slopes and knickpoints. (3) Regression of normalized steepness indices ($k_{sn}$) on a slope-area plot. $k_{sn}$ values are reported on the river profile. (4) Reconstruction of theoretical river profiles asociated to relict base-levels.*

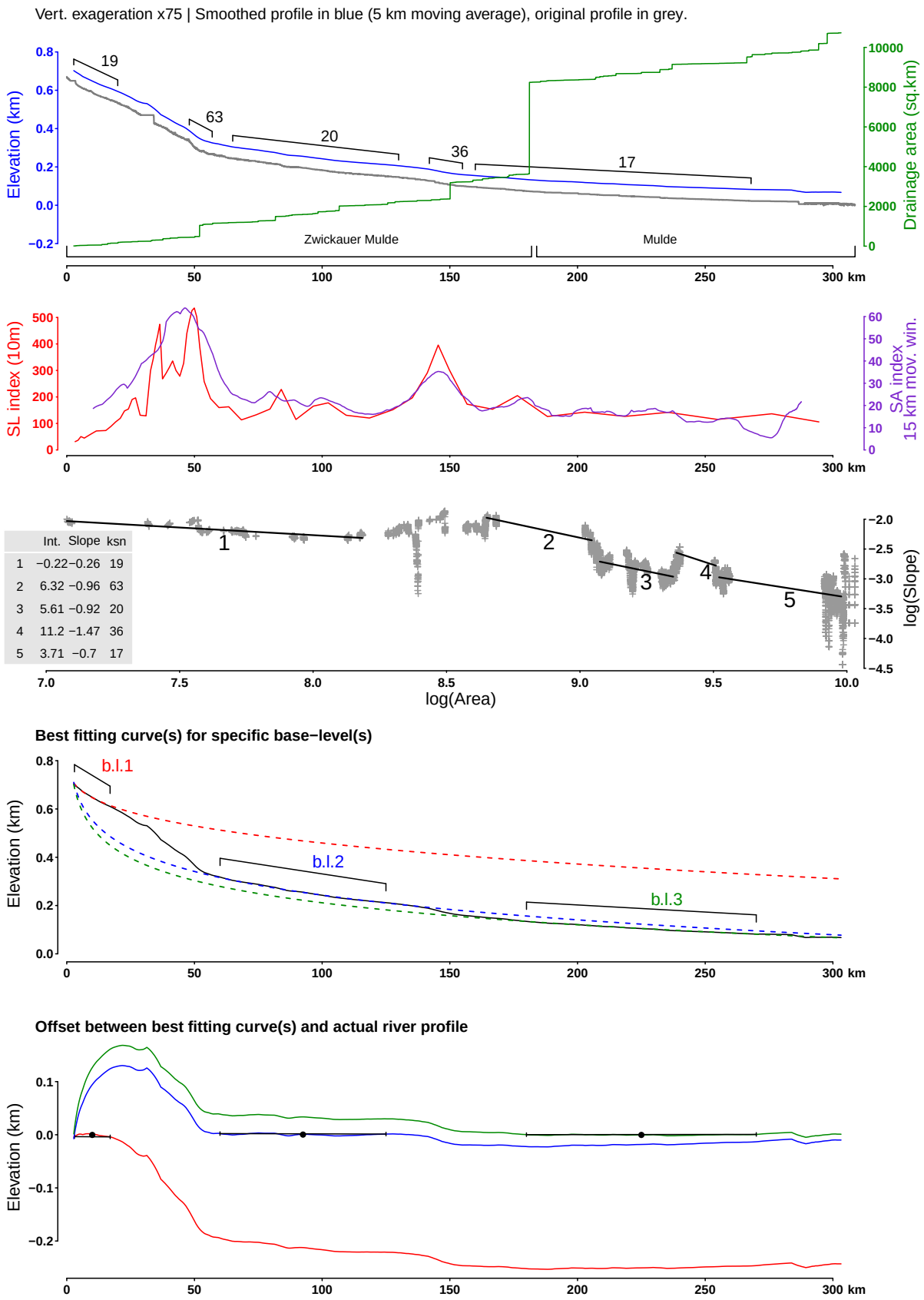


Fig. 2.11 – *Longitudinal profile analysis of the* **Zwickauer Mulde** *river. See location on Fig. 1.1. From top to bottom: (1) River profile and drainage area. (2) Stream-length gradient (SL) and Slope-Area (SA) indices. Peak values indicate anomalously steep slopes and knickpoints. (3) Regression of normalized steepness indices ($k_{sn}$) on a slope-area plot. $k_{sn}$ values are reported on the river profile. (4) Reconstruction of theoretical river profiles asociated to relict base-levels.*

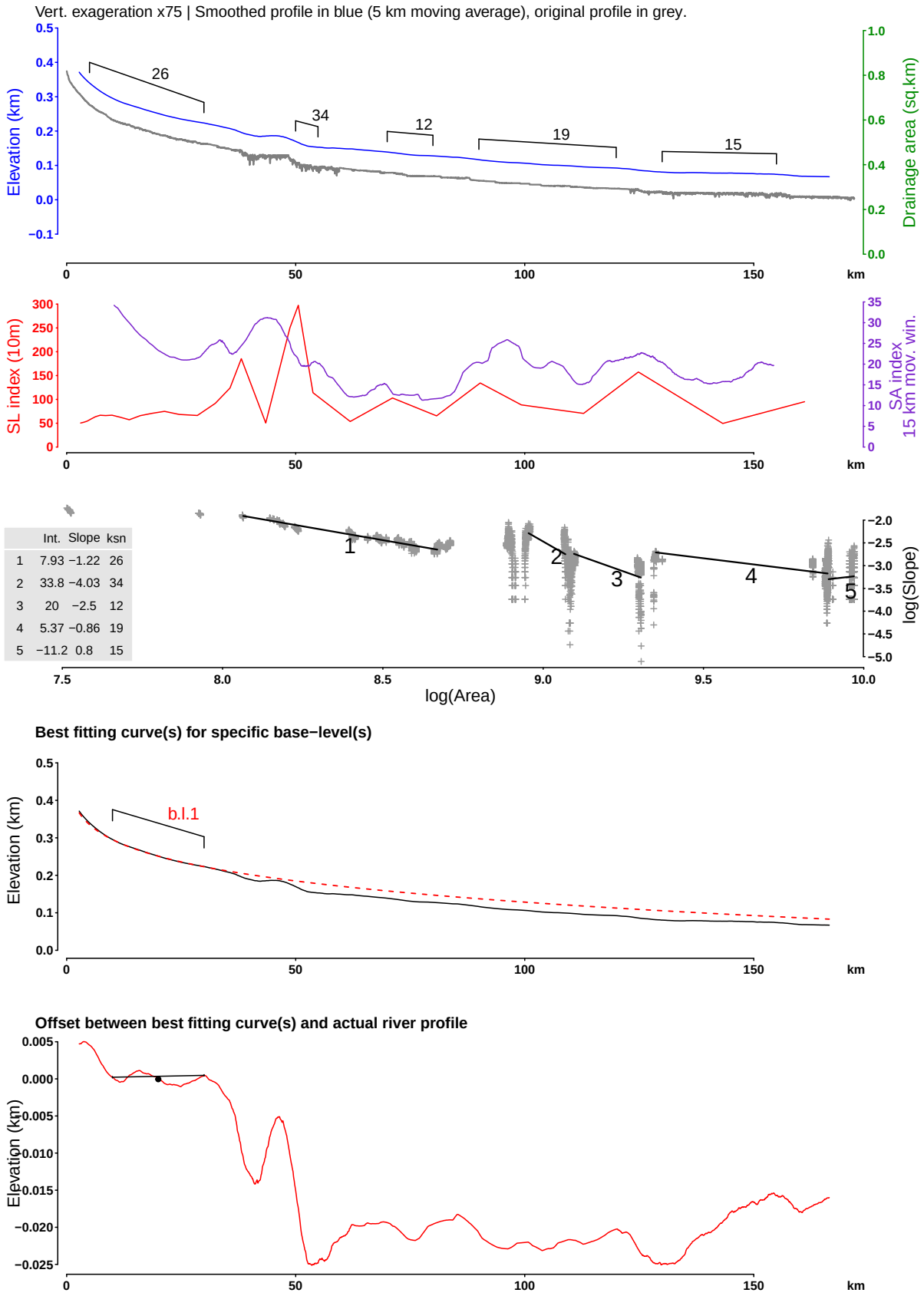


Fig. 2.12 – *Longitudinal profile analysis of the* **Pleiße** *river. See location on Fig. 1.1. From top to bottom: (1) River profile and drainage area. (2) Stream-length gradient (SL) and Slope-Area (SA) indices. Peak values indicate anomalously steep slopes and knickpoints. (3) Regression of normalized steepness indices ($k_{sn}$) on a slope-area plot. $k_{sn}$ values are reported on the river profile. (4) Reconstruction of theoretical river profiles asociated to relict base-levels.*

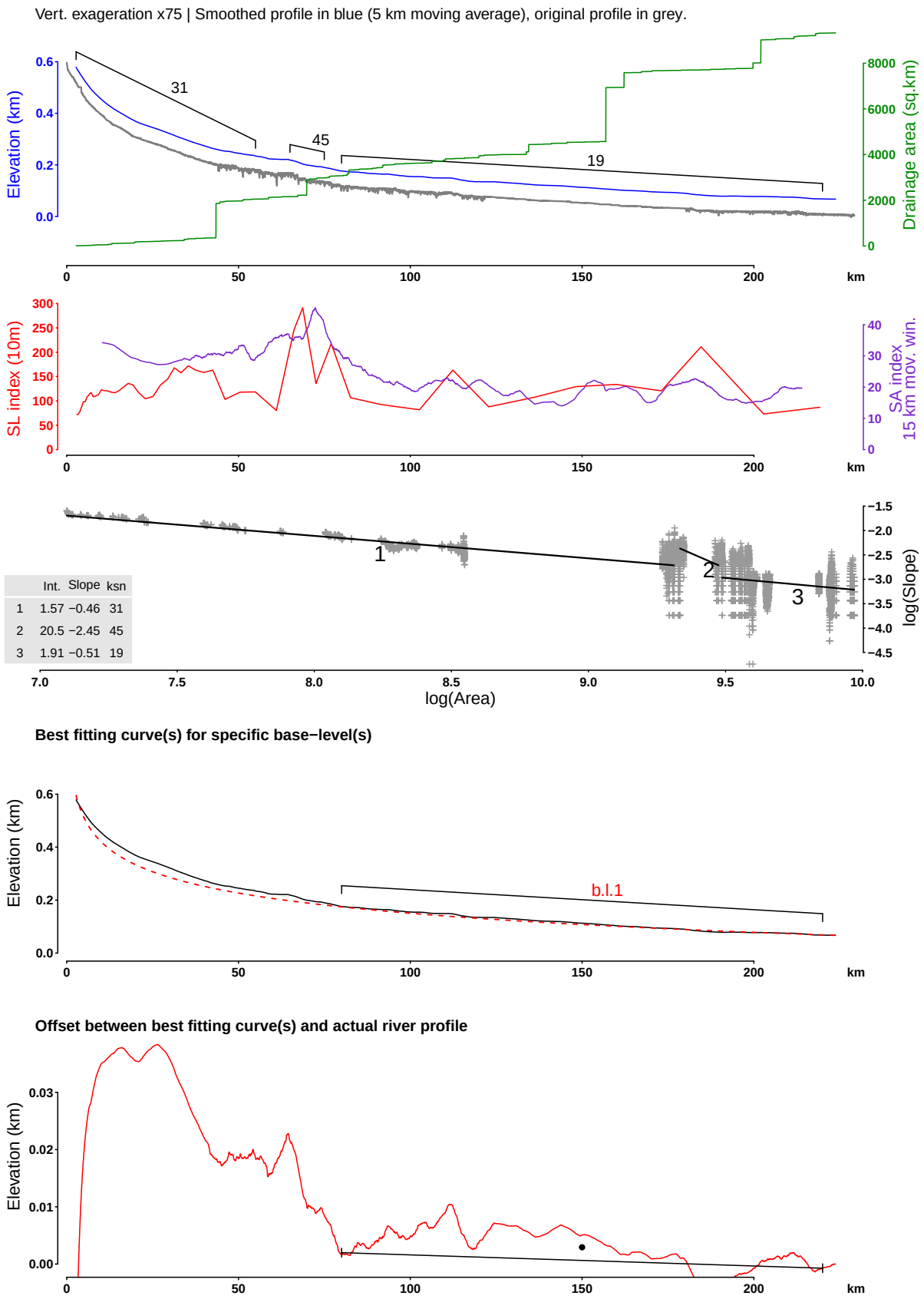


Fig. 2.13 – *Longitudinal profile analysis of the* **Göltzsch** *river. See location on Fig. 1.1. From top to bottom: (1) River profile and drainage area. (2) Stream-length gradient (SL) and Slope-Area (SA) indices. Peak values indicate anomalously steep slopes and knickpoints. (3) Regression of normalized steepness indices ($k_{sn}$) on a slope-area plot. $k_{sn}$ values are reported on the river profile. (4) Reconstruction of theoretical river profiles asociated to relict base-levels.*

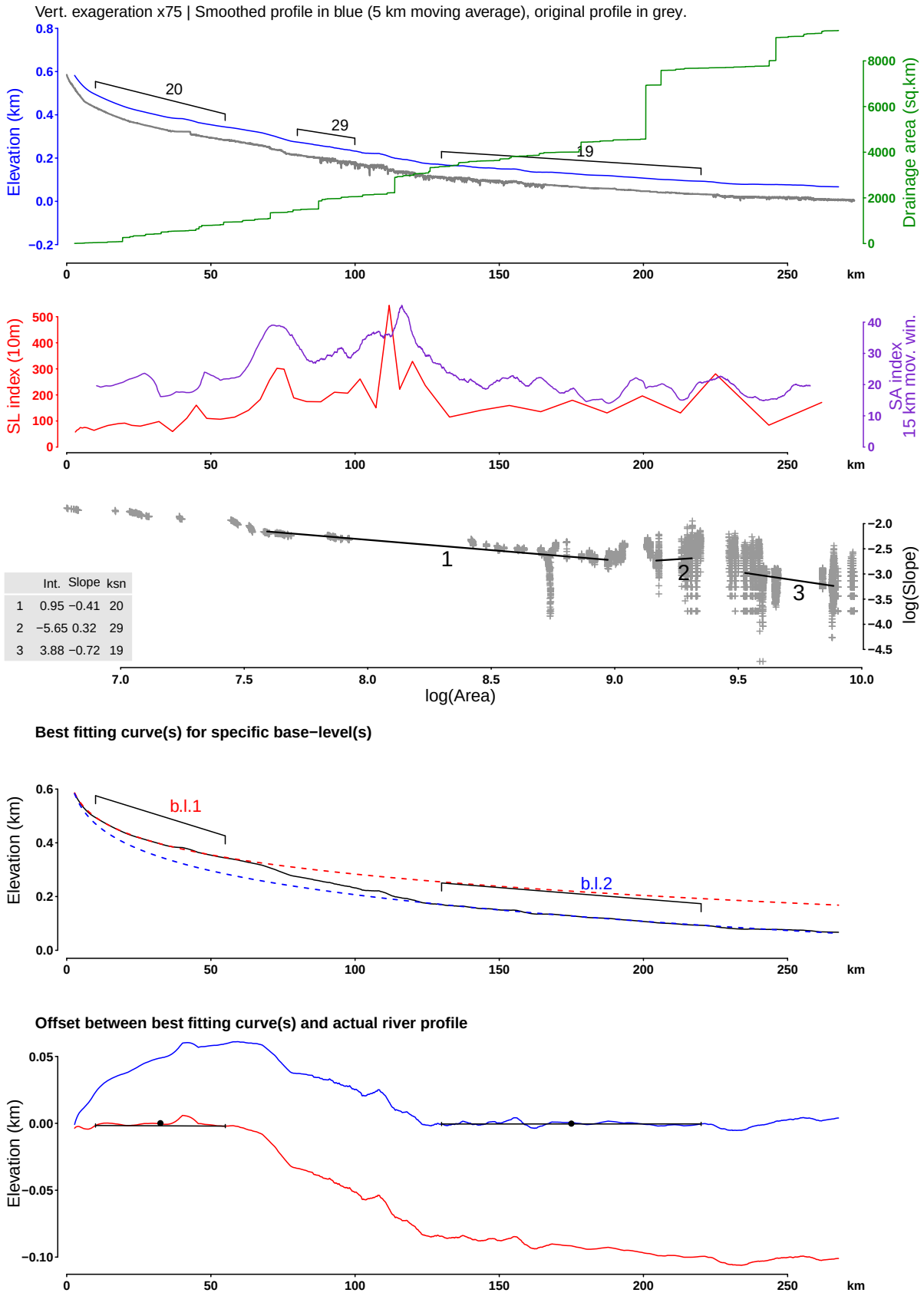


Fig. 2.14 – *Longitudinal profile analysis of the* **Weiße Elster** *river. See location on Fig. 1.1. From top to bottom: (1) River profile and drainage area. (2) Stream-length gradient (SL) and Slope-Area (SA) indices. Peak values indicate anomalously steep slopes and knickpoints. (3) Regression of normalized steepness indices ($k_{sn}$) on a slope-area plot. $k_{sn}$ values are reported on the river profile. (4) Reconstruction of theoretical river profiles asociated to relict base-levels.*